Spring 2022

Coalitional Game Theory for Stormwater Management and Green Infrastructure Practices

Carly Lawyer

COALITIONAL GAME THEORY FOR STORMWATER MANAGEMENT AND GREEN INFRASTRUCTURE PRACTICES

by

Carly Lawyer

Bachelor of Science
University of South Carolina, 2019

Submitted in Partial Fulfillment of the Requirements

For the Degree of Master of Science in

Civil Engineering

College of Engineering and Computing

University of South Carolina

2022

Accepted by:

Erfan Goharian, Director of Thesis

Enrica Viparelli, Committee Member

Hassan Tavakol-Davani, Committee Member

Tracey L. Weldon, Interim Vice Provost and Dean of the Graduate School

DEDICATION

Mom, your inability to consider I may fail at something keeps me up at night. Thank you for being a light, and for never doubting me.

Grandpa, the giant sheet cake you brought home to celebrate my commitment to graduate school fueled this whole project.

My partner and dearest best friend, thank you for every coffee, every midnight snack, and your endless encouragement.

ACKNOWLEDGEMENTS

I would like to express my sincerest gratitude for my supervisor, professor, and mentor, Dr. Erfan Goharian, for their unwavering support and assistance throughout my time as a graduate student. Thank you for pushing me forward, building me up, and giving me the opportunity to work with and learn from you. I am fortunate and honored to be your first graduating student. I would also like to thank the members of my committee, Dr. Enrica Viparelli and Dr. Hassan Tavakol-Davani, for offering me their time, expertise, and feedback.

Thank you to my officemates, without whom this whole experience would have been twice as difficult and half as fun. Thank you for sharing your knowledge with me, for your encouragement, and your friendship.

Finally, I would also like to thank all my friends and family members who offered support throughout my time as a graduate student. Your interest in my well-being and academic pursuits over the last few years was invaluable.

ABSTRACT

As global warming and climate Variability bring about more frequent and intense rainstorms and accelerate sea level rise, our social and built environments are at heightened risk of flood induced damages and consequent costs. This is particularly true for coastal areas, facing the coupled effects of these threats while serving as home to people, businesses, unique landscapes, and historic landmarks. Complex decisions at all levels of government and community planning stand to benefit from increased understanding of possible outcomes and pathways resulting from decentralized human behavior and decision making in the realm of water resources engineering and management. Game theory has allowed scientists to better understand and predict preferred strategies and interactions of rational self-interested actors in multi-player games. In coalitional games, players are able to work together to increase their individual utility payoffs through formation of strategic subsets, or coalitions. When applied to water resources management dilemmas such as infrastructure development and planning, this practice can be used to identify which and what variety of coalitions should form to benefit their overall hydrologic system. This research aims to determine ideal green infrastructure location and spending scenarios within Charleston, South Carolina's Market Street watershed using a coalitional game theory solution concept, the Shapley value, in combination with rainfall-runoff simulation. Results offer insights to stormwater services and flood managers concerning suggested areas of focus for green infrastructure

spending and advocacy for the purpose of reducing flooding and resulting property damages.

TABLE OF CONTENTS

LIST OF TABLES

LIST OF FIGURES

LIST OF ABBREVIATIONS

ABM ..... Agent-Based Model

AMC ..... Average Marginal Contribution

BMP ..... Best Management Practice

CHI ..... Computational Hydraulics International

CGT ..... Coalitional Game Theory

DDC ..... Depth-Damage Curve

DEM ..... Digital Elevation Model

EOP ..... Edge of Pavement

EPA ..... Environmental Protection Agency

FEMA ..... Federal Emergency Management Agency

GI ..... Green Infrastructure

GIS ..... Geographic Information Systems

IAT ..... Impervious Area Treated

ICPR ..... Interconnected Channel and Pond Routing

LID ..... Low Impact Development

NLCD ..... National Land Cover Database

NOAA ..... National Oceanic and Atmospheric Administration

PCSWMM ..... Personal Computer Stormwater Management Model

SHELDUS ..... Spatial Hazard Events and Losses Database for the United States

SSR ..... Spent-Saved Ratio

SWMM ..... Stormwater Management Model

CHAPTER 1

INTRODUCTION

1.1 BACKGROUND

Climate variations promise to disproportionately affect the world's coastal systems by way of exacerbated precipitation event frequency and intensity in tandem with sea level rise and increasing storm surge severity. With these changes come heightened and additional risks to infrastructure, ecological, and socio-economic systems in coastal settings. Property damage can mean not only physical and financial threats to individuals and businesses but increasing vulnerability for local economies and cultural landscapes by way of environmental degradation as well. As the effectiveness of existing traditional infrastructure designed under stationarity assumptions wanes in the light of these changes (Milly et al., 2008), potential for implementation of decentralized green infrastructure (GI) for stormwater management is on the rise (Meney & Pantelic, 2022). Governing and planning actors at all levels must address increasingly complex programming problems concerning placement, funding, and effectiveness of infrastructure projects. As such, these groups are increasingly advocating for individual home and business owner participation in local runoff and flood reduction strategies.

1.2 OBJECTIVES AND SCOPE

This research explores the applicability of coalitional game theory analysis to inform GI placement in an urban coastal watershed to demonstrate the potential system-

wide effects of the adoption of widespread, decentralized GI. The objectives of this study are as follows:

1. Provide an overview of the threats floods and related hazards pose to environmental, physical, and social systems within coastal communities and review existing methods of modeling human behavior and decision making in the realm of water resources management.
2. Discuss the benefits and drawbacks of various traditional and GI method deployment in these communities for the purpose of minimizing runoff and reducing local flooding.
3. Develop a 1D stormwater model to simulate various GI installation scenario effects on runoff volumes, flooding, and consequent property damages.
4. Investigate coalitional game theory concepts and their applicability to informing GI planning concerns, including cost effectiveness and placement.

1.3 LAYOUT OF THESIS

The layout of the presented research is as follows:

Chapter 2 provides an overview of climate variation induced challenges facing coastal communities and explains an ongoing need for the introduction of widespread decentralized GI in these areas to aid existing, aged traditional means of infrastructure through increased stormwater management capacity. Additionally, effects of increasing flood frequency on historically significant coastal areas, in the context of cultural preservation and tourism economy are discussed. A review of literature concerning

modeling human decision making in the field of water resources management is also included. Finally, motivation for the presented research is explained.

Chapter 3 details the choosing of the specified study area, the coastal county of Charleston, South Carolina. Context is provided concerning the area's economic and cultural significance, as well as the community's ongoing struggles with nuisance flooding and increasingly severe coastal hazards.

Chapter 4 outlines the methods, software, and data used to simulate rainfall-runoff interactions in the Charleston Peninsula as well as a more focused model of the peninsula's Market Street watershed. This chapter also explains the estimation and application of the coalitional game theory solution concept, the Shapley value, to inform GI placement in the Market Street watershed for the purpose of reducing flood-induced building damages.

Chapter 5 contains model validation information, results concerning GI placement scenarios and corresponding potential flood damage savings, cost efficiency tables, and discussion on recommended planning strategies based on the combined flood simulation and game theory results.

Finally, Chapter 6 summarizes research findings and provides suggestions for future work.

CHAPTER 2

LITERATURE REVIEW

2.1 CLIMATE CHANGE AND COASTAL COMMUNITIES

Climate change has impacted human and natural systems, globally, at every level of development. Changes in the hydrological cycle observed due to global warming over the last several decades include increased atmospheric water vapor content, altered precipitation patterns, intensity, and extremes, and changes in soil moisture (Bates et al., 2008). The United States has experienced an increasing percentage of intense single-day rain events between 1901 and 2014. Additionally, total annual precipitation has increased by 0.5% per decade across all 48 contiguous states, and 0.2% per decade over land areas worldwide (EPA, 2014). Much of our existing and aging water infrastructure is strained by these changes, whose designs were based in past hydrological experiences and stationarity assumptions (Bates et al., 2008; Milly et al., 2008; U.S. Global Change Research Program, 2017). However, the consequent costs of heightened temperatures and rising seas have not distributed their risks evenly and will continue to disproportionately affect built and environmental systems in coastal areas.

The combined and exacerbated impacts of more intense storms and sea level rise are particularly detrimental to coastal communities, threatening outdoor recreation reliant on surrounding natural systems as well as regional economies based in agriculture, fishing, and tourism (EPA, 2014; U.S. Global Change Research Program, 2017). As global temperatures increase, the rising sea impacts storm surge, high tide levels, coastal

erosion, and incites loss of crucial wetland areas, worsening effects of natural disasters (NOAA, 2022). 17 of the 18 warmest years on record have occurred since 2001, bringing with them over two thirds of the total hurricane damages recorded over the last century (Gaul, 2019). Experts' concern with these issues may be less extreme if it weren't for human propensity to settle around bodies of water; coastal areas constitute less than 10% of the land in the contiguous United States, but house nearly 40% of the country's population (NOAA, 2021). With an existing trillion-dollar coastal property market and many forms of public infrastructure at stake, high tide flooding is expected to continue to affect homes and businesses in these densely populated areas by overloading storm and wastewater systems while stressing surrounding estuarine ecosystems (NOAA, 2022; U.S. Global Change Research Program, 2017). As population growth, economic development, and urbanization are expected to continue and compound existing coastal community vulnerability, it is imperative that implemented adaptation and infrastructure decisions are considered in the context of long-term sustainable development (IPCC, 2014).

2.2 TRADITIONAL AND GREEN INFRASTRUCTURE

The introduction of impermeable surfaces, such as concrete pavement and roofing, which replace soils and vegetation that aid in mitigating runoff volumes through infiltration and evapotranspiration processes following storm events, cause significant variations in runoff volumes and flow patterns (Das, 2015). This is of additional concern in highly urbanized and densely populated coastal areas, which, like all communities, include vital means of transportation and business, which can be interrupted by both rainfall and tide induced nuisance flooding. In the past, engineers and city planners have

relied on traditional, or grey infrastructure methods, to move urban stormwater out of built environments, by way of gutters, drains, pipes, and collection systems (EPA, 2021). What each of these means of control have in common is a focus on conveying stormwater elsewhere, often untreated and into local water bodies. As climate variations and land use changes continue to alter existing hydrologic conditions, additional stormwater infrastructure to reduce excess runoff will be needed to aid existing means of grey infrastructure which may not be equipped to adequately handle these changes on their own.

To meet this challenge, a case for Green Infrastructure (GI) should be made. The Water Infrastructure Improvement Act defines GI as "the range of measures that use plant or soil systems, permeable pavement or other permeable surfaces or substrates, stormwater harvest and reuse, or landscaping to store, infiltrate, or evapotranspirate stormwater and reduce flows to sewer systems or to surface waters" (Water Infrastructure Improvement Act, 115 U.S.C. § 436, 2019). Low impact development (LID) strategies fall under the umbrella term of GI and describe an approach to stormwater management that mimics the natural processes within an environment to manage and treat stormwater close to its source, rather than conveying it elsewhere (EPA, 2018). LID implementation works to deter excess rainfall from common collection points through the creation, restoration, and preservation of green spaces and natural landscape features that effectively limit the amount of built and impermeable surfaces added to an area (Ellis et al., 2014; EPA, 2018). There is a vast body of research which explores the effectiveness of GI for urban runoff rate and volume reduction, be it through rainwater harvesting (Ahiablame et al., 2013; Jones & Hunt, 2010), permeable pavements (Randall et al.,

2020; Støvring et al., 2018; Zhang, Shouhong; Guo, 2014), bioretention cells (Davis, 2008; Wang et al., 2019), or green roofing (Bliss et al., 2009; William et al., 2016). These strategies work in tandem with, reduce stress on, and expand the capacity of existing stormwater infrastructure by intercepting rainfall before it reaches urban drainage systems (Ahern, 2011).

LID strategies are versatile in that they can not only be applied to new development projects, but redevelopment and retrofitting projects as well (Roseen et al., 2011). Most are easily accessible to homeowners and businesses and relatively affordable, particularly means of rainwater harvesting and bioretention in the form of rain gardens. Additionally, GI implementation provides an opportunity to add both aesthetic (Tupper, 2012) and monetary (Ichihara & Cohen, 2010; Voicu & Been, 2008) value to outdoor spaces and properties. For these reasons, and their ability to bolster the capabilities of existing and aged grey infrastructure, LID strategies have high potential to increase flood resilience in urban coastal communities.

2.3 CULTURAL HERITAGE PRESERVATION IN FLOOD-PRONE AREAS

Coastal areas often offer a combination of history and natural landscapes that cannot be experienced anywhere else. Visiting historic and cultural sites is one of the most popular tourist activities today, and heritage tourism has been recognized as the fastest growing niche market in the tourism industry (Baram, 2008; Hargrove, 2002). However, many landmarks and cultural heritage sites are now at risk due to climate change impacts including sea level rise, coastal erosion, increased flooding, and heavy rain, threatening archaeological resources, historic buildings, and cultural landscapes

while creating complex interactions within and between natural, cultural, economic, and social systems (Cassar et al., 2007; Holtz et al., 2014).

In turn, the tourism sector has become increasingly impacted by climate change and has much to lose by way of both economic and natural resources (Cassar et al., 2007). Attractions allow coastal communities to generate seasonal employment opportunities and contributions to the local economy. For example, the United States coastal tourism and recreation sector, which includes scenic water tours, parks, beach-going, marinas, and hotels and lodging, makes up nearly 75% of the employment of the country's entire marine economy (Office for Coastal Management, 2020).

Multiple studies have confirmed the effects of increasing environmental changes and flooding events on tourist activities. In one case, a negative relationship was found to exist between number of visitors and flooding patterns in Spain, citing fewer visitors to a thermal bath complex following heightened water levels in a nearby reservoir (Ara et al., 2019). Another reported direct flooding impacts on the tourism industry in Malaysia, finding declines in both numbers and hotel revenue in response to destruction of natural, cultural, and heritage attractions (Hamzah et al., 2012). Using parking revenue data, (Hino et al., 2019) found decreased visits to historic downtown Annapolis, Maryland due to frequent high-tide flooding. In another case, 45% of hotel reservations in Venice, Italy were cancelled following a historic flood event in 2019 which inundated nearly 90% of the city (Cerini, 2019; Insurance Journal, 2019).

The effects of flooding on historic sites are often overlooked, but can be devastating not only to historic structures, but their surrounding landscape and contents as well (Hamzah et al., 2012; Holický & Sýkora, 2010). These, coupled with the

intangible value of heritage itself, are the irreplaceable character defining elements that need to be protected for future generations to enjoy, which is necessary to maintain tourism's place in many local economies (Hargrove, 2002; Stovel, 1998; Wolch et al., 2014). The main challenge in implementing traditional stormwater mitigation techniques in culturally significant and visually impressive areas lies in the inability to make alterations to sites or structures that can cause loss of or obscure their historic designation or features (Holický & Sýkora, 2010). This is problematic as the literature that exists on vulnerability assessments for historic sites due to flooding focuses mainly on the structural integrity of historic buildings without putting emphasis on the surrounding landscape and other natural features (Gandini, 2018; Promsaka et al., 2012; Wolch et al., 2014).

It has been established that if coastal economies dependent on tourism are to remain unaffected by the combined effects of climate change and urbanization, additional flood protection is needed. Simultaneously, these areas must maintain their aesthetic appeal while managing the highly unequal distribution of adverse climate change effects. LID strategies, due to their aesthetic qualities, make them well-suited for historically significant areas with flood vulnerabilities, particularly those containing historic buildings and surrounding green spaces. However, choices about spending and placement remain a complex water resources management problem.

2.4 WATER RESOURCES MANAGEMENT AND MODELING HUMAN BEHAVIOR

Increased flood frequency and associated risks affect decision making by individuals and businesses as well as water resources planners and managers. Planners must collaborate with numerous community institutions while ensuring that decisions

take into consideration long-term impacts on future generations and fit into present budget constraints as well as highly developed urban spaces (Ahern, 2011; Loucks & Beek, 2017). There are plentiful studies which have aimed to inform LID placement and design decisions using rainfall-runoff simulations in the Environmental Protection Agency's (EPA) Stormwater Management Model (SWMM) (Bai et al., 2018; Kim et al., 2018; Qin et al., 2013; Simpson, 2010; York et al., 2015; Zahmatkesh et al., 2014) as well as a variety of studies which have coupled SWMM simulations with optimization algorithms (Eckart et al., 2018; Ghodsi et al., 2020; Macro et al., 2019; Raei et al., 2019; Tavakol-Davani et al., 2019; Xu et al., 2017). This category of study is suitable for informing centralized decision-making surrounding GI but neglects the drivers of and human behaviors behind decentralized GI decisions.

LIDs are a decentralized form of infrastructure, able to be procured and installed by individual property owners, with or without financial incentives from governing bodies. This accessibility is a tradeoff for smaller service area, therefore widespread adoption through community participation is needed in order to see systemwide benefits (Ahiablame & Shakya, 2016; Baptiste et al., 2015; Montalto et al., 2013; Ureta et al., 2021). Multiple studies have attempted to identify community barriers to GI participation, with findings ranging from household characteristics (Ureta et al., 2021), lack of public understanding about individual roles in stormwater management (Chaffin et al., 2016), lack of trust and communication between stakeholder groups (Van De Meene et al., 2009), property restrictions (Coleman et al., 2018), and lack of direct financial incentives (Carter & Fowler, 2008).

It is the combination of these beliefs and barriers across communities which work together to produce system-wide collective and emergent behavior. Agent-Based Modeling (ABM) methods offer a means of simulating these diverse behaviors, relationships, and interactions among individuals, or actors, within their environment (Macal & North, 2010). Applications for water resources management are still relatively limited (Berglund, 2015), but ABM has the potential to allow modelers to observe, plan for, and understand the long- and short-term outcomes of ecological, environmental, economic, and social changes, which are all important aspects of the water resource system planning and management process (Loucks & Beek, 2017). ABM has been used previously to investigate possible outcomes and emergent responses to various climate, policy, flood, and subsidy scenarios (An et al., 2005; Manson, 2001; D. C. Parker et al., 2003), some coupled with hydraulic models (Abebe et al., 2019a, 2019b, 2020; Dawson et al., 2011; Hyun et al., 2019; Michaelis et al., 2020). Additional coastal climate change adaptation literature which utilizes ABM are summarized in Table 3.1. While ABMs are particularly suited to aid in the study of local-global interactions, effects of heterogeneity on emergence, and decentralized decision-making (Bandini et al., 2009), there is a lack of data on agents themselves, limiting reliability of parametrized human behaviors (Macal & North, 2010; Michaelis et al., 2020; Patt & Siebenhüner, 2005; Yang et al., 2018). Extensive data collection requirements and challenges in modeling both communications and complex interactions among individuals makes this method of study a non-trivial task (Niazi & Hussain, 2012) for water management researchers.

Game Theory analysis, not yet implemented to a great extent in the field of water resources management, allows for the prediction of human behavior in response to

Table 3.1: Coastal Adaptation Strategies and Associated Studies Which Utilize ABM

Adaptation Type	Secondary Categories	Example Strategies	ABM Studies
Accom-modation	Land use changes	Flood resistant agriculture	Troost et al. 2012; Morgan and Daigneault 2015; Jenkins et al. 2017; Crick, Jenkins, and Surminski 2018; Abebe et al. 2019b
		Replacement of armored with living shorelines	
		Adjusted land use planning	
	Flood proofing	Retrofitted building	Brown and Ferreira 2013; Montalto et al. 2013; Haer et al. 2017, 2020; Crick, Jenkins, and Surminski 2018; Tonn and Guikema 2018; Yang et al. 2018; Abebe et al. 2019b, 2020; Zhuo et al. 2019; Chandra-Putra and Andrews 2020; Han et al. 2020; Michaelis et al. 2020
		Building and contents elevation*	
		Elevation of low-lying infrastructure	
		Green infrastructure*	
	Evacuation planning	Improved evacuation routes*	R. J. Dawson, Peppe, and Wang 2011
		Improved flood shelters	
	Flood forecasting and projection	Flood hazard mapping	Haer et al. 2017, 2020; Jenkins et al. 2017; Karanci, Berglund, and Overton 2017; Crick, Jenkins, and Surminski 2018; Tonn and Guikema 2018; Yang et al. 2018; Zhuo et al. 2019; Abebe et al. 2020; Chandra-Putra and Andrews 2020; Han et al. 2020
		Flood warning systems	
		Flood insurance	
		Government subsidies*	
		Flood information campaigns*	
Protection	Hard structures	Seawalls	Tonn and Guikema 2018; Abebe et al. 2019b; Zhuo et al. 2019; Haer et al. 2020; Han et al. 2020; Michaelis et al. 2020
		Dikes	
		Storm surge barriers	
	Coastal management	Beach and dune nourishment	Karanci, Berglund, and Overton 2017
		Artificial dunes	
		Removal of invasive and restoration of native species	
		Enhancement of coastal vegetation	

Retreat	Land reclamation	Allow wetlands to migrate inland	Crick, Jenkins, and Surminski 2018; Abebe et al. 2019b
		Shoreline setbacks	
		Deny development approval in flood prone areas*	
	Climate migration	Managed community retreat	Berman et al. 2004; Hassani-Mahmooei and Parris 2012; Jenkins et al. 2017; Karanci, Berglund, and Overton 2017; Tonn and Guikema 2018; Chandra-Putra and Andrews 2020
		Selling property in flood prone areas*	

conflict and omits the need for behavioral data as well as the modeling challenges presented by agent-based modeling methods (Madani, 2010; Parrachino et al., 2006). Predicted game theory outcomes often differ from those found using traditional optimization methods, as they take into consideration and prioritize individual stakeholder objectives rather than system objectives, and allow modelers to observe how individual goals affect system outcomes and evolution (Madani, 2010). Game theory can incorporate decision makers' potential actions, preferences, and strategic choices in the face of conflict, allowing researchers to predict individual decisions in differing scenarios, give advice to relevant parties, and inform future decisions (Farooqui & Niazi, 2016) in planning, policy, and design conflicts (Madani, 2010). Cooperative game theory, in which agents are able to work together and bargain with one another, offers solutions to allocation problems which can serve as a basis for, for example, agreements among parties dealing with cost sharing conflicts or benefits allocation following player cooperation (Myerson, 1991; Parrachino et al., 2006). Applications of cooperative game theory in water resources dilemmas include allocation of maintenance cost for a shared irrigation system (Hamers et al., 2003), electricity and production cost from shared hydroelectric power (Gately, 1974), pollution allowance (Kilgour et al., 1988), aquifer resources (Just & Netanyahu, 2004), and water rights (Braden et al., 1991). However, the use of Game Theory to consider socio-economic impacts of flood management and stormwater management practice installation has not been well-established.

A recent study (William et al., 2017) used cooperative game theory to investigate the impacts of various stormwater management policies to incentivize GI implementation for community participation in bioretention cell installation in an urban watershed.

Results provide insights concerning spatial bargaining power in the study area, with analysis revealing which subbasins are adequately reimbursed in terms of decreased stormwater pollutant loads versus the expenses they incurred for GI installation. Still, there are no studies, to my knowledge, which leverage cooperative game theory concepts in this manner to inform cost effective LID placement for the purpose of stormwater capture and consequent local flood damage reduction.

2.5 RESEARCH MOTIVATION

Heavier precipitation events, sea level rise, and increasingly severe storm surge are expected to cause lasting damage to existing coastal properties and infrastructure. Aging means of traditional stormwater infrastructure in these areas are expected to not be able to adequately handle these changes and would benefit by alleviated stress and increased capacity by way of widespread GI installation. Planners, governing bodies, and relevant stakeholders would greatly benefit from further knowledge surrounding increasing community participation in stormwater management efforts, as well as means of informed predictions for where LID projects will be most beneficial and cost-effective in the long-term. For this reason, this research proposes the use of coalitional game theory (CLT) analysis to inform LID placement, spending, and GI advocacy focus in coastal Charleston, South Carolina. Results from this study will potentially provide insights concerning spatial flood damage and flood reduction benefit information as well as study subarea bargaining power, with analysis revealing areas in Charleston which would be adequately reimbursed in terms of decreased flooding and economic damage for the cost incurred for various GI installation scenarios.

CHAPTER 3

STUDY AREA: CHARLESTON, SOUTH CAROLINA

3.1 ECONOMIC AND CULTURAL SIGNIFICANCE

The City of Charleston, South Carolina, a major and scenic port along the southeastern coast of the United States, is situated on an inlet of the Atlantic Ocean formed by the confluence of the Ashley and Cooper Rivers (Charleston County, 2010). It is South Carolina's oldest city, home to a 1,750-acre historic district designated by the National Register of Historic Places (Morris & Renken, 2020) and over 1,000 historic buildings which line the city's colorful and frequently crowded downtown streets (Spanger-Siegfried et al., 2014). The city is an economic engine for the state, by way of both trade and manufacturing, but the core of its revenue is reliant on an enduring heritage tourism industry (Morris & Renken, 2020; Platt, 2020). Following an influx of nearly 7 million visitors, over 2.5 million attraction attendees, and nearly $7.3 million in economic impact, history and historic sites were deemed the Greater Charleston Area's greatest asset in 2018 (Office of Tourism Analysis, 2018). However, having experienced drainage and flooding problems since its founding (City of Charleston, 2015), sea level rise and increased flooding instances are significant threats to both Charleston's lucrative tourism economy and business community (Williams & Moore, 2020).

3.2 FLOOD VULNERABILITY

The City of Charleston is an economic engine and travel destination which is facing an existential threat due to compound flooding (Peterson & Porter, 2020). The area

is expected to face extensive flooding from high tides alone by 2030 (Spanger-Siegfried et al., 2014). In the 1970s, Charleston experienced an average of two days of tidal flooding per year, an average of more than two dozen days in 2014, and is predicted to experience 180 days of flooding in 2045 (City of Charleston, 2015; Spanger-Siegfried et al., 2014). Nuisance flooding incidence has increased due to compounding effects of sea level rise, land subsidence, and urban development, and is worsening due to ongoing population growth and approval for additional development projects (Morris & Renken, 2020). The city experienced an all-time record of 89 tidal floods in 2019, translating to a flood event nearly every five days, following a previous record of 58 events in 2015 (Peterson & Porter, 2020). Tidal threshold exceedances show an upward trend since the early 1920's, and are expected to continue to increase (Figure 3.1) (NOAA & National Weather Service, 2022). These 'sunny day' flood events, which occur even without rainfall aiding in overwhelming the city's aging stormwater drainage system, inhibit tourists in historic downtown Charleston as well as the mobility of motor vehicles and foot traffic alike, resulting in closed businesses, flooded homes, and damaged infrastructure (Spanger-Siegfried et al., 2014). The city reported 80 instances of closed roads due to flooded conditions between 2015 and the summer of 2021 in the Market Street watershed alone (Figure 3.2) (City of Charleston, 2021). As sunny day flooding instances increase, the city must also contend with increasingly severe storms and heavy rains.

Currently, the most commonly used form of stormwater infrastructure in South Carolina's coastal zone is detention ponds (Vandiver & Hernandez, 2010). Out of approximately 21,500 detention ponds in coastal South Carolina, over 3,700 of them are

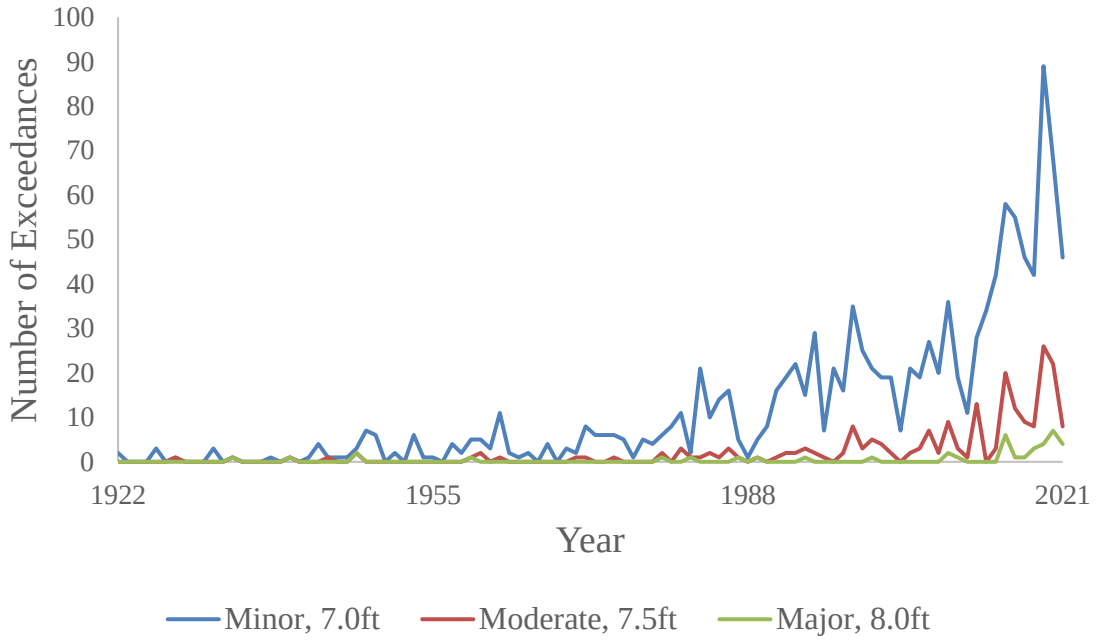

Figure 3.1: Charleston Harbor Tide Threshold Exceedances 1922-2021

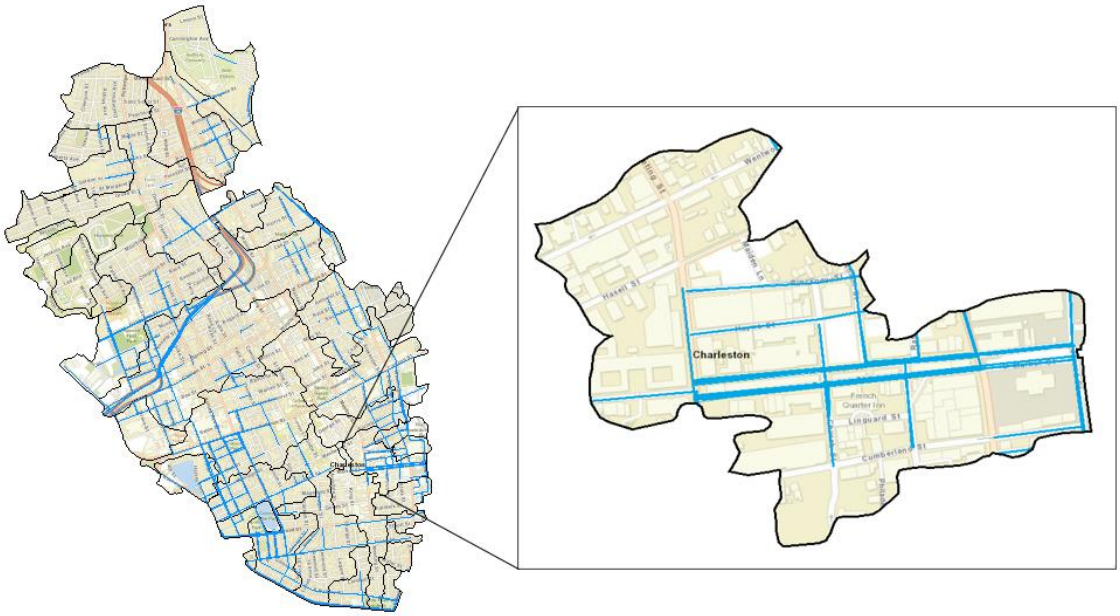

Figure 3.2: Charleston Peninsula and Market Street Watershed Flood Induced Road Closure Locations 2015-2021

in Charleston County, and are largely located in residential areas (Cotti-Rausch et al., 2019; Stormwater Ponds Research and Management Collaborative, 2014). The National Oceanic and Atmospheric Administration (NOAA) predicts up to a foot of sea level rise for United States coastlines by 2050 and a minimum of two feet by 2100 (NOAA, 2022). Detention ponds may be deemed ineffective once they are merged or submerged by this change in sea level. My preliminary analysis provides that, from overlaying NOAA sea level rise estimates (NOAA, 2019) with Charleston County's existing ponds, an estimated one-foot change in sea level will result in a loss of over 160 detention ponds, nearly 40% of which are in Residential areas (Lawyer & Goharian, 2021, 2020). As an example, Figure 3.3 illustrates at varying degrees of sea level rise inland ponds in Charleston's urban Mount Pleasant community which become ineffectual as a means of stormwater capture. Figure 3.4 shows what percentages of total stormwater ponds on residential and commercial developments are expected to be affected at different sea levels, estimating a loss of nearly 5% residential and 2% commercial ponds by 2050 and over 12% residential and 4% commercial ponds by 2100. Even without these predicted losses, it is recommended that ponds be coupled with other best management practices (BMP), such as LID strategies, to enhance removal and retention of stormwater (Vandiver & Hernandez, 2010).

The United States Federal Emergency Management Agency (FEMA) provides a National Risk Index, which indicates the potential of a community to suffer negative impacts as a result of a natural hazard based on the following equation (FEMA, 2022):

$$Risk\ Index = \frac{Expected\ Annual\ Loss * Social\ Vulnerability}{Community\ Resilience}$$

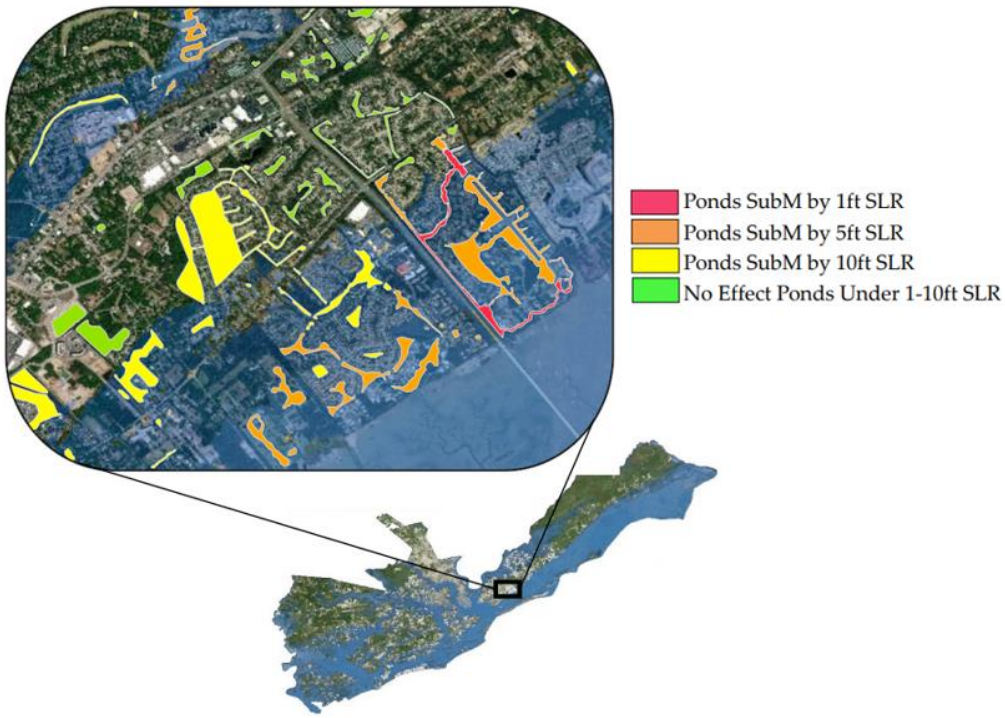

Figure 3.3: Overlay of NOAA Sea Level Rise Estimates and Existing Charleston County Stormwater Ponds

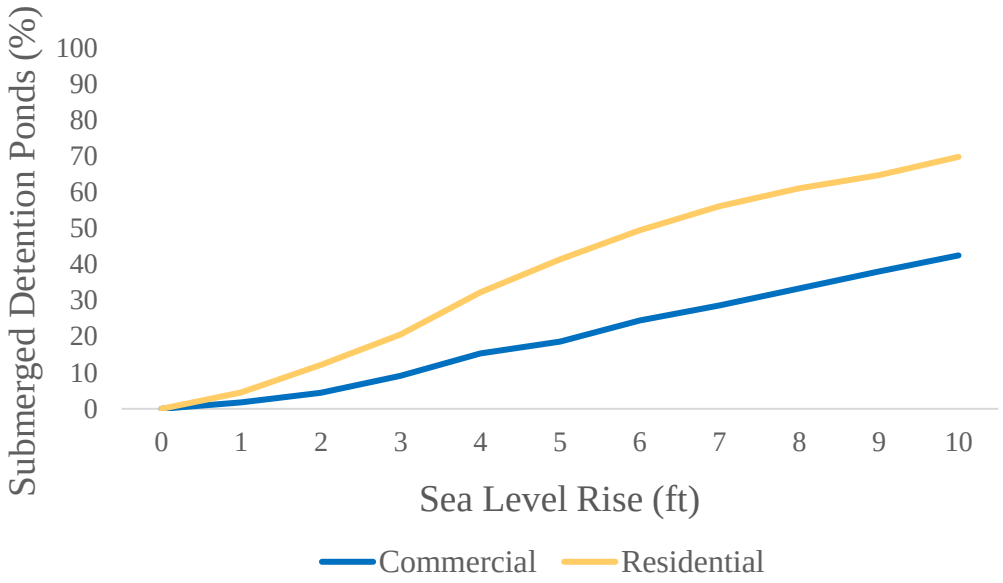

Figure 3.4: Percentage of Submerged Charleston County Residential and Commercial Stormwater Ponds According to NOAA Sea Level Rise Estimates

The study area, part of the Old Historic District, lies predominantly in Census tract 45019005100 which has a Risk Index rating of Relatively High and lies within the top 14% of counties in the country, and the top 6% of counties in the state of South Carolina (Figure 3.5). Although the area has a Relatively low Social Vulnerability score and a Very High Community Resilience score, it has a Relatively High Expected Annual Loss score, within the top 9% for the country, totaling an expected $1.2 billion.

Coastal areas also face a slew of additional engineering challenges, from high and tidally influenced groundwater tables and flat terrain to poorly draining soils. South Carolina's Coastal Plain has the second highest average annual rainfall in the United States, averaging 50 to 52 inches per year (Ellis et al., 2014; South Carolina Climatology Office, 2013). The City of Charleston's drainage system, some of which dates back to the 1800s, struggles to contend with precipitation as is, as many of the system's outfalls are tidally influenced. When the tide is high, the stormwater collection system has inadequate room for stormwater runoff, causing lengthy drainage times and unwanted surface ponding (Figure 3.6) (Charleston County, 1999). In addition to higher-than-average rainfall, coastal environments are vulnerable to storm surge damage and tropical storms, hurricanes, and other coastal hazards. The Spatial Hazard Events and Losses Database for the United States (SHELDUS) reported an aggregated property damage cost of nearly $54 billion for Charleston County between 2000 and 2019, nearly 85% of which was reportedly caused by hurricane, tropical storm, and flooding events, even though these categories accounted for only 32% of the total hazard events experienced in that time frame (Center for Emergency Management and Homeland Security, 2020). One of these

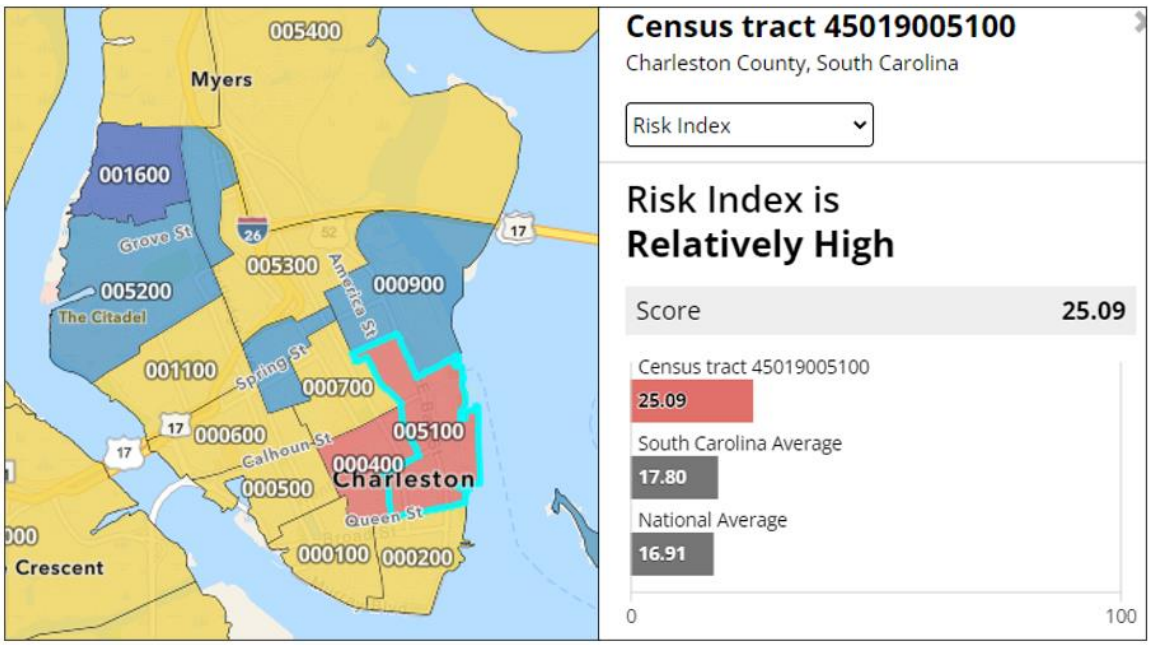

Figure 3.5: FEMA National Risk Index Map for Charleston Peninsula (FEMA, 2022)

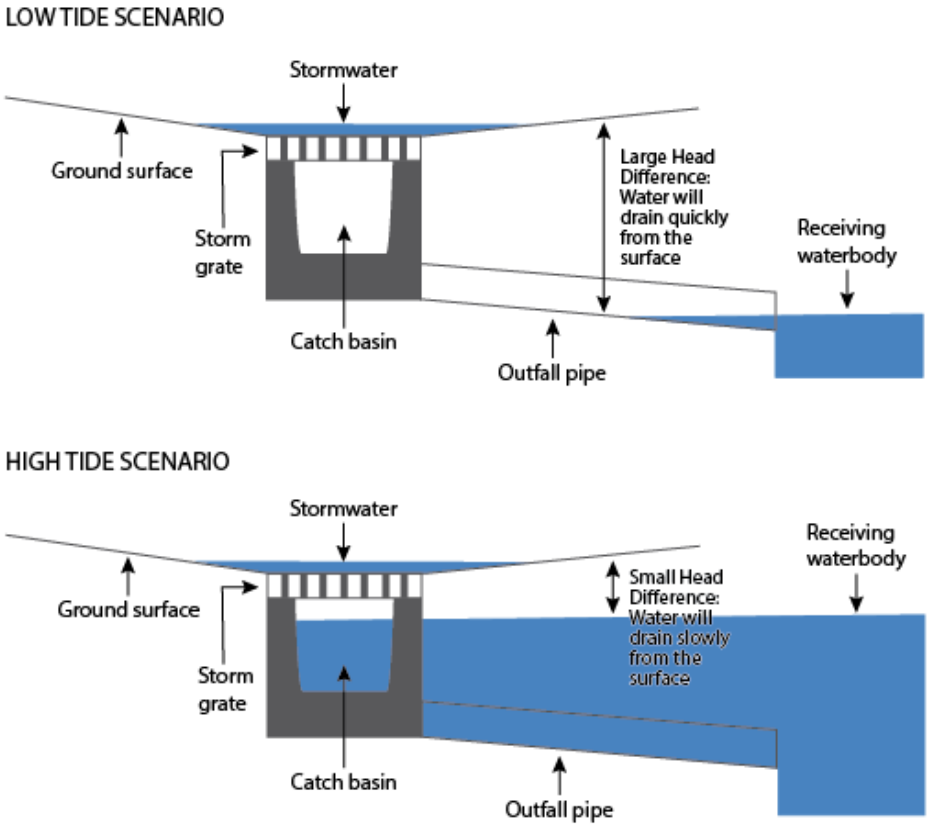

Figure 3.6: Depiction of Low and Hide Tide Effects on Stormwater Drainage (Charleston County, 1999)

events was the historic South Carolina flood, also referred to as the infamous '1,000-year flood', which occurred over the course of five days in early October of 2015 (Figure 3.7) (City of Charleston, 2015; Weather Underground, 2015). Widespread, heavy rainfall flooded central and coastal areas of the state, with many locations recording rainfall rates as high as 2 inches per hour, costing an estimated $1.5 billion in damages (NOAA, 2016). The City of Charleston experienced both extreme rainfall and tide elevations and was hit with a record-breaking 11.5 inches of rain in 24 hours on October 3rd, and more than 23 inches of rain over the course of the whole event (City of Charleston, 2015; Weather Underground, 2015). This event will serve as the case study for this research to investigate the ability of widespread, decentralized GI installation to reduce flood damage costs in urban coastal environments.

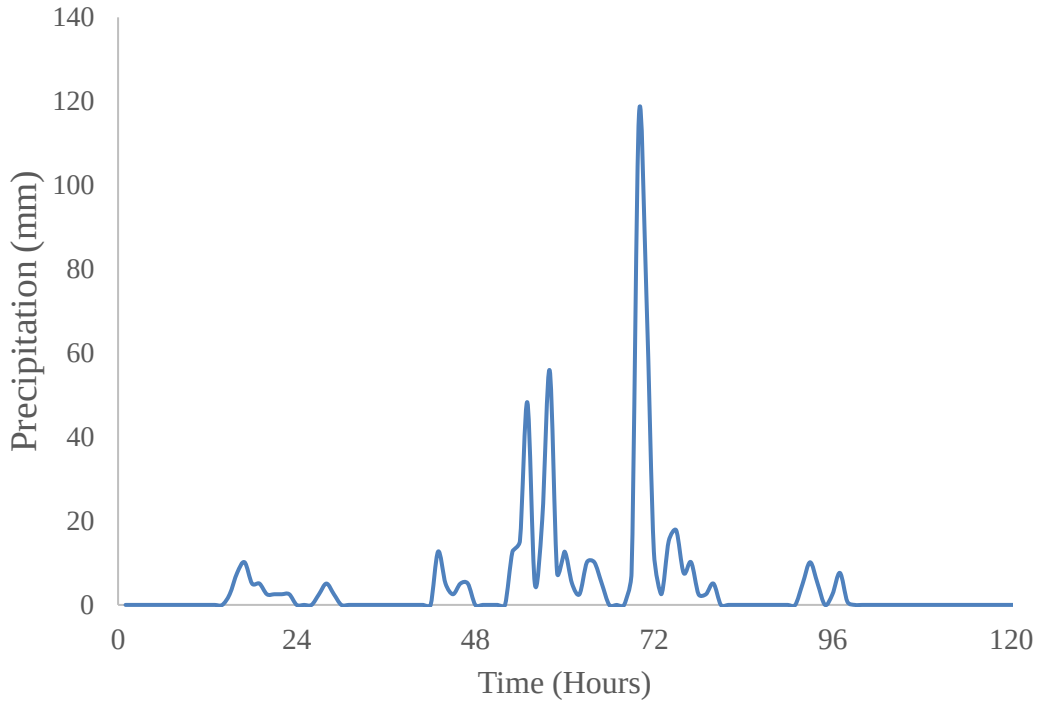

Figure 3.7: Charleston International Airport Rain Gauge Hourly Precipitation Over the Duration of the 2015 Historic South Carolina Flood Event

CHAPTER 4

METHODS

4.1 STORM WATER MANAGEMENT MODELING

The United States Environmental Protection Agency's (EPA) Storm Water Management Model (SWMM) is a widely implemented dynamic rainfall-runoff simulation model which allows the user to monitor both runoff quality and quantity over single and continuous events (USEPA & Rossman, 2015). Study areas are divided into smaller subcatchments with specified properties, including pervious and impervious fractions, depression storage depths, surface slopes, and roughness values. Overland flow can be routed between these subcatchments or through drainage system inlets connected to any variety of pipes, channels, storage units, and diversion structures. SWMM accounts for a number of hydrologic processes, including but not limited to surface water evaporation, time-varying rainfall, groundwater and drainage system interactions, and infiltration (Figure 4.1). Common applications of this software include drainage system component sizing for flood control, sizing of flood control detention facilities, studying best management practice (BMP) effectiveness on pollutant load reduction, and examining rainfall and runoff capture capabilities of low impact development (LID) strategies.

Developed by Computational Hydraulics International (CHI), Personal Computer Storm Water Management Model (PCSWMM) (CHI, 2020) is a spatial decision support system (CHI, 2022c) which enhances EPA SWMM software use by offering, among

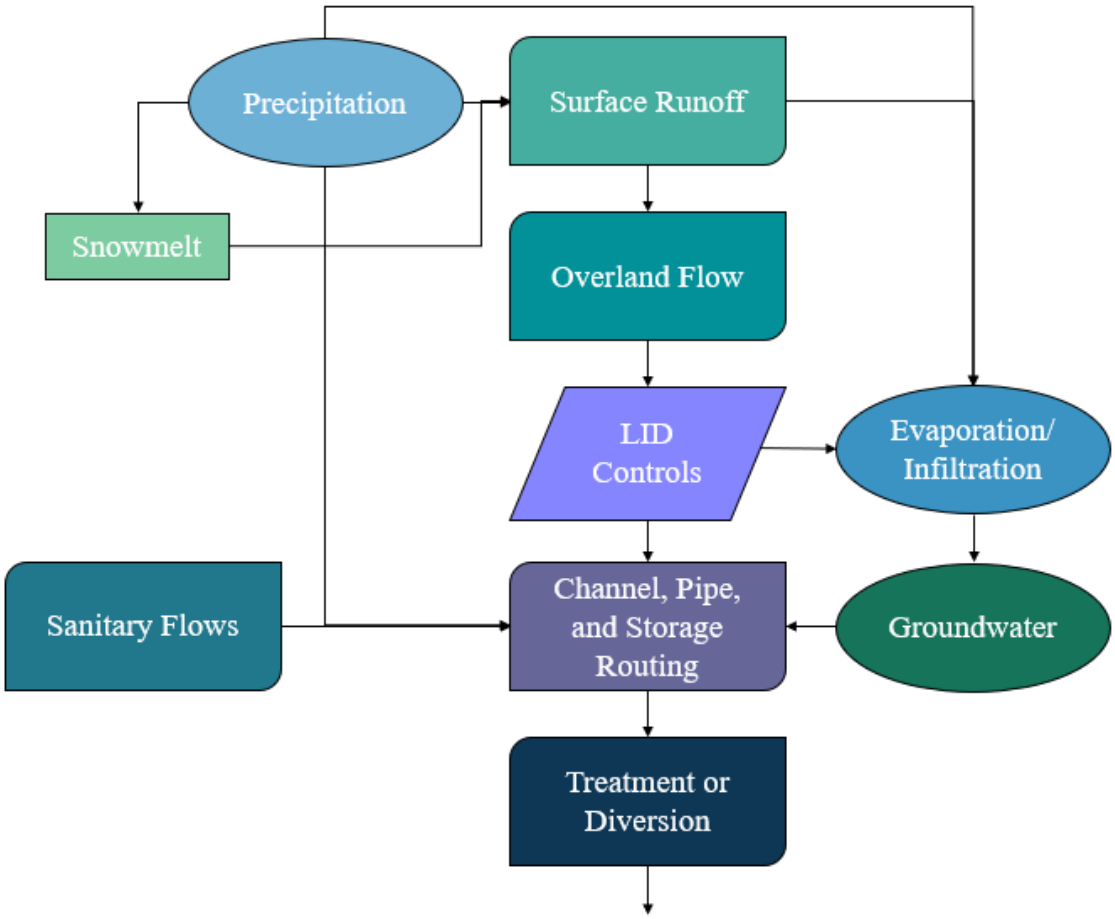

Figure 4.1: SWMM Operations (Diagram excludes pollutant processes)

other features, a graphical interface, a comprehensive Geographic Information Systems (GIS) toolset, integrated 1D-2D modeling, automated sensitivity, calibration and error analysis, and output visualization and reporting (CHI, 2022b). All models created for this research were configured in PCSWMM in accordance with requirements and suggestions within the Storm Water Management Model User's Manual Version 5.1 (USEPA & Rossman, 2015).

4.1.1 Configuring the Charleston Peninsula Model in PCSWMM

The following paragraphs describe parameter and input sources for a 1D model in PCSWMM containing rainfall, runoff, evaporation, and infiltration processes. The model runs using a 15-minute time step for the total 120-hour duration, starting analysis at time 0:00:00 October 1, 2015, and ending at 0:00:00 October 6, 2015, to allow for flood analysis during the historic flood events which took place across much of the state of South Carolina (Figure 3.7).

Charleston's peninsula, a significant portion of which makes up an area coined the Old Historic District, consists of 43 watersheds. The watershed boundary shapefile and corresponding attributes used were obtained from the City of Charleston's GIS Division Open Data (City of Charleston, 2021) and land cover information was obtained from the National Land Cover Database (NLCD) (Multi-Resolution Land Characteristics Consortium, 2011) (Figure 4.2). Raster data was imported to ArcMap v. 10.8.1 (ESRI, 2020) and a weighted average of impervious cover percentages per land use classification was used to determine the impervious cover per basin to be input in PCSWMM. Average surface slope per basin was also determined in ArcMap using a 3-meter National Elevation Dataset to be input in PCSWMM (USDA & NRCS, 2017) (Figure 4.3).

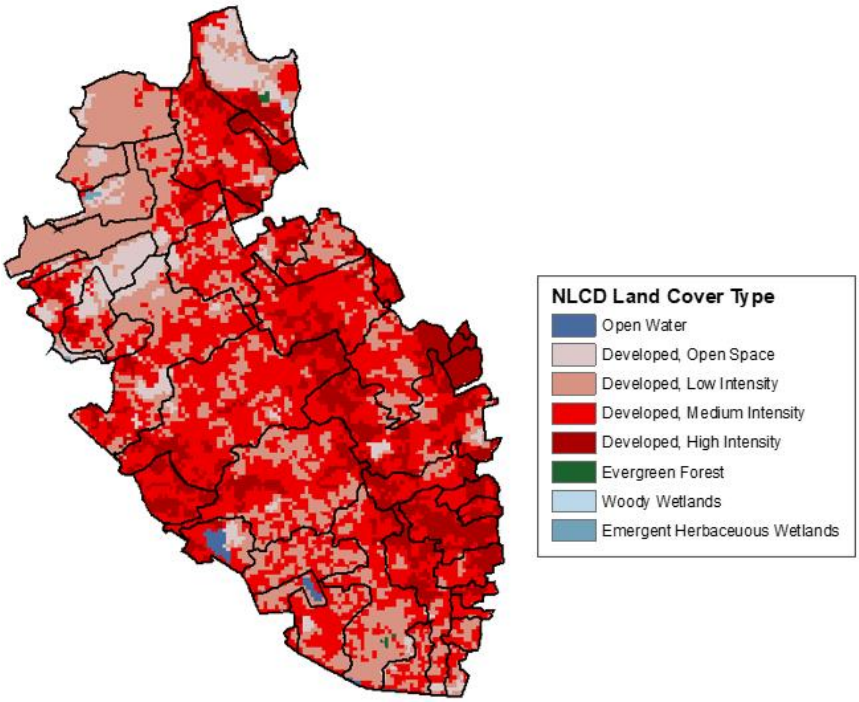

Figure 4.2: National Land Cover Database Raster of the Charleston Peninsula with Watershed Boundaries

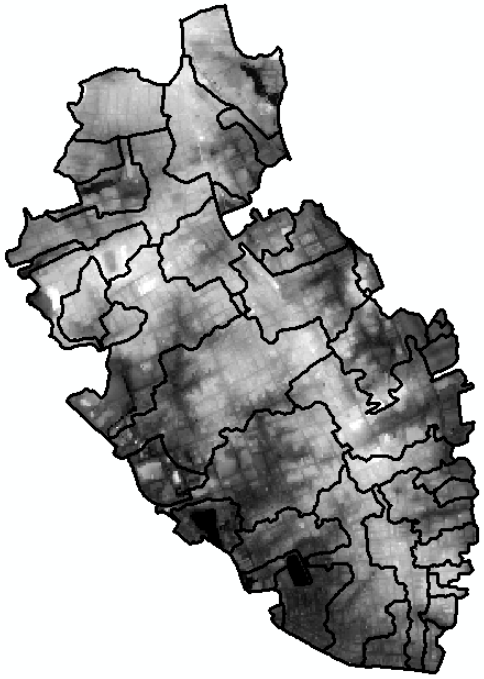

Figure 4.3: 3-Meter DEM of the Charleston Peninsula with Watershed Boundaries

All impervious and pervious areas were assigned depression storage values of 1.25mm and 2.5mm, the values corresponding to impervious surfaces and lawns, respectively (ASCE, 1992). Additionally, every basin maintains the default software assumption that 25% of the impervious area per basin has zero depression storage.

All impervious and pervious areas were assigned Manning's roughness coefficients for overland flow of 0.012 and 0.15, the values corresponding to smooth concrete and grass, respectively (CHI, 2022a). Conduits, according to the drainage map, were assigned Manning's roughness coefficients of 0.012 or 0.015 for reinforced concrete or brick, respectively (Chow, 1959). The Manning formula, which estimates mean liquid velocity in open channels, is as follows,

$$V = \frac{1}{n} R^{\frac{2}{3}} S^{\frac{1}{2}}$$

where V is mean flow velocity in meters per second, n is Manning's roughness coefficient, R is the hydraulic radius of the flow channel, and S is energy line slope.

The Modified Green-Ampt method was selected as the infiltration model for this project, and the corresponding equation is shown below (Mein, R.G & Larson, 1973; Morbidelli et al., 2018),

$$F = F_p - \psi_{av}(\theta_s - \theta_i) ln \left[\frac{F - \psi_{av}(\theta_s - \theta_i)}{F_p - \psi_{av}(\theta_s - \theta_i)} \right] + K_s(t - t_p)$$

where F denotes the cumulative depth of infiltrated water, Ψ_{av} is the capillary head at the wetting front, r is the rainfall rate, θ is the volumetric water content, for which i and s indicate initial and saturation quantities, K is the hydraulic conductivity of the soil, and t and t_p denote time and time to ponding, respectively. To determine parameters required

for PCSWMM's infiltration calculations, a soil map of the Charleston Peninsula (Bonsteel & Carr, 1904) was used to determine the approximate soil type distribution for each basin (Figure 4.4). This information was then used to assign corresponding hydraulic conductivity, suction head, and initial soil moisture deficit inputs for PCWMM per basin (Rawls et al., 1983). Groundwater processes and interactions are not considered.

Dynamic wave routing was selected as the model's flow routing method, which utilizes the Saint-Venant equations, which consist of Continuity and Momentum equations for one-dimensional flow (Chow et al., 1988). The Continuity equation states that control volume inflows and outflows are equivalent to change in control volume, and is presented in the following equation,

$$\frac{\partial Q}{\partial x} + \frac{\partial A}{\partial t} = 0$$

where Q represents flow rate, x is conduit or channel length, A is the cross-sectional area of the conduit or channel, and t is time. The Momentum equation specifies that the sum of a flow's local acceleration, convective acceleration, and pressure force is equal to the sum of gravity force and friction force, and is presented in the following equation,

$$\frac{1}{A}\frac{\partial Q}{\partial t} + \frac{1}{A}\frac{\partial}{\partial x}\left(\frac{Q^2}{A}\right) + g\frac{\partial y}{\partial x} - g\left(S_o - S_f\right) = 0$$

where S_o and S_f represent conduit slope and friction slope, respectively.

To simulate the historic rainfall events over the Carolinas in October 2015, evaporation, rainfall, and tidal data were obtained. Daily evaporation depth values were input in PCSWMM for the duration of the storm event (Climate Engine, 2021). Rainfall data was obtained in the form of hourly precipitation for the specified simulation

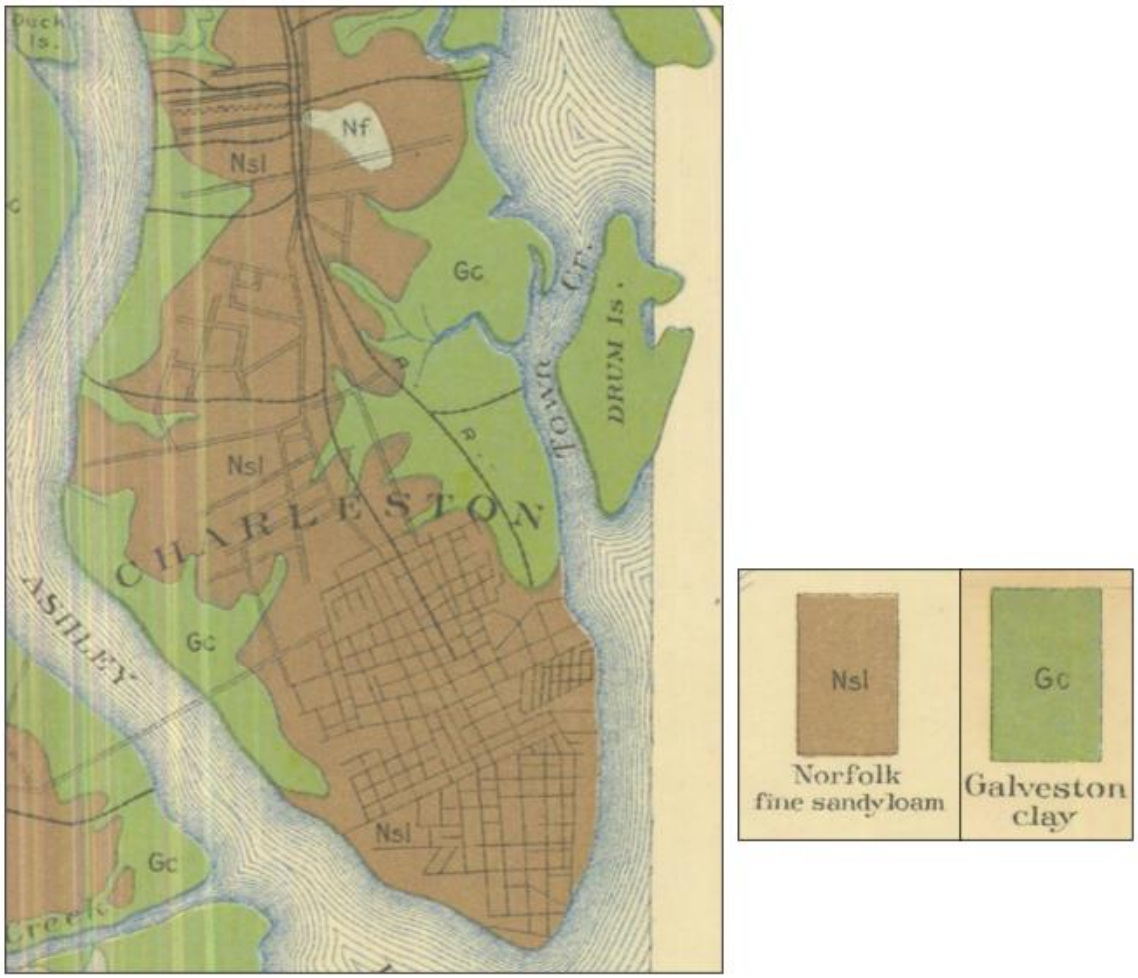

Figure 4.4: 1904 Soil Map of the Charleston Peninsula (Bonsteel & Carr, 1904)

date range from the Charleston International Airport Station (Weather Underground, 2015). This rainfall time series was assigned to each of the peninsula basins' rain gages. Corresponding water level data was obtained from the Charleston Cooper River Entrance Station and assigned to each of the peninsula basins' outfalls to account for backwater flows when applicable (NOAA, 2015).

Finally, a reduced version of the peninsula's existing drainage system was implemented. Using a map of the drainage system (Howe, 1950) which includes hand-written specifications for conduit location, sizing, shape, direction of flow, and material, conduits were manually drawn in PCSWMM and allocated their corresponding specifications (Figure 4.5). Junctions were drawn according to street intersections and locations where conduit flow was shown to meet and disperse to connected conduits in conflicting directions. Junction rim elevations were set equal to their respective location's ground elevation, and junction invert elevations were calculated by subtracting each junction's corresponding channel diameter and an assumed two feet of freeboard. Ponding at junctions was not considered. Outfalls were placed according to their location on the drainage map and assumed to empty into the peninsula's surrounding water bodies. Rather than transposing the entire drainage system, each basin has an outfall and two or fewer connected conduits, usually the largest in the basin, which serve as the collection areas for other smaller conduits in each basin. The innermost node connected to each of these outfalls in each basin is assumed to be each basin's respective outlet, or each basin's main runoff collection node. The described drainage system created in PCSWMM is shown in Figure 4.6.

Figure 4.5: 1950 Drainage Map of the Charleston Peninsula (Howe, 1950)

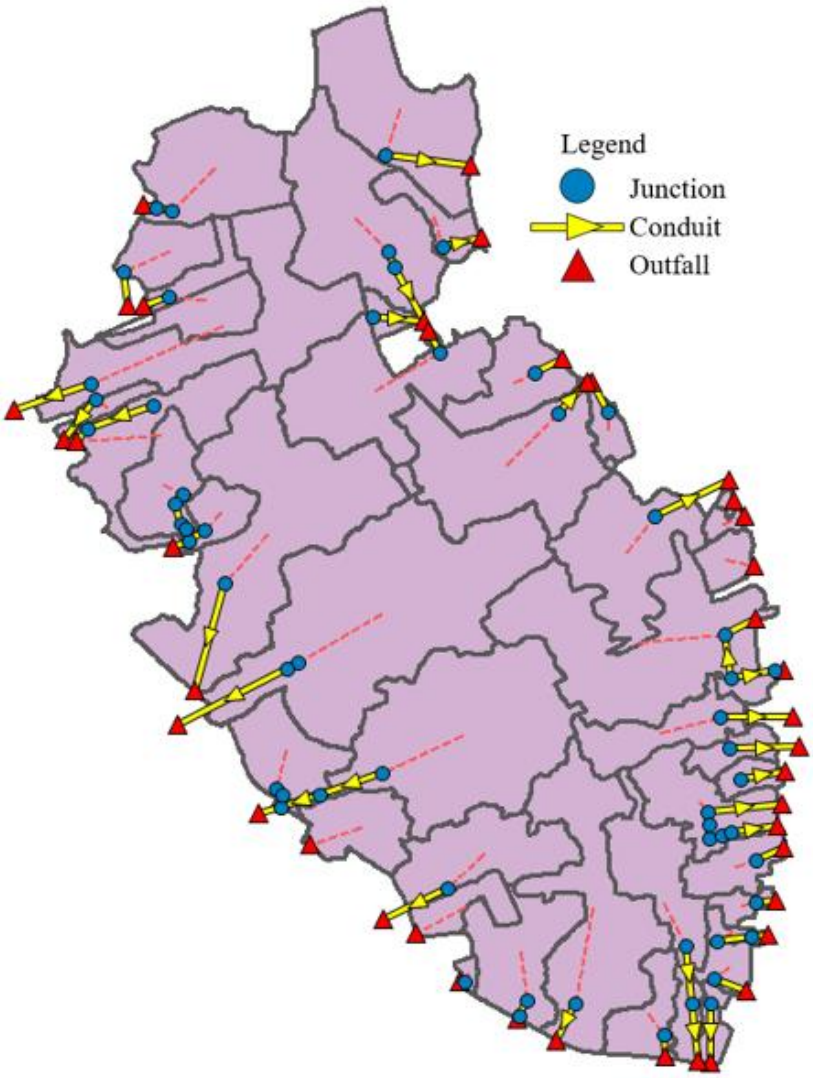

Figure 4.6: Charleston Peninsula Drainage System in PCSWMM

4.1.2 Configuring the Market Street Basin in PCSWMM

To allow for a more concentrated analysis of GI and rainfall-runoff interactions, the study area within PCSWMM was reduced to the Market Street basin only, an area which experiences high tourist visitation and frequent nuisance flooding. To create the multiple players needed for cooperative game theory analysis, the Market Street basin was divided further into five hypothetical subbasins (Figure 4.7). The division was made based on the location of Market Street itself as well as zoning information provided by the City of Charleston (City of Charleston, 2021) (Figure 4.8). The way the subbasin boundaries have been drawn, most of Market Street is contained to one subbasin and each subbasin has a unique distribution of building types provided by the zoning data. The building types within the basins are limited to Residential, Commercial, and Industrial. For the purposes of this study, the latter two categories have been combined and will be referred to as Commercial buildings, or Businesses, henceforth. All Residential type buildings are assumed to be single-family households, and the terms Residential building and Household will be used interchangeably.

While some PCSWMM parameters remained the same as described for the Charleston Peninsula model, such as Manning's roughness coefficients, soil types and infiltration parameters, depression storage depths, and water level and rainfall time series, the following were recalibrated for the Market Street Basin model. Impervious and pervious percentages for each subbasin were determined using the previously utilized NLCD raster data. Average slope for each subbasin was calculated in ArcMap, this time using a 1-meter LiDAR Elevation Dataset (USDA & NRCS, 2019) (Figure 4.9). Finally, using the previously referenced peninsula drainage map, the drainage system for the

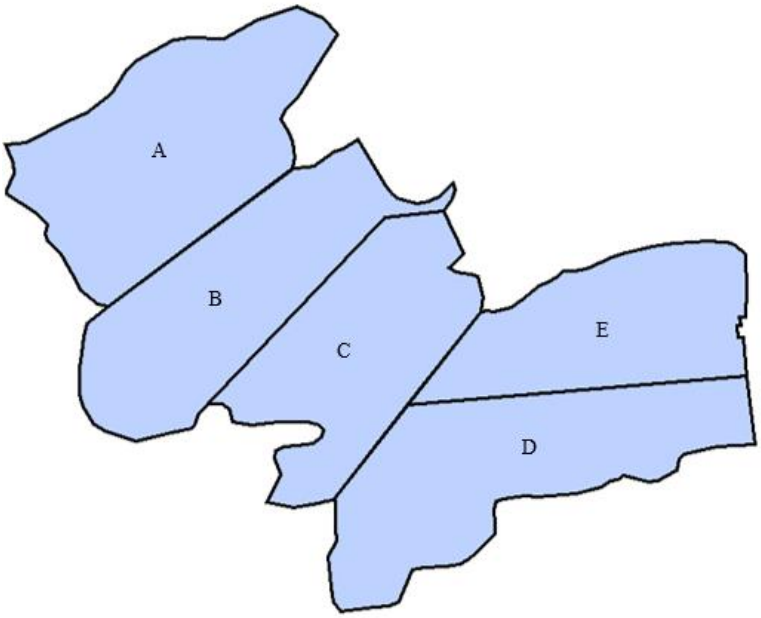

Figure 4.7: Market Street Subbasin Designations

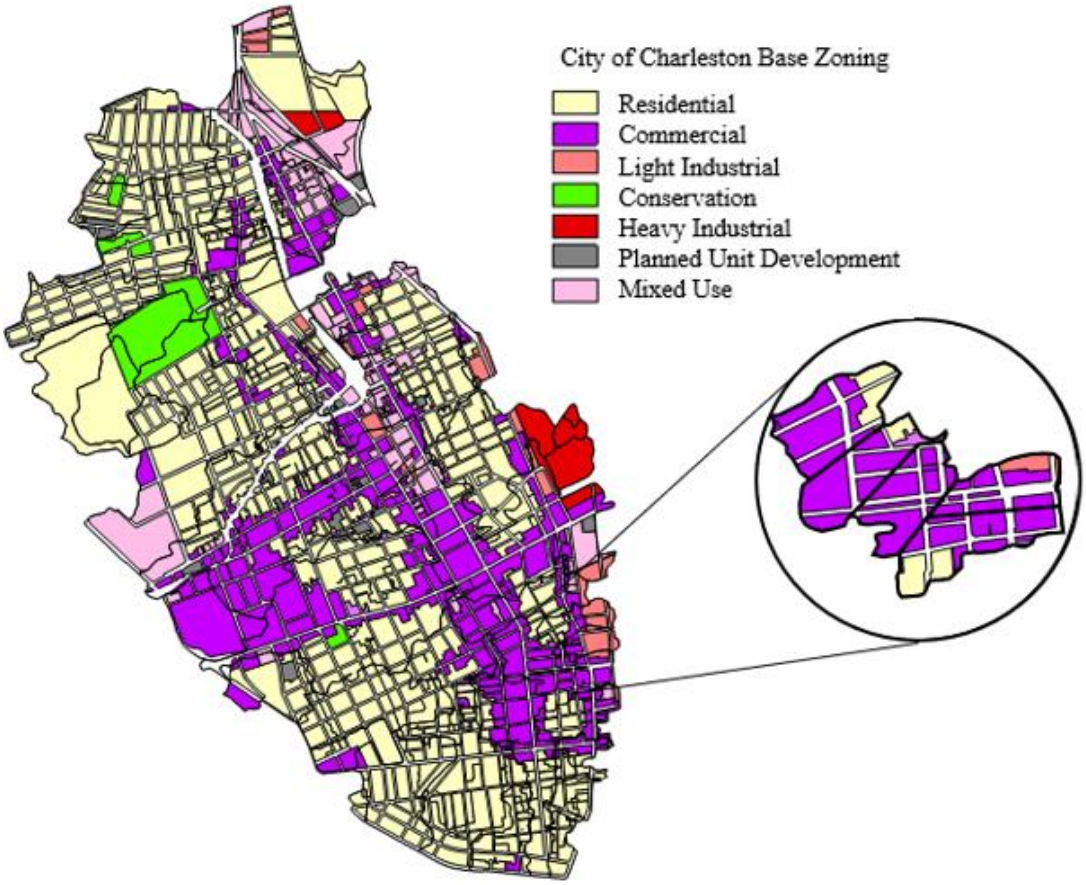

Figure 4.8: City of Charleston Zoning Designations with Watershed Boundaries

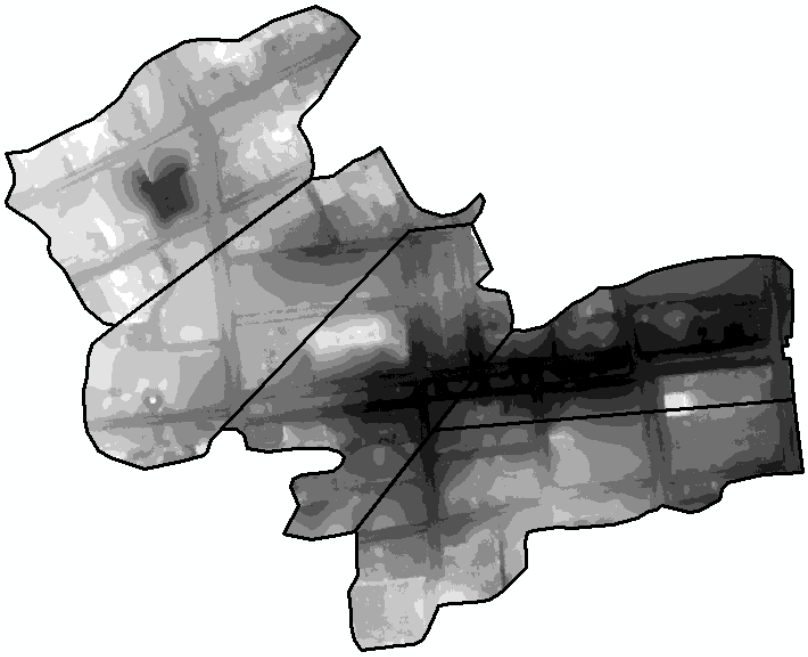

Figure 4.9: 1-Meter LiDAR Elevation Map of the Market Street Basin with Subbasin Boundaries

Market Street Basin was replicated in detail in PCSWMM to the fullest extent possible. This model is shown in Figure 4.10, Market Street Basin Drainage System in PCSWMM.

4.2 COALITIONAL GAME THEORY AND THE SHAPLEY VALUE

Game theory (Von Neumann & Morgenstern, 1944) is a means of decision analysis which allows us to model conflict, cooperation, and communication between two or more individuals whose decisions affect each other's welfare (Farooqui & Niazi, 2016; Myerson, 1991). Any situation involving two or more players can be classified as a game, where players are assumed to be 1) rational, in that they make self-interested decisions which maximize some expected game payoff measured by some utility, and 2) intelligent, in that the player knows everything about the game the modeler knows and can make any inferences about the game the modeler can make (Myerson, 1991). A game with finite players can be represented as a matrix, displaying player strategies, payoffs, and possible combinations therein. In strategic, or normal form, game Γ is represented by the following equation,

$$\Gamma = (N, (C_i)_{i \epsilon N}, (u_i)_{i \epsilon N})$$

where N is a nonempty set of game players, and each player i has a set of available strategies, C_i. The strategy profile describes possible strategy combinations that game players may choose, and C represents the set of all possible strategy profiles in the following form:

$$C = \mathop{\mathrm{X}}_{j \epsilon N} C_j$$

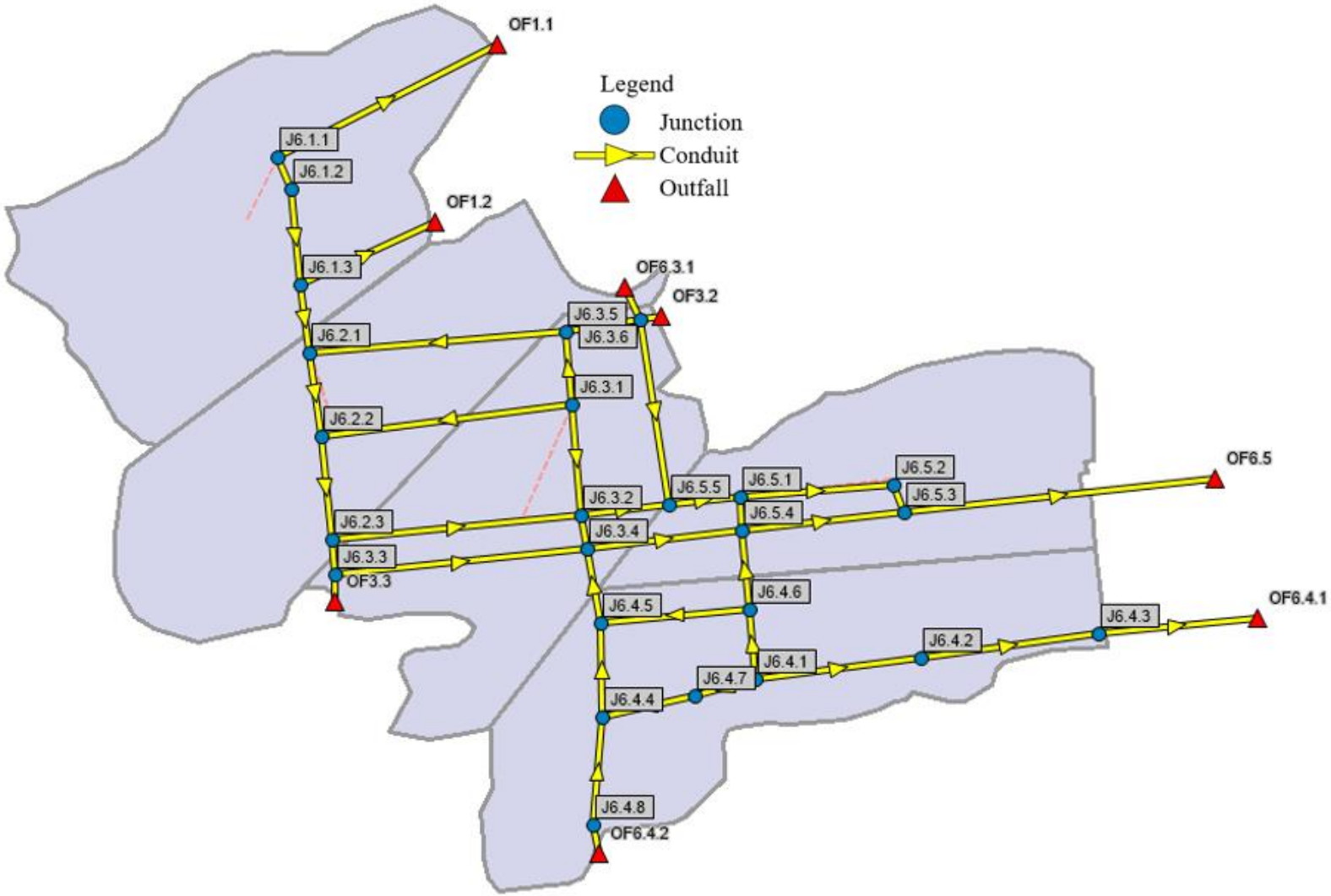

Figure 4.10: Market Street Basin Drainage System in PCSWM

For any strategy profile within this set *C* where $c = (c_j)_{j \epsilon N}$, where *c* is the implemented strategy combination, the number $u_i(c)$ represents the expected utility payoff for player *i*. (Myerson, 1991).

There are numerous game distinctions, but the most common are non-cooperative and cooperative. Intuitively, non-cooperative games involve players who compete and make independent decisions whereas cooperative games involve players who are able to make collective decisions, negotiate, and allocate the benefits of doing so (Madani, 2010). Cooperative games with three or more players must employ a theory of coalitional analysis in order to account for the formation of possible multiplayer coalitions (Myerson, 1991).

In coalitional game theory (CGT), game analysis takes into consideration that cooperative subsets, or coalitions, may form within the group of players in their entirety, referred to as the grand coalition (Myerson, 1991). CGT allows for game theorists to model the capabilities of groups of individuals rather than the individuals themselves (Shoham & Leyton-Brown, 2008). A central solution concept in CGT, the Shapley value (Shapley, 1953), associates a unique game payoff value to each coalition member (Hart, 2008). In other terms, a player's Shapley value is the player's average marginal contribution (AMC) to a game payout, weighted and summed over all possible player combinations (Molnar, 2022; Shoham & Leyton-Brown, 2008). In this sense, it is a useful measure of individual players' power in a coalitional game (Myerson, 1991). It is also used as a measure of fairness when allocating game payouts, according to symmetry, dummy player, and additivity axioms (Myerson, 1991; Shapley, 1953; Shoham & Leyton-Brown, 2008). The Shapley value of player *i*, ϕ_i, in game (*N*, *v*), can be calculated

using the following equation, in which *N* represents the grand coalition, or set of all players, *S* is a given coalition, and *v*(*S*) is the contribution of coalition *S*:

$$\phi_i(N, v) = \frac{1}{|N|!} \sum_{S \subseteq N \setminus \{i\}} |S|! \, (|N| - |S| - 1)! \, [v(S \cup \{i\}) - v(S)]$$

Included in the above equation, characteristic function *v* assigns a number value *v*(*S*), or worth, to every coalition *S*. This is possible due to the Shapley value concept's underlying assumption of the existence of transferable utility. This assumption states that game players may freely transfer units of commodity, usually in the form of money, among themselves. With each unit of commodity a player gains, their payoff increases (Myerson, 1991). The following section explains how these concepts are applied to stormwater management to inform GI spending and planning decisions.

4.2.1 Game Design and Implementation

This research seeks to employ the CGT solution concept of the Shapley value to inform GI allocation across the five Market Street watershed subbasins by observing total watershed flood damage cost reductions following the historic 2015 flood under different installation scenarios. Four unique games and two variations of one of these games were designed and implemented for the Market Street watershed model which is executed in PCSWMM.

Subbasin buildings have been categorized according to the previously presented zoning data and have been limited to either Residential (Household) or Commercial (Business) identifiers. Building counts and areas were calculated using ArcMap (City of Charleston, 2021). Additionally, GI types considered in the presented games are limited to rooftop-connected rain barrels and rain cisterns. In all presented games it is assumed

that a maximum of one rain barrel may be installed per Residential building and a maximum of one rain cistern may be installed per Commercial building. As PCSWMM does not allow users to assign LIDs to specific buildings, impervious area treated in each basin was calculated using the average size of each building type per subbasin. For example, the impervious area treated in Subbasin B by two cisterns is assumed to be equal to two times the average area of Commercial buildings in Subbasin B. Employed rainwater harvesting costs and design specification are shown in Table 4.1.

Unique games are proposed to observe the effects of varying hypothetical spending amounts, GI grants, impervious area treatment minimums, and minimum rainwater storage requirements (Table 4.2). Each game was simulated with the following conditions:

- Barrels and cisterns have no underdrains, so the barrels and cisterns employed only fill one time over the course of the simulation.
- Barrels and cisterns have a 12-hour drain delay. In PCSWMM, drain delays occur after rainfall has ceased for 12 hours.

For the storm event used in this study, barrels and cisterns drained twice over the course of the simulation; once at hour 40, at approximately 4pm on October 3rd, and again at hour 110, at approximately 2pm on October 5th. When applicable, drains were assigned a 2-inch diameter, an offset height of 6-inches, and drain coefficients were calculated according SWMM manual procedures (USEPA & Rossman, 2015). Each game was implemented in PCSWMM using the software's LID Usage Editor to place LIDs according to the game descriptions. An *n* player coalitional game produces

Table 4.1: Rain Barrel and Cistern Design Specifications and Costs

	Rain Barrel	Rain Cistern A	Rain Cistern B
Building Type	Residential	Commercial	Commercial
Size (gal)	60	2,000	5,000
Cost (USD)	115	1,680	4,300
Unit Area (sqm)	0.29	4.1	5.3
Unit Height (m)	0.9	2.4	3.9

Table 4.2: Games Executed in PCSWMM and Game Specifications

Scenario Name	Game Specifications
1. Maxed	Every Residential building has one 60-gallon rain barrel, and every Commercial building has one 2,000-gallon cistern. Subbasin total costs and quantities vary. This serves as the maximum rainwater harvesting scenario within user-set barrel size and building type restrictions.
2. Equal Storage	Each subbasin has 14 identical 2,000-gallon cisterns and each subbasin has a total cistern cost of $23,520. A quantity of 14 was selected because it is the number of Commercial buildings in the subbasin with the fewest Commercial buildings. This serves as an identical spending and rainwater storage scenario across all subbasins.
3. 20% Impervious Area Treated (IAT)	Each subbasin treats a minimum of and as close to 20% of its impervious area as possible using only 2,000-gallon cisterns. Subbasin total costs and quantities vary. This serves as a feasibility test for GI rebate programs which only consider treated area requirements.
4. Maxed, 5,000-gallon Cisterns in Subbasin E	Maxed (Game 1) scenario funding for Subbasin A (cisterns only) is transferred to Subbasin E and is added to Subbasin E's existing Maxed scenario funding. With this additional funding, Subbasin E replaces its 16 2,000-gallon cisterns with 16 5,000-gallon cisterns. This serves as a suggested scenario.
5. Maxed, Rebate A	Same as Maxed (Game 1) scenario, but subbasins are reimbursed $5,000 for every 10% of impervious area treated.
6. Maxed, Rebate B	Same as Maxed (Game 1) scenario, but subbasins are reimbursed $7,000 for every 15% of impervious area treated.

2^{n-1} possible player combinations, therefore each game required 31 model runs in PCSWMM, each simulating different subbasin combinations of LID installation. PCSWMM produced the total flood volumes resulting from each scenario, which were used to calculate total flood damage costs for each subbasin and the whole Market Street watershed system. This process is discussed in detail in Section 4.3.

In terms of the Shapley solution concept, the contribution value of each subbasin coalition, $v(S)$, is represented by each subbasin's capacity to reduce flood damage cost for the entire Market Street watershed. Coalition S can consist of any combination of players, represented by the five Market Street subbasins. These subbasins have been designated identifiers A through E (Figure 4.7). If a subbasin is in a coalition, it is assumed to have participated in some form of LID implementation. For example, coalition A describes a scenario in which Subbasin A installed LIDs according to game rules, and Subbasins B, C, D, and E did not. Hence, the Shapley value of Subbasin A, ϕ_A, represents the average marginal contribution (AMC) of Subbasin A to the total system flood damage cost reduction after considering its contribution to the system in every possible coalition combination. The grand coalition will henceforth refer to coalition ABCDE, the player combination in which all subbasins participate in LID installation, and alternately, the empty set describes the baseline scenario in which none of the players partake in LID installation.

The Shapley value serves as a metric of power for each subbasin, illustrating which subbasins contribute most to overall system flood damage reduction, informing future planning decisions, either in terms of where GI advocacy efforts should be focused, incentives offered, or LID projects installed. Additionally, in running every

combination of subbasin participation in GI installation, it is possible to compare cost effectiveness for each subbasin by observing GI cost per basin and individual subbasin flood damage cost reductions.

4.3 FLOOD DAMAGE COST CALCULATIONS

Shapley values were calculated using building flood damage cost reductions as a metric to inform LID placement decisions. These costs were estimated using PCSWMM Total Flood Volume outputs and the Federal Emergency Management Agency's (FEMA) HAZUS Flood Model Depth-Damage Curves (FEMA, 2021) to estimate Residential and Commercial building total repair costs (TRC) per subbasin and then summing them for the Market Street watershed (Figure 4.11). To establish the empty coalition TRC, or the baseline TRC, Total Flood Volume for all junctions in each Market Street subbasin were summed to determine the total flood volume with no LIDs in place. To approximate subbasin flood depths, the following equation was used:

$$Flood\ Depth_i = \frac{Total\ Flood\ Volume_i}{Area_{Basin(i)} - Area_{Buildings(i)}}$$

Once subbasin flood depths were established, all buildings within each subbasin were assumed to experience a uniform level of flooding. Residential TRCs per subbasin were calculated by multiplying the total Residential building area per subbasin by the corresponding HAZUS Depth-Damage Curve (DDC) percent damage value assigned to Single Family Household, Luxury, No Basement homes and the HAZUS designated repair cost per flooded square foot (Table 4.3). Commercial building TRCs were calculated following the same procedure, using HAZUS DDC values and repair costs for Entertainment and Recreation buildings. These damages were then summed for each subbasin and ultimately the entire Market Street Basin to find TRC for the system. This

Table 4.3: HAZUS Repair Costs per Square Foot

Building Category	HAZUS Building Type	Repair Cost per Square Foot (USD)
Residential	Single-Family Household, Luxury, No Basement	187.14
Commercial	Entertainment and Recreation	195.68

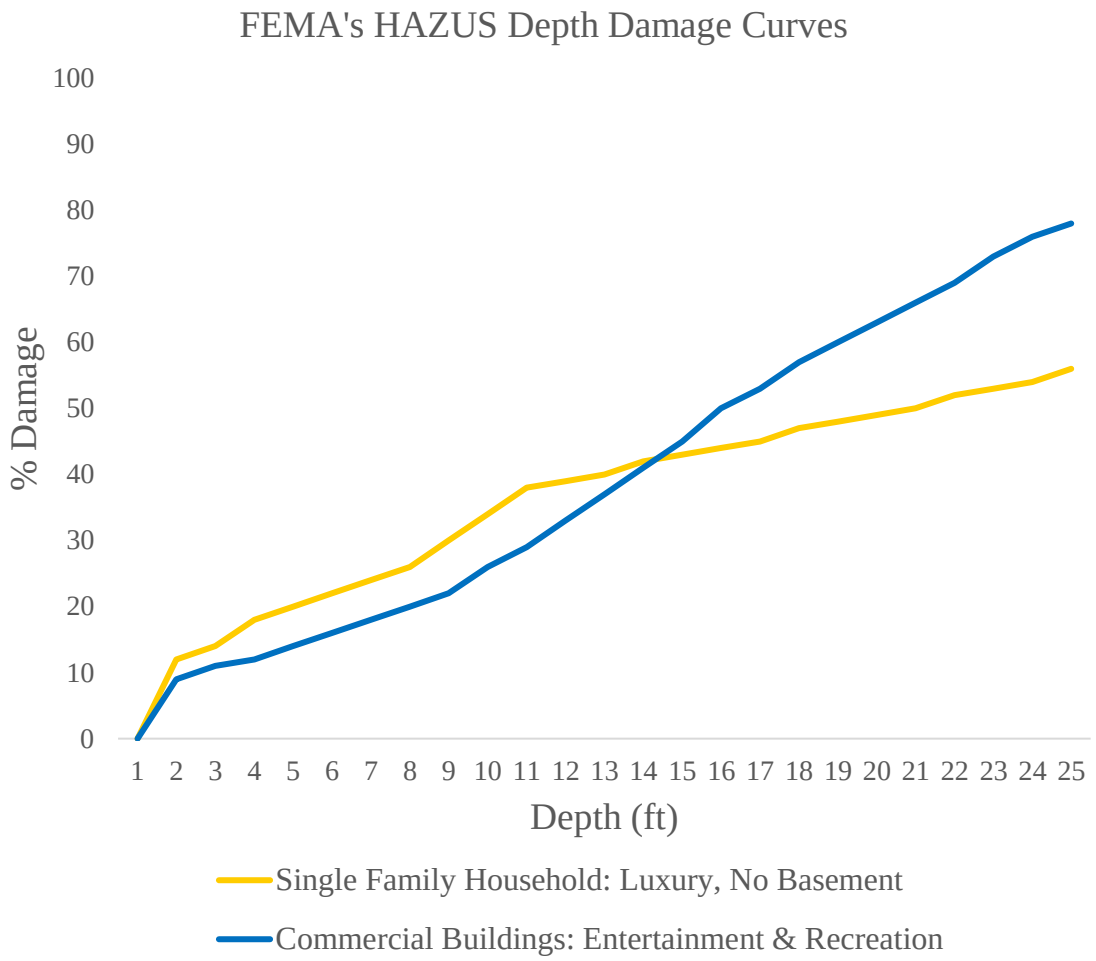

Figure 4.11: FEMA's HAZUS Depth-Damage Curves for Specified Residential and Commercial Building Type

procedure is summarized in the following equation:

$$Market\ Street\ Basin\ TRC = \sum (Building\ Area_{Commercial(i)} * \frac{DDC\ Value}{100} * Repair\ Cost_{Commercial} + Building\ Area_{Residential(i)} * \frac{DDC\ Value}{100} * Repair\ Cost_{Residential})$$

This process was repeated for every coalition combination for every game scenario. To calculate subbasin TRC reduction for each of these instances, each TRC for every coalition combination for every game was subtracted from the baseline TRC. These values were used to calculate subbasin Shapley values for each game.

CHAPTER 5

RESULTS

5.1 MODEL VALIDATION

The 1D Charleston Peninsula model configured in PCSWMM, later used to develop the PCSWMM Market Street watershed model, was validated by comparing flow rate results for a segment of the peninsula's drainage network to those achieved in a fully coupled compound flood Interconnected Channel and Pond Routing (ICPR) model for the Charleston peninsula under identical rainfall and tide conditions (Tanim & Goharian, in review). The ICPR is has been calibrated and validated based on historical data and flood information for the Charleston peninsula, and thus, was used as a benchmark to validate the PCSWMM model presented in this study.

ICPR employs a triangulated irregular network that preserves complex land use features and basin hydrology at very fine temporal and spatial scales, whose drainage network components include tidal creeks, tidal channels, wetlands, underground sewer networks, and detention ponds. The Charleston ICPR model employed 0.5-meter DEM and Digital Surface Model (DSM) data to account for overland flow representation and building layout. ICPR simulates compound flooding and was validated using South Carolina Department of Transportation flood induced road closure data. Model efficiency comparing this data with the ICPR model's detected road closure locations is 98.35% for the historic South Carolina flood event and 100% for a nuisance tidal flooding event, further validated by United States Geological Survey high water mark data.

The Charleston peninsula model configured in PCSWMM was validated by comparing flow rate results for the Market Street watershed and conduit discharges to those obtained by the peninsula model built in ICPR. The ICPR model is used as a benchmark as there is no water level, discharge, or velocity information available for Charleston, including the Market Street watershed. Conduit location is shown in Figure 5.1, and flow rate comparisons over the course of the 2015 South Carolina historic flood event are shown in Figure 5.2. In general, the flow rate is very similar to the ICPR model. However, the main differences which occur largely at the beginning of the run are due to 1) ICPR's distributed modeling of hydrological processes as well as 2D surface water modeling, whereas PCSWMM is essentially a lump and 1D hydrological model, thus model parameters are spatially and temporally constant over the run time, and 2) ICPR models the whole system, while the PCSWMM has static boundary conditions. Thus, water cannot leave the system and enter other watersheds and instead discharges to the sea, as a result causing all runoff to drain to the limited number of pipes. Moreover, PCSWMM Charleston peninsula simulations reported a runoff continuity error of 0.43% and -0.23% respectively and Market Street watershed simulations reported a runoff continuity error of -0.66% and -0.3% respectively. Thus, the PCSWMM is capable of simulating flood scenarios, in particular the historic 2015 flood for the Charleston peninsula and Market Street watershed as it presents very similar results to the benchmark model.

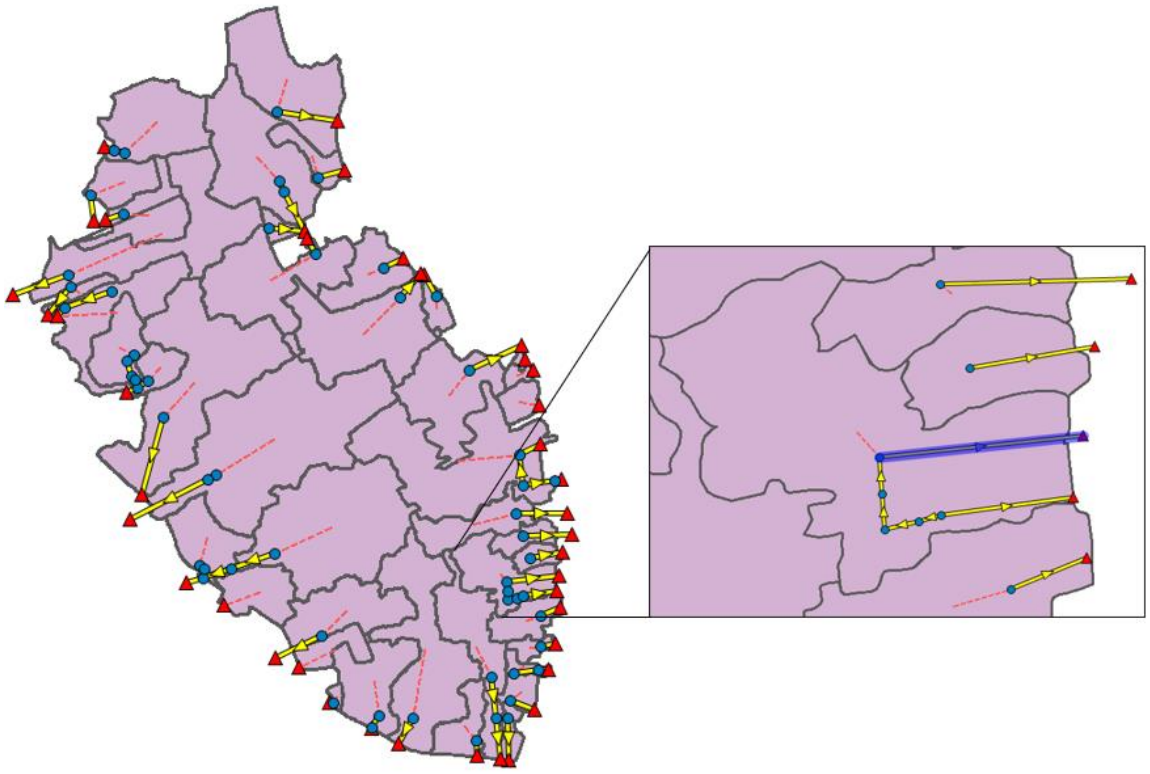

Figure 5.1: Conduit Used for ICPR Flow Rate Comparison and PCSWMM Model Validation

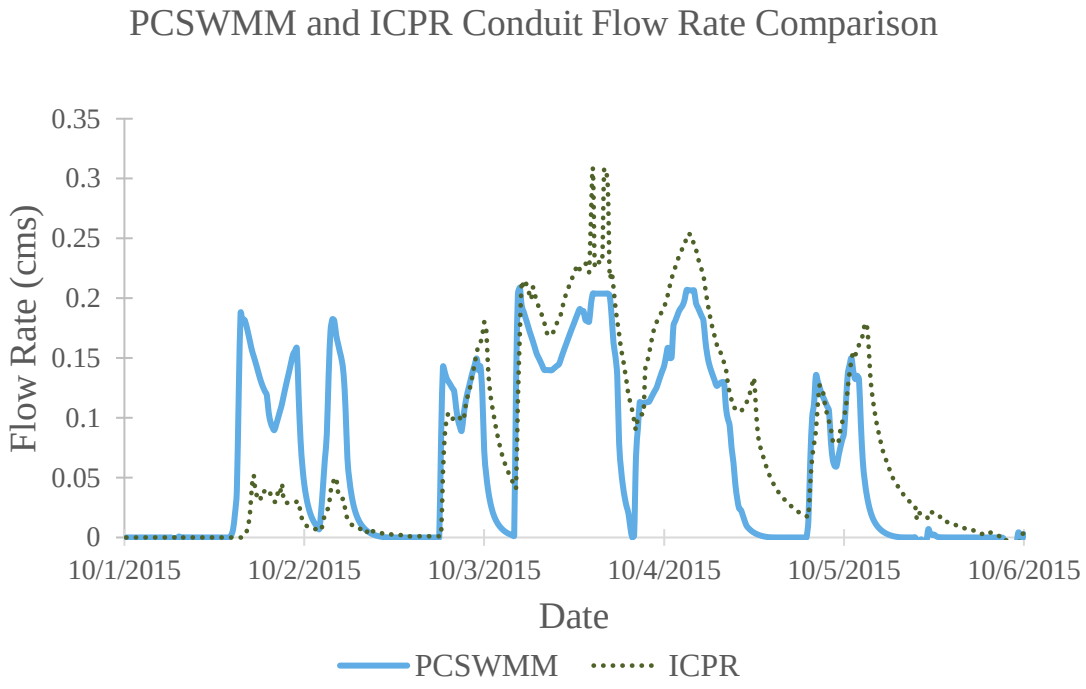

Figure 5.2: Comparison of ICPR and PCSWMM Market Street Conduit Flow Rate for Historic 2015 South Carolina Flood Event

5.2 BASELINE RESULTS

5.2.1 Subbasin Characteristics

Characteristics of each of the Market Street subbasins related to area and building density are summarized in Table 5.1 and Figures 5.3, 5.4, and 5.5. Building counts and areas per subbasin are listed in Table 5.2 and are illustrated in Figures 5.6 and 5.7. A map of Residential and Commercial buildings is provided in Figure 5.8. NLCD land cover distributions are summarized in Table 5.3 and Figure 5.9. Developed land cover, in terms of impervious area covered by buildings and edge of pavement (EOP) (City of Charleston, 2021) are listed in Table 5.4 and illustrated in Figures 5.10 and 5.11. Figure 12 provides a map of buildings and EOP cover. This information was required to create game theory games which met the physical restraints of each subbasin, as well as to calculate potential treated area in PCSWMM for each subbasin under different LID conditions. All subbasin properties provided in this section will lend physical context to and be discussed alongside Shapley value results.

5.2.2 Baseline Total Repair Cost

Total Repair Cost (TRC) for the baseline scenario, the empty set in each coalitional game in which no LIDs have been in installed in any subbasins, was estimated using the described flood damage cost calculation methods described in section 4.3 and rounding up to the nearest dollar. The TRC for the baseline scenario is estimated to be $10,357,415. Results for the baseline scenario run in PCSWMM, shown in Figures 5.13 and 5.14, indicate that flood volume was not distributed evenly across the subbasins, as Subbasin C accounted for 35% of the total volume, followed by 30% in Subbasin E, and

Table 5.1: Area and Building Distributions for Market Street Watershed Subbasins

Subbasin	% Area of Market Street Watershed	% Total Buildings in Market Street Watershed	% Building Area in Market Street Watershed
A	23	42	24
B	20	17	24
C	18	11	19
D	22	18	17
E	16	13	16

Table 5.2: Number and Area per Building Type per Market Street Subbasin

Subbasin	Total Residential Buildings	Total Residential Building Area (sqm)	Total Commercial Buildings	Total Commercial Building Area (sqm)
A	27	5,920	25	27,958
B	4	1,420	17	33,219
C	0	0	14	27,078
D	8	2,819	14	20,882
E	0	0	16	22,689

Table 5.3: Distribution of NLCD Land Cover Types per Market Street Watershed Subbasin

Subbasin	Developed, High Intensity	Developed, Medium Intensity	Developed, Low Intensity
A	50.6	49.4	0.0
B	58.0	42.0	0.0
C	80.9	19.1	0.0
D	50.0	47.4	2.6
E	88.0	12.0	0.0

Table 5.4: Developed Land Cover Type Distribution per Market Street Watershed Subbasin

Subbasin	% Impervious Area	% Impervious Area Consisting of:		
		Buildings	EOP	Other
A	89.6	48	39	13
B	91.2	57	41	2
C	96.0	47	41	12
D	88.7	36	48	16
E	97.5	43	40	17

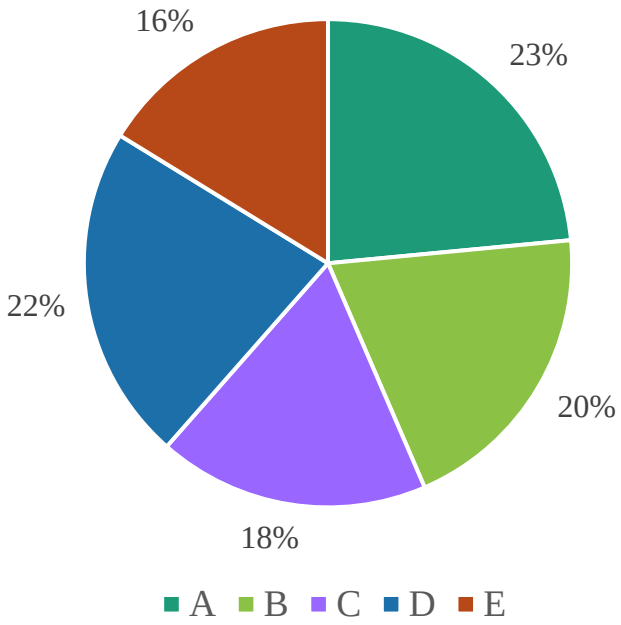

Figure 5.3: Distribution of Total Market Street Watershed Area per Subbasin

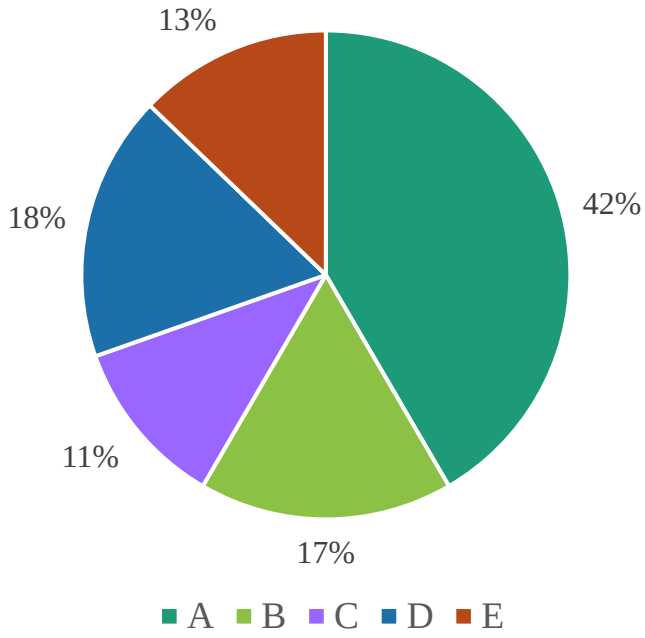

Figure 5.4: Distribution of Total Market Street Watershed Buildings per Subbasin

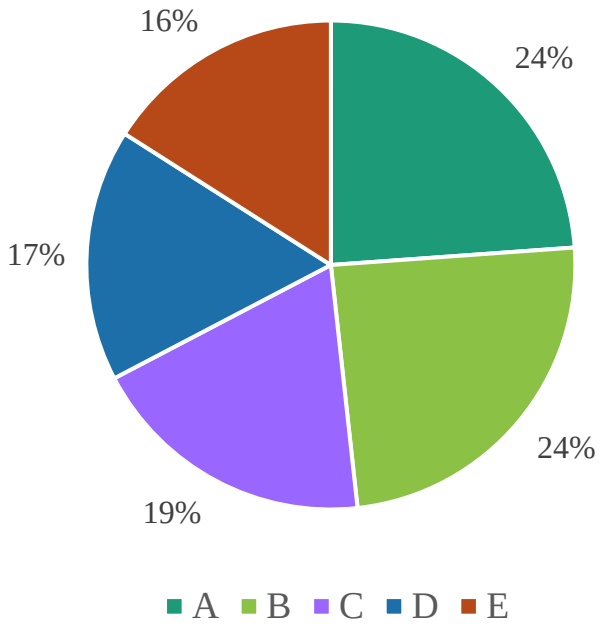

Figure 5.5: Distribution of Total Market Street Watershed Building Area per Subbasin

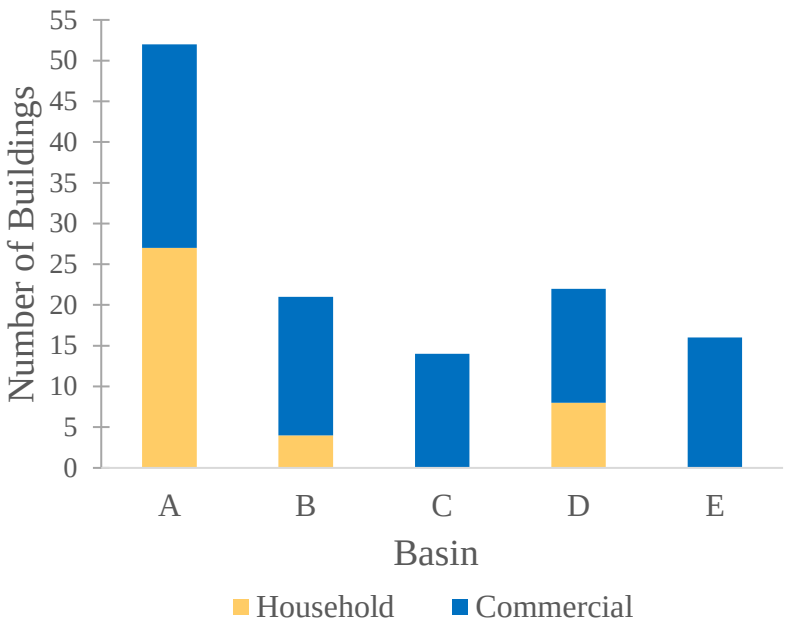

Figure 5.6: Distribution of Building Number and Type per Market Street Watershed Subbasin

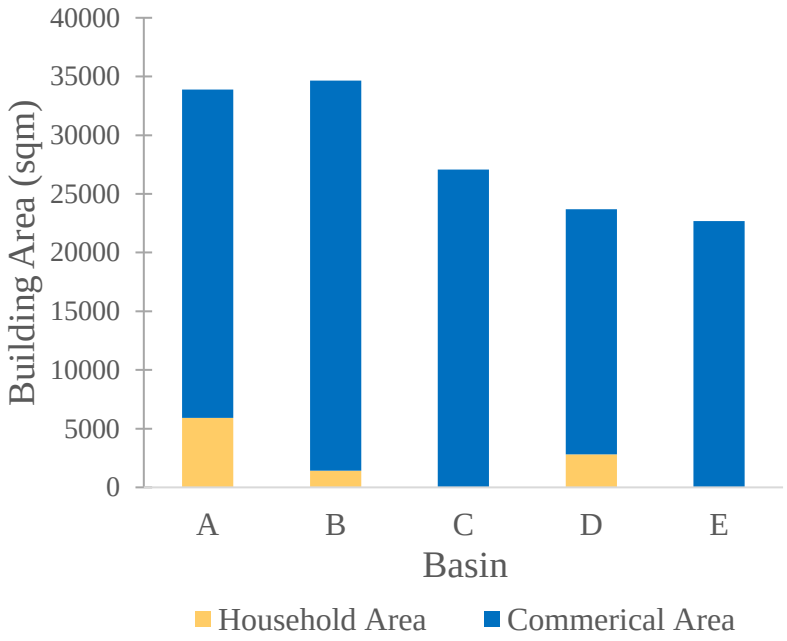

Figure 5.7: Distribution of Building Area and Building Type per Market Street Watershed Subbasin

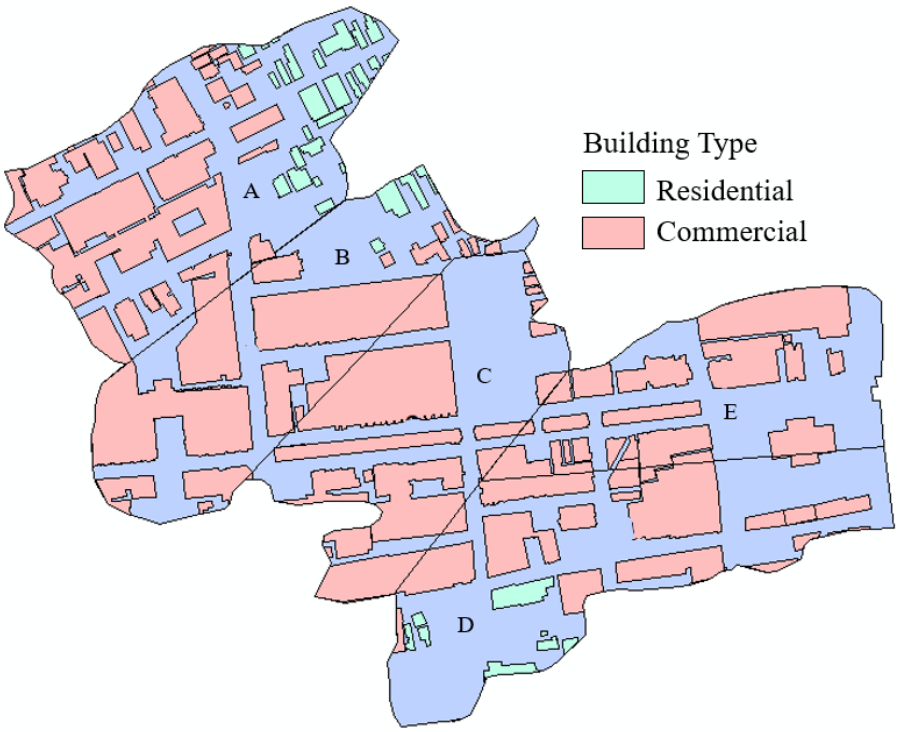

Figure 5.8: Map of Residential and Commercial Buildings per Market Street Subbasin

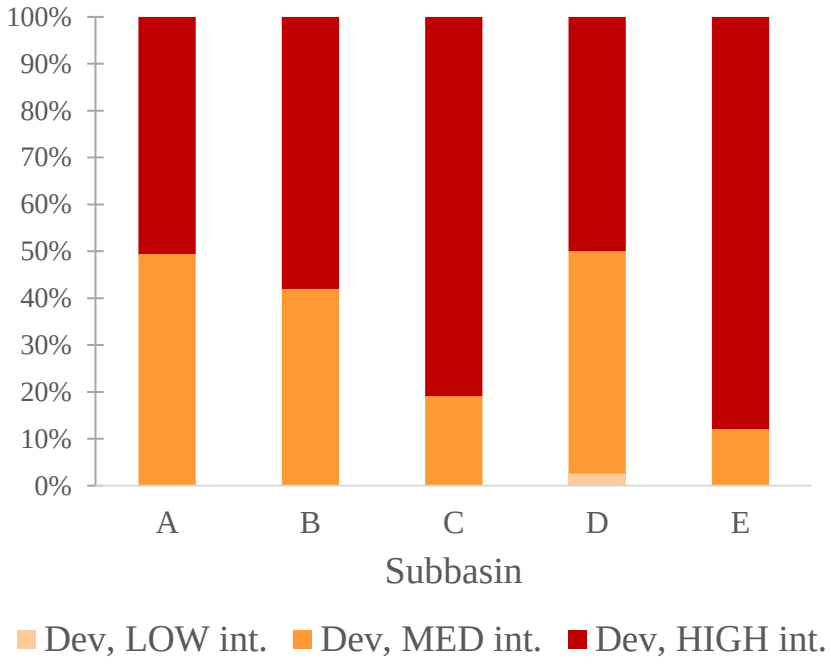

Figure 5.9: NLCD Land Cover Distribution per Market Street Watershed Subbasin

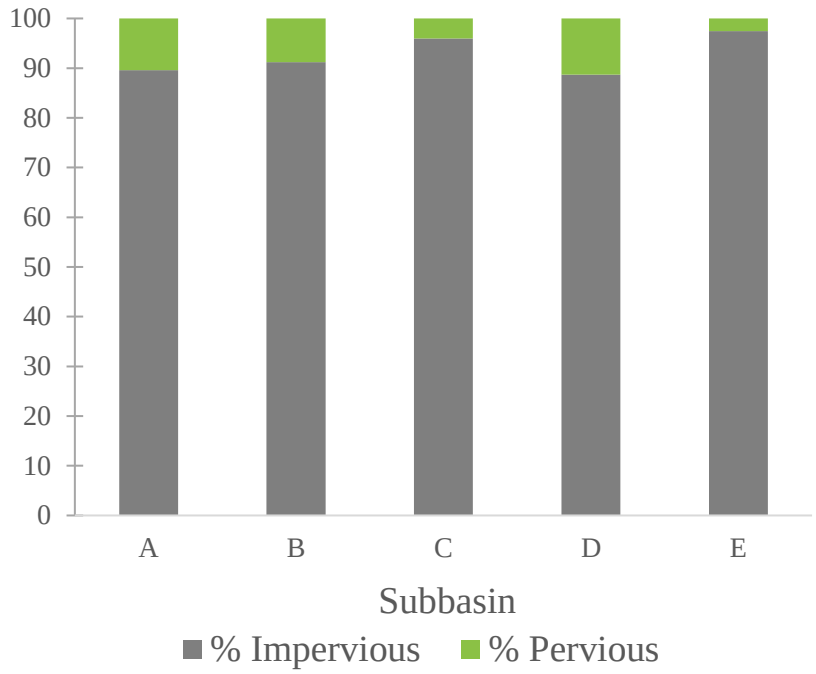

Figure 5.10: Impervious and Pervious Area Distribution per Market Street Watershed Subbasin

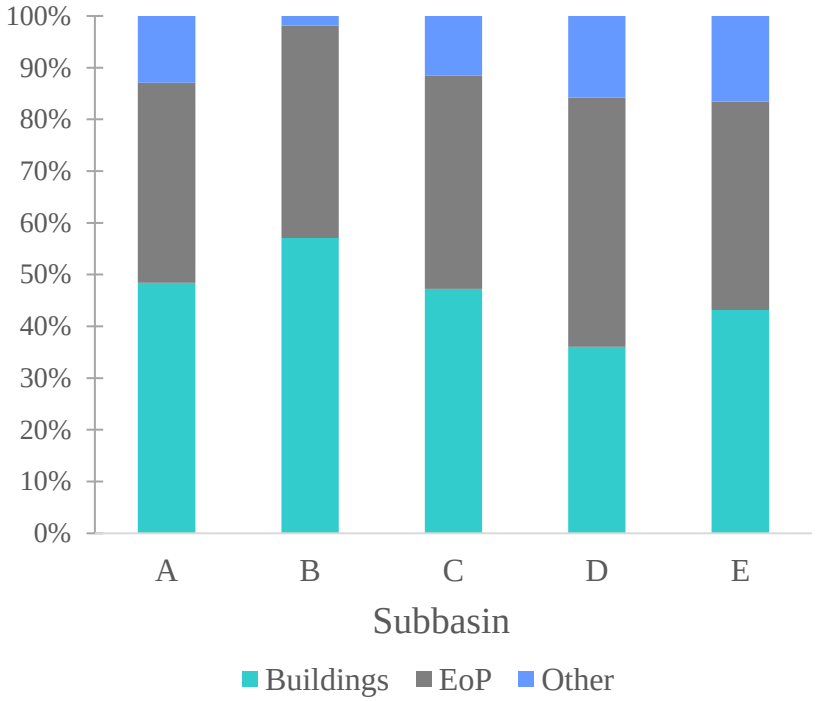

Figure 5.11: Developed Land Cover Distribution per Market Street Watershed Subbasin

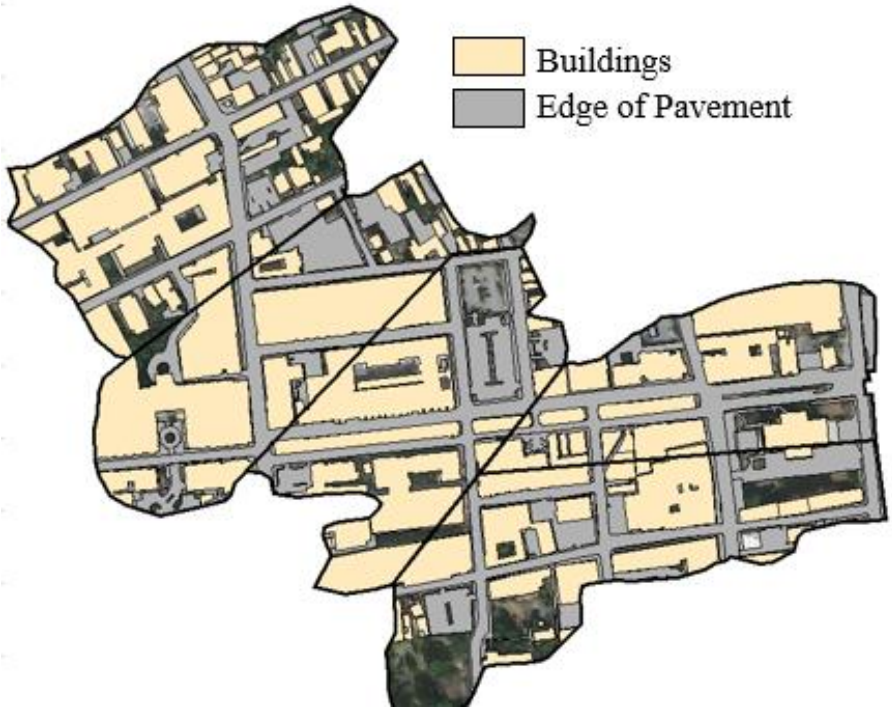

Figure 5.12: Map of Market Street Watershed Building and Edge of Pavement Cover

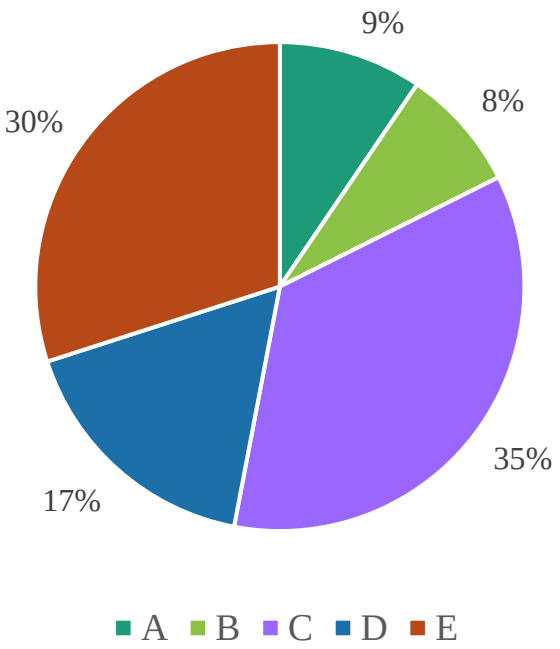

Figure 5.13: Baseline (Empty Set) Subbasin Flood Volume Distribution

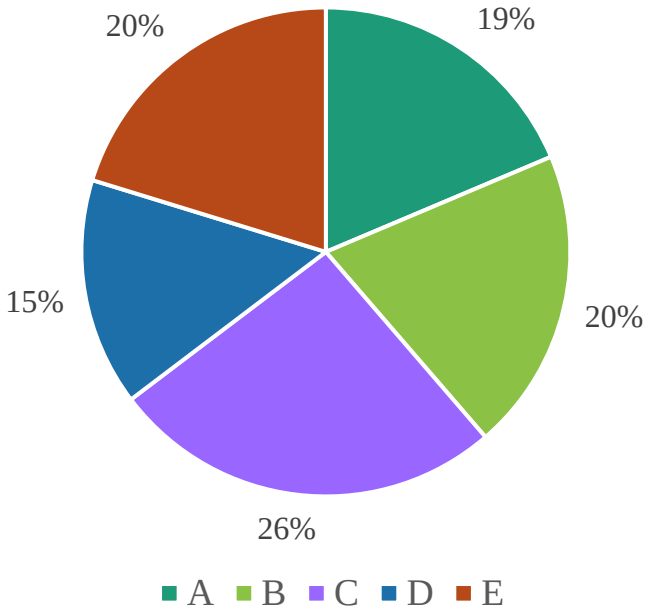

Figure 5.14: Baseline (Empty Set) Subbasin Flood Damage Cost Distribution

17%, 9%, and 8% in Subbasins D, A, and B, respectively. Thus, Subbasin C bore the highest flood damage cost, accounting for 26% of the TRC, followed by Subbasin B and E accounting for 20% each, Subbasin A for 19%, and Subbasin D for 15%. Differences in shares of flood volume versus flood damage cost are the result of different land use types as well as variation in number and type of buildings in each subbasin. 93% of the watershed TRC is attributed to Commercial building costs, mostly attributed to Subbasins C and E, as these subbasins had the highest flood volumes. Neither subbasin contains Residential buildings, and the utilized HAZUS Commercial repair cost per square foot exceeds that of Residential buildings. TRC reductions will be calculated for all game coalition combinations by subtracting each coalition's TRC from the baseline TRC and will be used to measure subbasin Shapley values.

5.3 GAME ANALYSIS: SHAPLEY VALUE AND COST COMPARISONS

Shapley values for each developed game, previously described in Table 4.2, will be presented in this section. In the first game scenario, "Maxed", all Households install one 60-gallon barrel, and all Businesses install one 2,000-gallon cistern. Subbasins have varying storage capacities and LID costs. Number and percentage of participating players, total GI cost, and impervious area treated (IAT) as input in PCSWMM's LID Usage Editor will be provided for each game and are shown for this scenario in Table 5.5. Shapley value results and total spending are presented for the no underdrain and 12-hour drain delay Maxed scenarios in Figure 5.15. Coalition flood damage cost reductions, or TRC savings, per scenario are shown in Figure 5.16. Cost effectiveness, shown as TRC savings per GI dollar spent, henceforth referred to as the spent-saved ratio (SSR), are shown for both scenarios in Figure 5.17. In the no underdrains scenario, Subbasin E has

Table 5.5: Game 1: Maxed, LID Quantities, Costs, and IAT

Subbasin	Households with LIDs		Businesses with LIDs		IAT (%)	GI Cost (USD)
	Number	% of Total	Number	% of Total		
A	27	100%	25	100%	48.5	$45,105
B	4	100%	17	100%	57.0	$29,020
C	-	-	14	100%	47.2	$23,520
D	8	100%	14	100%	36.6	$24,440
E	-	-	16	100%	43.2	$26,880

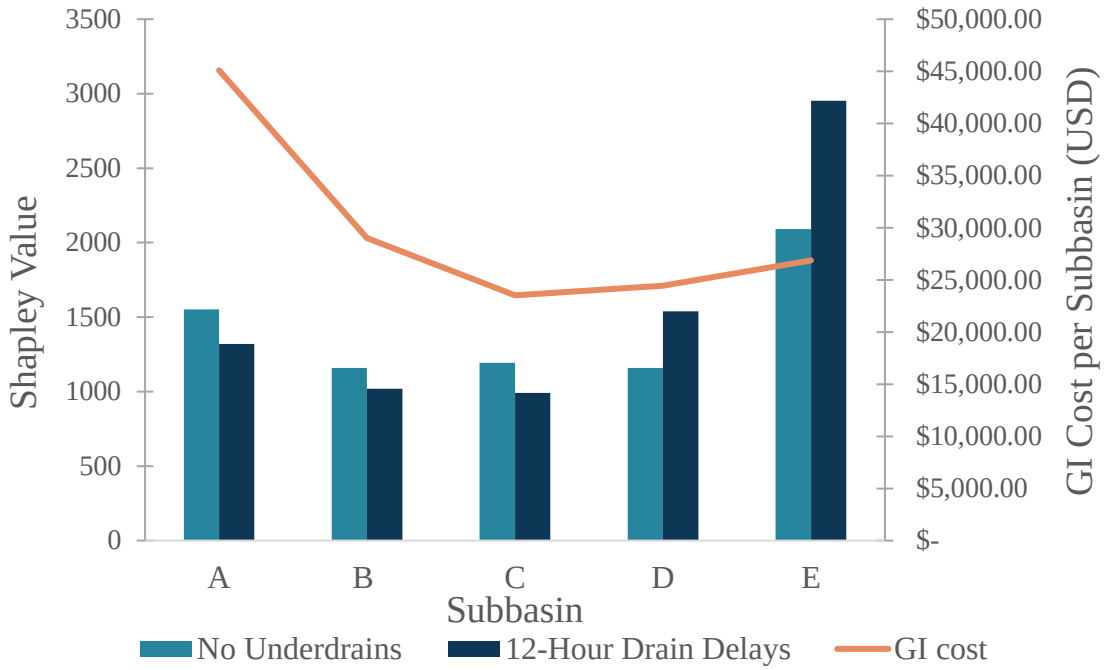

Figure 5.15: Game 1: Maxed Scenario, Subbasin Shapley Values and Total GI Costs

Game 1: Maxed	No Underdrains	12-Hour Drain Delays
Coalition	Damage Savings	Damage Savings
Empty	$ -	$ -
A	$ 2,406.42	$ 4,115.35
B	$ 1,949.94	$ 3,492.79
C	$ 2,187.26	$ 3,979.23
D	$ 2,153.25	$ 4,798.45
E	$ 3,376.06	$ 7,508.73
AB	$ 4,584.38	$ 8,029.02
AC	$ 4,110.96	$ 8,029.20
AD	$ 4,272.14	$ 8,641.51
AE	$ 5,645.06	$ 11,458.00
BC	$ 3,817.50	$ 7,615.61
BD	$ 3,786.02	$ 8,142.63
BE	$ 5,123.02	$ 10,769.87
CD	$ 3,785.06	$ 8,246.21
CE	$ 5,279.54	$ 10,841.11
DE	$ 5,341.88	$ 11,850.70
ABC	$ 6,359.72	$ 11,796.83
ABD	$ 6,364.38	$ 11,839.53
ABE	$ 7,251.13	$ 13,344.00
ACD	$ 6,082.45	$ 11,865.79
ACE	$ 7,390.01	$ 13,395.16
ADE	$ 7,309.73	$ 14,782.24
BCD	$ 5,673.42	$ 11,751.72
BCE	$ 7,050.41	$ 12,963.89
BDE	$ 6,417.16	$ 14,204.69
CDE	$ 6,669.68	$ 13,215.61
ABCD	$ 7,721.76	$ 12,473.92
ABCE	$ 8,621.39	$ 13,490.30
ABDE	$ 8,659.31	$ 13,915.54
ACDE	$ 8,821.98	$ 13,947.45
BCDE	$ 8,316.80	$ 13,781.06
ABCDE	$ 9,568.60	$ 12,602.58

Figure 5.16: Game 1: Maxed Scenario Coalition TRC Reductions

Maxed, No Underdrains	
Coalition	$ Spent/$ Saved
Empty	0
E	8.0
CE	9.5
DE	9.6
C	10.8
BE	10.9
CDE	11.2
BCE	11.3
D	11.4
BCDE	12.49
BDE	12.52
CD	12.7
AE	12.8
ACE	12.9
ADE	13.2
BCD	13.57
ACDE	13.60
BC	13.8
ABE	13.9
BD	14.1
ABCE	14.4
ABDE	14.5
B	14.9
ACD	15.3
ABC	15.4
ABD	15.5
ABCDE	15.6
ABCD	15.8
AB	16.2
AD	16.3
AC	16.7
A	18.7

Maxed, 12-Hour Drain Delay	
Coalition	$ Spent/$ Saved
Empty	0
E	3.6
DE	4.3
CE	4.6
D	5.1
BE	5.2
BDE	5.656
CDE	5.663
CD	5.8
C	5.9
BCE	6.1
AE	6.3
ADE	6.5
BCD	6.55
BD	6.57
BC	6.9
ACE	7.1
BCDE	7.5
ABE	7.6
ACD	7.8
AD	8.0
ABC	8.28
B	8.31
ABD	8.33
AC	8.5
ACDE	8.6
ABDE	9.0
ABCE	9.231
AB	9.232
ABCD	9.79
A	11.0
ABCDE	11.8

Figure 5.17: Game 1: Maxed Scenario Coalition GI Dollars Spent per TRC Dollars Saved

the highest Shapley value, and therefore the highest AMC of all subbasins to watershed TRC savings, while also having the third lowest GI cost. Subbasin A has the second highest Shapley value but a significantly higher cost, nearly double that of Subbasin E, as it has the highest number of both Residential and Commercial buildings, and consequently the highest number of purchased barrels and cisterns. The AMC of Subbasin E is nearly double that of Subbasins B, C, and D, only with additional spending of nearly $2,000. In this case, the grand coalition provides the watershed with the highest overall flood damage savings, but is not the most cost-effective coalition, as it is not the coalition with the lowest SSR. The lowest SSR belongs to the coalition only containing Subbasin E, followed by coalitions DE, CE, C, BE, D, CDE, and so forth, illustrating that the most cost-effective GI planning options are those which include spending in Subbasin E and exclude spending in Subbasin A, the latter of which has the highest SSR, making Subbasin A the least cost-effective place to focus GI spending for flood damage reduction purposes. The grand coalition generated the highest overall flood damage savings of $9,569 (rounded to the nearest dollar). These findings are significant as they indicate watershed GI spending would go farther in the way of flood reduction in Subbasin E than any other subbasin.

With 12-hour drain delays, Subbasin E still offers the highest Shapley value, which is also greater than in the no underdrain scenario. Subbasin D, which shared the lowest Shapley value with Subbasin B in the previous scenario, has the second highest Shapley value, exceeding Subbasin A at approximately half the GI cost. Subbasin E still has the lowest SSR, followed by coalitions DE, CE, D, BE, BDE, and CDE. However, in this case, the grand coalition does have the highest TRC reduction, and has the highest

SSR, acting as the least cost-effective option for flood damage savings. The grand coalition saves the watershed $12,603, which is greater than the grand coalition savings in the no underdrain scenario, but lower than coalition ADE in the 12-hour drain delay scenario, which has the potential to save the watershed a total of $14,782.

The differences in Shapley value distributions for the two underdrain scenarios make it apparent that upstream barrel and cistern drain release times in each subbasin have an effect on downstream subbasin flood damage reduction abilities. Hydrographs illustrating these changes for all games can be referenced in Appendices A through D.

In the second game scenario, “Equal Storage”, all subbasins install 14 cisterns and therefore have equivalent GI costs as well as equivalent rainfall storage capacities while treating different amounts of impervious area, as these values are dependent on subbasin average Commercial building sizes. Number and percentage of participating players, total GI cost, and IAT are shown in Table 5.6. Shapley values and spending for the two drainage scenarios are shown in Figure 5.18. TRC savings per scenario are shown in Figure 5.19. SSRs are shown in Figure 5.20. In the no underdrain scenario, Subbasin E has the highest Shapley value. The coalition which is able to save the system the most in flood damage repairs is the one which consists of only Subbasin E, and also has the lowest SSR, making it the most cost-effective GI plan. Again, it is found that coalitions which contain Subbasin E are the most cost effective, with coalitions DE, CE, BE, D, C, and CDE following Subbasin E with the next lowest SSR values. Subbasin A is still the least cost-efficient option. The grand coalition saves the system $8,656 in TRC.

When cisterns have a 12-hour drain delay, Shapley values increase for all subbasins, but maintain the same relation to one another as in the no underdrain scenario,

Table 5.6: Game 2: Equal Storage; LID Quantities, Costs, and IAT

Subbasin	Households with LIDs		Businesses with LIDs		IAT (%)	GI Cost (USD)
	Number	% of Total	Number	% of Total		
A	0	0%	14	56%	22.4	$23,520
B	0	0%	14	82.4%	45.1	$23,520
C	-	-	14	100%	47.2	$23,520
D	0	0%	14	100%	31.8	$23,520
E	-	-	14	87.5%	37.8	$23,520

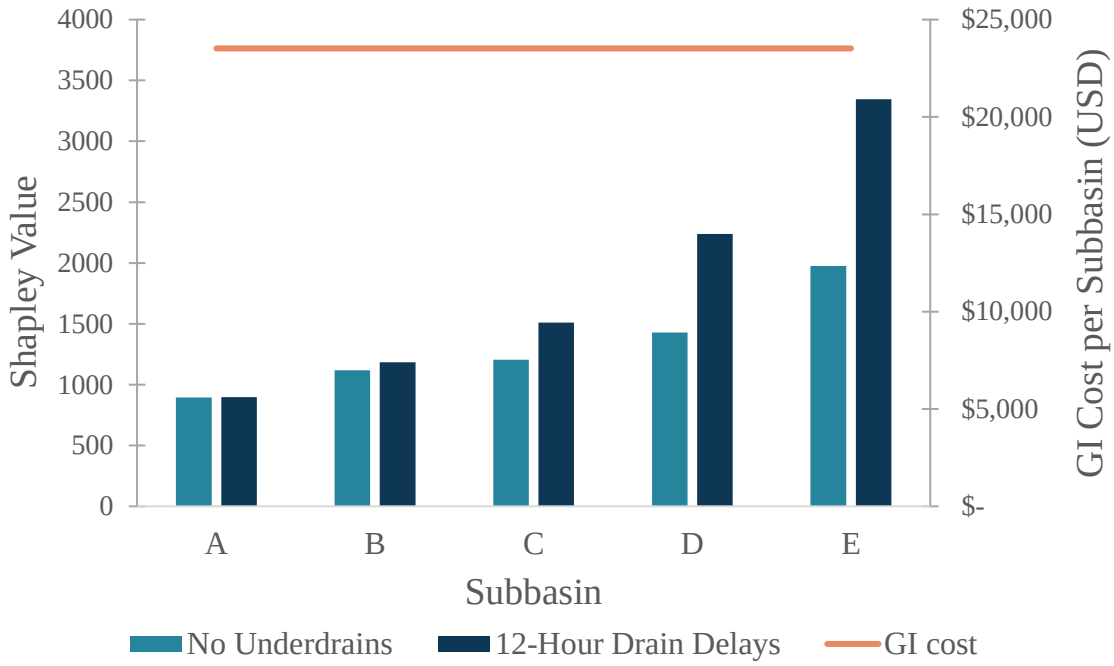

Figure 5.18: Game 2: Equal Storage Scenario, Subbasin Shapley Values and Total GI Costs

Game 2: Equal Storage	No Underdrains	12-Hour Drain Delays
Coalition	Damage Savings	Damage Savings
Empty	$ -	$ -
A	$ 1,171.96	$ 1,928.09
B	$ 1,695.82	$ 2,893.38
C	$ 2,187.26	$ 3,979.23
D	$ 2,188.21	$ 4,717.85
E	$ 2,945.81	$ 6,630.23
AB	$ 2,972.68	$ 5,258.54
AC	$ 2,871.62	$ 5,776.18
AD	$ 3,285.88	$ 6,336.48
AE	$ 4,052.21	$ 8,492.76
BC	$ 3,452.18	$ 7,101.44
BD	$ 3,514.08	$ 7,471.37
BE	$ 4,393.12	$ 9,170.22
CD	$ 3,820.03	$ 8,211.25
CE	$ 4,875.20	$ 10,237.96
DE	$ 4,952.89	$ 11,125.18
ABC	$ 5,095.31	$ 9,645.17
ABD	$ 5,027.64	$ 9,842.82
ABE	$ 5,741.53	$ 11,600.31
ACD	$ 5,166.19	$ 10,615.11
ACE	$ 5,588.03	$ 11,774.92
ADE	$ 5,769.56	$ 12,739.44
BCD	$ 5,493.99	$ 11,410.57
BCE	$ 6,022.11	$ 12,123.53
BDE	$ 6,127.72	$ 13,193.75
CDE	$ 6,346.25	$ 13,010.19
ABCD	$ 6,428.55	$ 11,919.05
ABCE	$ 7,010.94	$ 12,802.04
ABDE	$ 7,650.02	$ 14,217.80
ACDE	$ 7,600.63	$ 14,277.69
BCDE	$ 7,635.60	$ 13,644.18
ABCDE	$ 8,656.45	$ 13,205.11

Figure 5.19: Game 2: Equal Storage Scenario Coalition TRC Reductions

Equal Storage, No Underdrains	
Coalition	$ Spent/$ Saved
Empty	0
E	8.0
DE	9.5
CE	9.6
BE	10.7
D	10.7
C	10.8
CDE	11.1
BDE	11.5
AE	11.6
BCE	11.7
ADE	12.2
ABE	12.29
ABDE	12.30
CD	12.31
BCDE	12.32
ACDE	12.4
ACE	12.6
BCD	12.8
BD	13.39
ABCE	13.42
ABCDE	13.59
BC	13.63
ACD	13.7
ABC	13.8
B	13.9
ABD	14.0
AD	14.3
ABCD	14.6
AB	15.8
AC	16.4
A	20.1

Equal Storage, 12-Hour Drain Delay	
Coalition	$ Spent/$ Saved
Empty	0
E	3.5
DE	4.2
CE	4.6
D	5.0
BE	5.1
BDE	5.3
CDE	5.4
ADE	5.5
AE	5.5
CD	5.7
BCE	5.8
C	5.9
ACE	6.0
ABE	6.1
BCD	6.2
BD	6.3
ACDE	6.59
ABDE	6.617
BC	6.624
ACD	6.65
BCDE	6.9
ABD	7.2
ABC	7.32
ABCE	7.35
AD	7.4
ABCD	7.9
B	8.13
AC	8.14
ABCDE	8.91
AB	8.95
A	12.2

Figure 5.20: Game 2: Equal Storage Scenario Coalition GI Dollars Spent per TRC Dollars Saved (Spent/Saved Ratio)

increasing from Subbasin A to Subbasin E. Subbasin A is still contributing the least to overall TRC reduction, only treating 22.4% of its impervious area in this game versus 100% in the previous game and is still the least cost-efficient option. The grand coalition saves the system $13,205 in TRC, but the highest TRC savings for this game scenario are brought about by coalition ACDE, saving $14,278, implying that the addition of and spending on GI with 12-hour drain delays in Subbasin B creates additional flood damages. Here, it is again shown that drain delays on widely distributed GI has the ability to affect hydrological processes and outcomes within the watershed.

In Game 3, “20% IAT”, each subbasin treats a minimum of and as close to 20% of its impervious area using 2,000-gallon cisterns. Number and percentage of participating players, total GI cost, and IAT are shown in Table 5.7. Shapley value results and total spending are presented for the two drain scenarios in Figure 5.21. TRC savings per scenario are shown in Figure 5.22. SSRs are shown for both scenarios in Figure 5.23. With no underdrains, Subbasin E again has the highest Shapley value, having the highest AMC to flood damage savings for the entire watershed and treating approximately 20% of its area at a lower cost than both Subbasins A and D. As in the previous games, Subbasin E has the lowest SSR and is therefore the most cost-effective option for GI installation, and Subbasin A has the highest SSR. The grand coalition in this case saves the watershed $5,590 in TRC and is the coalition with the highest TRC savings.

When 12-hour cistern drain delays are considered, Shapley values increase for all subbasins, and Subbasin E's value more than doubles. The subbasins remain in the same order of increasing AMCs as in the no underdrain scenario, aside from Subbasin C having the lowest Shapley value rather than Subbasin B. As in the previous scenario,

Table 5.7: Game 3: 20% IAT Scenario LID Quantities, Costs, and IAT

Subbasin	Households with LIDs		Businesses with LIDs		IAT (%)	GI Cost (USD)
	Number	% of Total	Number	% of Total		
A	0	0%	13	52%	20.8	$21,840
B	0	0%	7	41.2%	22.5	$11,760
C	-	-	6	42.9%	20.3	$10,080
D	0	0%	9	64.3%	20.4	$15,120
E	-	-	8	50%	21.6	$13,440

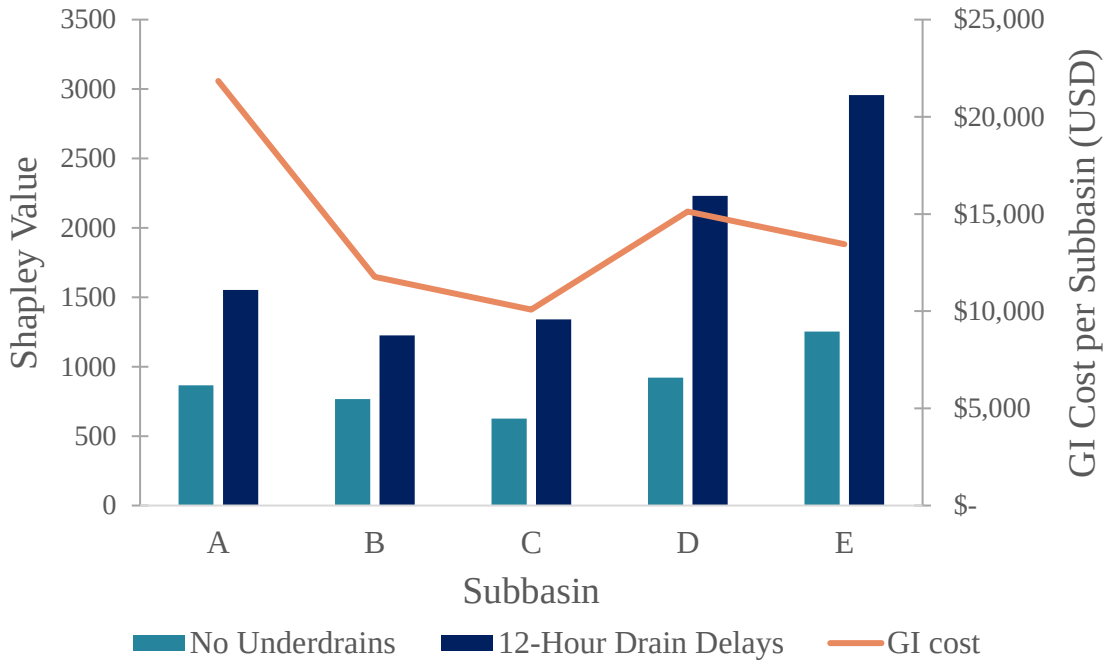

Figure 5.21: Game 3: 20% IAT Scenario, Subbasin Shapley Values and Total GI Costs

Game 3: 20% IAT	No Underdrains	12-Hour Drain Delays
Coalition	Damage Savings	Damage Savings
Empty	$ -	$ -
A	$ 1,102.03	$ 1,757.63
B	$ 812.94	$ 1,258.75
C	$ 869.76	$ 1,499.14
D	$ 1,277.06	$ 3,036.01
E	$ 1,726.40	$ 3,780.59
AB	$ 1,954.31	$ 3,352.93
AC	$ 1,982.47	$ 3,599.61
AD	$ 2,344.13	$ 4,748.00
AE	$ 2,797.83	$ 5,568.81
BC	$ 1,783.23	$ 3,059.46
BD	$ 2,090.01	$ 4,183.56
BE	$ 2,574.31	$ 5,008.74
CD	$ 2,177.42	$ 4,458.91
CE	$ 2,530.60	$ 5,214.16
DE	$ 3,003.46	$ 6,709.77
ABC	$ 2,850.30	$ 5,214.82
ABD	$ 3,222.63	$ 5,774.78
ABE	$ 3,680.71	$ 7,102.92
ACD	$ 2,928.65	$ 6,169.44
ACE	$ 3,713.24	$ 7,314.64
ADE	$ 4,004.97	$ 8,493.62
BCD	$ 2,985.99	$ 5,944.93
BCE	$ 3,378.51	$ 6,844.42
BDE	$ 3,750.85	$ 7,902.96
CDE	$ 3,117.20	$ 8,204.53
ABCD	$ 4,218.95	$ 8,100.30
ABCE	$ 4,480.54	$ 8,934.22
ABDE	$ 4,852.88	$ 9,997.13
ACDE	$ 4,558.89	$ 9,858.24
BCDE	$ 4,620.61	$ 9,633.74
ABCDE	$ 5,590.02	$ 11,571.19

Figure 5.22: Game 3: 20% IAT Scenario Coalition TRC Reductions

20% IAT, No Underdrains	
Coalition	$ Spent/$ Saved
Empty	0
E	7.8
CE	9.3
DE	9.5
BE	9.8
BCE	10.4
BDE	10.7
BCDE	10.9
CD	11.57
C	11.59
D	11.8
ACE	12.22
BC	12.25
BCD	12.38
CDE	12.40
ADE	12.58
AE	12.61
ABCE	12.7
ABE	12.78
ABDE	12.81
BD	12.86
ABCDE	12.92
ACDE	13.3
ABCD	13.9
B	14.5
ABD	15.1
ABC	15.3
AD	15.8
ACD	16.1
AC	16.1
AB	17.2
A	19.8

20% IAT, 12-Hour Drain Delay	
Coalition	$ Spent/$ Saved
Empty	0
E	3.6
DE	4.3
CE	4.5
CDE	4.7
D	4.98
BE	5.03
BDE	5.1
BCE	5.15
BCDE	5.23
CD	5.7
ADE	5.9
ACDE	6.1
ACE	6.20
BCD	6.22
ABDE	6.22
ABCDE	6.24
AE	6.3
ABCE	6.39
BD	6.43
ABE	6.6
C	6.7
BC	7.1
ABCD	7.3
ACD	7.6
AD	7.8
ABC	8.38
ABD	8.44
AC	8.9
B	9.3
AB	10.0
A	12.4

Figure 5.23: Game 3: 20% IAT Scenario Coalition GI Dollars Spent per TRC Dollars Saved (Spent/Saved Ratio)

Subbasins E and A remain the most and least cost-effective locations for GI focus, respectively. The grand coalition in this instance saves the watershed $11,571 in TRCs. This is the first game in which the no underdrain and delayed drain scenario grand coalitions have both resulted in the highest TRC savings. This may be due to considerably higher IAT values across the subbasins in the first two games, so the stormwater volume released after the two drain delays does not have a significant effect on neighboring subbasins by way of increased flood depth.

In Game 4, “Maxed, 5,000-Gallon Cisterns in Subbasin E”, game set up is the same for most subbasins as in the first Maxed game, but to address that Subbasin E is the most cost-effective location for GI placement in all the other games and Subbasin A is the least, in this scenario a portion of Subbasin A’s GI funding is given to Subbasin E. Subbasin A keeps its Residential barrels, but no longer has funding for its 25 Commercial building cisterns. The cost of these 25 2000-gallon cisterns is given to Subbasin E and used to install 5,000-gallon cisterns on all 16 of its Commercial buildings rather than the 16 2,000-gallon cisterns it had previously. Updated number and percentage of participating players, total GI cost, and IAT are shown in Table 5.8. Shapley value results and total spending are presented for the two drain scenarios in Figure 5.24. TRC savings per scenario are shown in Figure 5.25. SSRs are shown for both scenarios in Figure 5.26. As expected, in the no underdrains scenario, Subbasin A only installs barrels for its Residential properties and has the lowest GI cost and Shapley value, and Subbasin E spends more than double than Subbasins B, C, and D, and has a Shapley value approximately 5 times greater. Similar to previous games, Subbasins E and A have the

Table 5.8: Game 4: Maxed, 5,000-gallon Cisterns in Subbasin E Scenario LID Quantities, Costs, and IAT

Subbasin	Households with LIDs		Businesses with LIDs		IAT (%)	GI Cost (USD)
	Number	% of Total	Number	% of Total		
A	27	100%	0	0%	8.5	$3,105
B	4	100%	17	100%	57.0	$29,020
C	-	-	14	100%	47.2	$23,520
D	8	100%	14	100%	36.6	$24,440
E	-	-	16	100%	43.2	$68,880

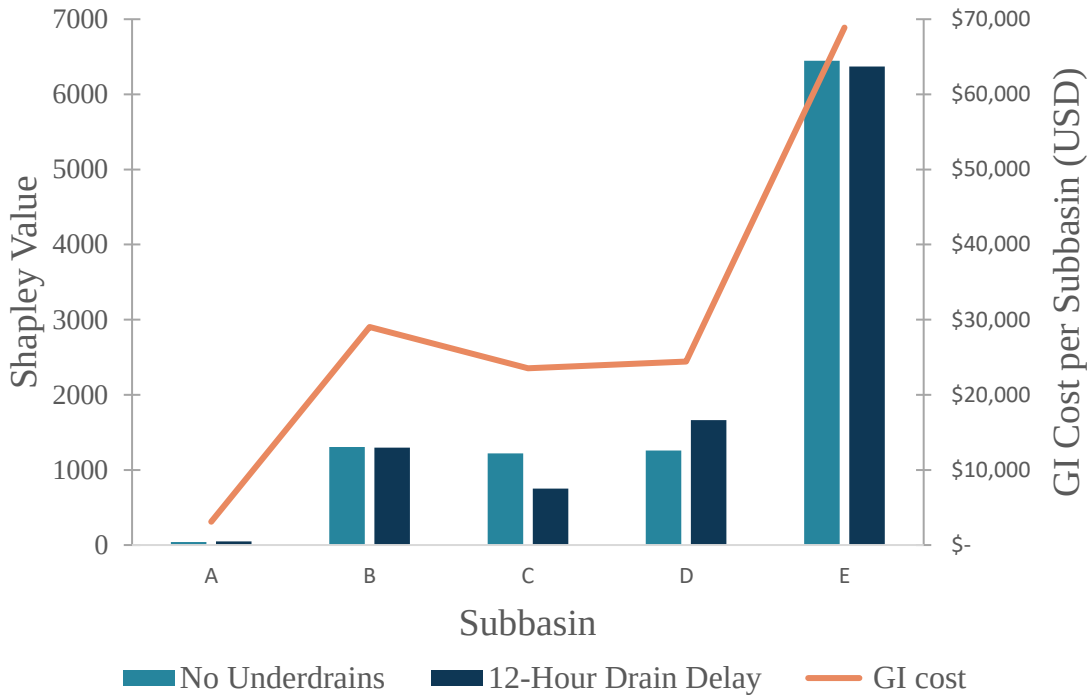

Figure 5.24: Game 4: Maxed, 5,000-gallon Cisterns in Subbasin E Scenario, Subbasin Shapley Values and Total GI Costs

Game 4: Maxed, Subbasin E 5,000gal Cisterns	No Underdrains	12-Hour Drain Delays
Coalition	Damage Savings	Damage Savings
Empty	$ -	$ -
A	$ 80.60	$ 115.57
B	$ 2,019.87	$ 3,492.79
C	$ 2,187.26	$ 3,979.23
D	$ 2,153.25	$ 4,687.25
E	$ 8,557.68	$ 13,557.66
AB	$ 2,019.87	$ 3,593.31
AC	$ 2,252.82	$ 4,049.16
AD	$ 2,173.17	$ 4,757.18
AE	$ 8,638.28	$ 13,592.63
BC	$ 3,817.50	$ 7,650.57
BD	$ 4,013.65	$ 8,107.67
BE	$ 10,365.63	$ 15,435.56
CD	$ 3,785.06	$ 8,246.21
CE	$ 10,476.21	$ 14,492.82
DE	$ 10,503.57	$ 15,911.01
ABC	$ 3,735.08	$ 7,821.03
ABD	$ 4,044.24	$ 8,348.06
ABE	$ 10,400.60	$ 15,509.87
ACD	$ 3,785.06	$ 8,381.70
ACE	$ 10,546.14	$ 14,593.34
ADE	$ 10,534.17	$ 15,980.94
BCD	$ 5,738.98	$ 11,751.72
BCE	$ 12,102.84	$ 15,621.22
BDE	$ 12,147.37	$ 17,172.34
CDE	$ 11,827.00	$ 15,680.64
ABCD	$ 5,704.02	$ 11,862.92
ABCE	$ 12,172.77	$ 15,695.53
ABDE	$ 12,177.97	$ 17,176.71
ACDE	$ 11,896.94	$ 15,820.50
BCDE	$ 13,164.67	$ 15,331.24
ABCDE	$ 13,269.56	$ 15,296.27

Figure 5.25: Game 4: Maxed, 5,000-gallon Cisterns in Subbasin E Scenario Coalition TRC Reductions

Maxed, Subbasin E 5,000gal Cisterns, No Underdrains	
Coalition	$ Spent/$ Saved
Empty	0
E	8.0
AE	8.3
CE	8.8
DE	8.9
ACE	9.1
ADE	9.2
BE	9.4
ABE	9.7
CDE	9.9
BCE	10
BDE	10.07
ACDE	10.08
ABCE	10.2
ABDE	10.3
C	10.8
BCDE	11.1
ABCDE	11.2
D	11.4
AC	11.8
CD	12.67
AD	12.68
BD	13.3
BCD	13.4
ACD	13.5
BC	13.8
ABD	13.99
ABCD	14.04
B	14.4
ABC	14.9
AB	15.9
A	38.5

Maxed, Subbasin E 5,000gal Cisterns, 12-Hour Drain Delay	
Coalition	$ Spent/$ Saved
Empty	0
E	5.1
D	5.2
AE	5.3
AD	5.79
CD	5.82
DE	5.87
C	5.91
ADE	6.0
ACD	6.1
BE	6.3
CE	6.4
ABE	6.51
ACE	6.54
BCD	6.55
AC	6.58
BD	6.59
ABCD	6.75
ABD	6.78
BC	6.9
ABC	7.11
BDE	7.12
ABDE	7.3
CDE	7.5
ACDE	7.6
BCE	7.8
ABCE	7.9
B	8.3
AB	8.9
BCDE	9.5
ABCDE	9.7
A	26.9

Figure 5.26: Game 4: Maxed, 5,000-gallon Cisterns in Subbasin E Scenario Coalition GI Dollars Spent per TRC Dollars Saved (Spent/Saved Ratio)

lowest and highest SSR values, respectively. The grand coalition results in the watersheds highest TRC savings, a total of $13,270.

In the 12-hour drain delay scenario, Subbasins A and E still have the lowest and highest Shapley values, respectively, as well as the highest and lowest SSRs, respectively. Shapley values do not strictly increase with GI spending in this case, as AMCs to TRC savings decrease for Subbasins B, C, D, and E. The grand coalition provides a TRC reduction of $15,296, but flood damage cost reductions are higher under coalition ABDE, which produces $17,177 in savings, the highest of all games considered thus far.

Finally, to observe the effects of GI rebates on cost effectiveness across the watershed, two variations of the Game 1: "Maxed" scenario are considered. In the first, Game 5: "Maxed, Rebate A", each subbasin is reimbursed $5,000 in GI cost for every 10% of its IAT through rainwater harvesting. The number and percentage of participating players and IAT, which are unchanged from those in Game 1, are shown with the updated GI costs which take Rebate A's savings into account in Table 5.9. Shapley values are unchanged, but they are shown for both drainage scenarios against new rebate-affected GI costs in Figure 5.27. Coalition flood damage savings are unchanged from Game 1 are referenced in Figure 5.16. Rebate updated SSRs for the no underdrain and 12-hour drain delay scenarios are shown in Figure 5.28.

In Game 6, "Maxed, Rebate B", each subbasin's GI cost is reimbursed $7,000 per 15% of its impervious area treated through rainwater harvesting. Maxed scenario player information and updated GI costs are shown in Table 5.10. Shapley values and new costs

Table 5.9: Game 5: Maxed, Rebate A Scenario LID Quantities, Costs, and IAT

Subbasin	Households with LIDs		Businesses with LIDs		IAT (%)	GI Cost with Rebate (USD)
	Number	% of Total	Number	% of Total		
A	27	100%	25	100%	48.5	$25,105
B	4	100%	17	100%	57.0	$4,020
C	-	-	14	100%	47.2	$3,520
D	8	100%	14	100%	36.6	$9,440
E	-	-	16	100%	43.2	$6,880

Table 5.10: Game 6: Maxed, Rebate B Scenario; LID Quantities, Costs, and IAT

Subbasin	Households with LIDs		Businesses with LIDs		IAT (%)	GI Cost with Rebate (USD)
	Number	% of Total	Number	% of Total		
A	27	100%	25	100%	48.5	$22,472
B	4	100%	17	100%	57.0	$2,420
C	-	-	14	100%	47.2	$1,493
D	8	100%	14	100%	36.6	$7,360
E	-	-	16	100%	43.2	$6,720

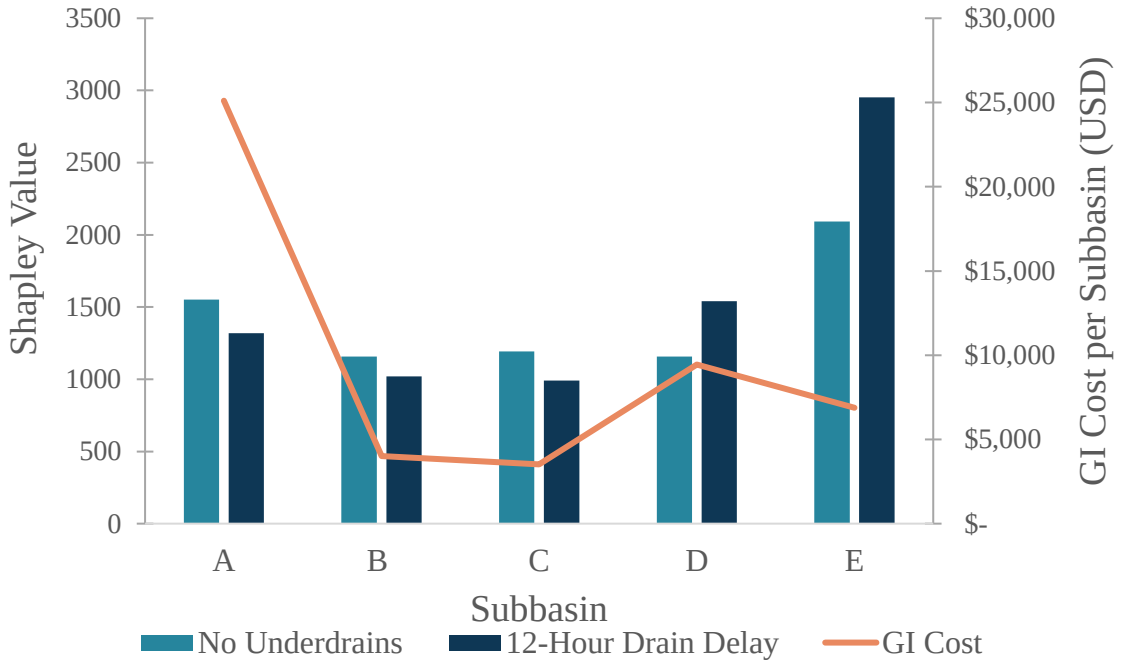

Figure 5.27: Game 5: Maxed, Rebate A Scenario, Subbasin Shapley Values and Total GI Costs

Maxed, Rebate A, No Underdrains	
Coalition	$ Spent/$ Saved
Empty	0
C	1.6
CE	1.97
BC	1.98
E	2.04
BCE	2.05
B	2.06
BE	2.13
BCDE	2.9
CDE	2.97
BCD	2.99
DE	3.1
BDE	3.2
CD	3.4
BD	3.6
D	4.4
ABCE	4.6
ACE	4.8
ABE	5.0
ACDE	5.09
ABCDE	5.12
ABC	5.13
ABDE	5.2
ABCD	5.5
AE	5.67
ADE	5.67
ABD	6.1
ACD	6.3
AB	6.4
AC	7.0
AD	8.1
A	10.4

Maxed, Rebate A, 12-Hour Drain Delay	
Coalition	$ Spent / $ Saved
Empty	0
C	0.88
E	0.92
CE	0.96
BC	0.99
BE	1.01
BCE	1.1
B	1.2
DE	1.4
BDE	1.4
BCD	1.4
CDE	1.5
CD	1.6
BD	1.65
BCDE	1.73
D	2.0
ACE	2.65
ABE	2.70
ABC	2.77
AE	2.79
ADE	2.80
ABCE	2.9
ACD	3.21
ACDE	3.22
ABD	3.26
ABDE	3.27
ABCD	3.4
AC	3.57
AB	3.63
ABCDE	3.9
AD	4.0
A	6.1

Figure 5.28: Game 5: Maxed, Rebate A Scenario Coalition GI Dollars Spent per TRC Dollars Saved (Spent/Saved Ratio

for both drainage scenarios against new rebate affected GI costs are shown in Figure 5.29. Coalition flood damage savings are still unchanged from Game 1 and can also be referenced in Figure 5.16, and rebate updated SSRs for both drain scenarios are shown in Figure 5.30. Total rebate savings for Games 5 and 6 are shown in Table 5.11. Subbasins B, D, and E save more on GI spending under the application of Rebate A while Subbasins A and C save more under Rebate B. In both cases and for all drain scenarios, Subbasin A remains the least cost-effective option, saving the lowest amount of flood reduction dollars per GI dollar spent. Most notably, in Games 5 and 6, for the first time Subbasin E does not have the lowest SSR. In all drain scenarios where rebates are enacted, Subbasin C has the lowest SSR. In both scenarios with no underdrains, the most cost-effective coalition C is followed by CE, BC, and E. Under Rebate A, the 12-hour drain delay scenario lowest SSR coalition is C, followed directly by coalition E. Under Rebate B, the 12-hour drain release again demonstrates an effect on subbasin storage capacity, as Subbasin E has the fifth lowest SSR in this case, the highest value it has had in any game.

5.4 DISCUSSION

Shapley values and cost comparisons for varying GI implementation plans under historic South Carolina 2015 flood event conditions, using urban flood modeling tool PCSWM, were estimated and used to identify which subarea, or subareas, of the Market Street watershed should be the focus of governing bodies and planners aiming to either implement GI or focus GI advocacy for the purpose of reducing property damages due to a combination of tide and rainfall induced flooding.

Table 5.12 contains a summary of findings for all considered games. Across all tested GI plans, Subbasin E had the highest AMC to flood induced building replacement

Table 5.11: GI Cost Rebate Savings per Subbasin

Subbasin	Game 5: Rebate A	Game 6: Rebate B
A	$20,000	$21,000
B	$25,000	$21,000
C	$20,000	$21,000
D	$15,000	$14,000
E	$20,000	$14,000

Table 5.12: Summary of Game Results: Shapley Values, SSRs, and Coalition TRC Savings

Games	Drain Scenario	Highest Shapley Value		Lowest Shapley Value		Highest TRC Savings			Lowest SSR		
		Subbasin	Value	Subbasin	Value	Coalition	Savings	SSR	Coalition	Savings	SSR
Game 1: Maxed	No Underdrain	E	2092	B, D	1158	ABCDE	$ 9,569	15.6	E	$ 3,376	8.0
	12-Hour Delay	E	2953	C	991	ADE	$ 14,782	6.5	E	$ 7,509	3.6
Game 2: Equal Storage	No Underdrain	E	1975	A	893	ABCDE	$ 8,656	13.6	E	$ 2,946	8.0
	12-Hour Delay	E	3347	A	898	ACDE	$ 14,278	6.6	E	$ 6,630	3.5
Game 3: 20% IAT	No Underdrain	E	1253	C	627	ABCDE	$ 5,590	12.9	E	$ 1,726	7.8
	12-Hour Delay	E	2956	B	1226	ABCDE	$ 11,571	6.2	E	$ 3,781	3.6
Game 4: Maxed, 5,000gal Cisterns in Subbasin E	No Underdrain	E	6446	A	39	ABCDE	$ 13,270	11.2	E	$ 8,558	8.0
	12-Hour Delay	E	6369	A	50	ABDE	$ 17,177	7.3	E	$13,558	5.1
Game 5: Maxed, Rebate A	No Underdrain	E	2092	B, D	1158	ABCDE	$ 9,569	5.1	C	$ 3,376	1.6
	12-Hour Delay	E	2953	C	991	ADE	$ 14,782	2.8	C	$ 7,509	0.9
Game 6: Maxed, Rebate B	No Underdrain	E	2092	B, D	1158	ABCDE	$ 9,569	6.1	C	$ 3,376	1.2
	12-Hour Delay	E	2953	C	991	ADE	$ 14,782	3.2	C	$ 7,509	0.6

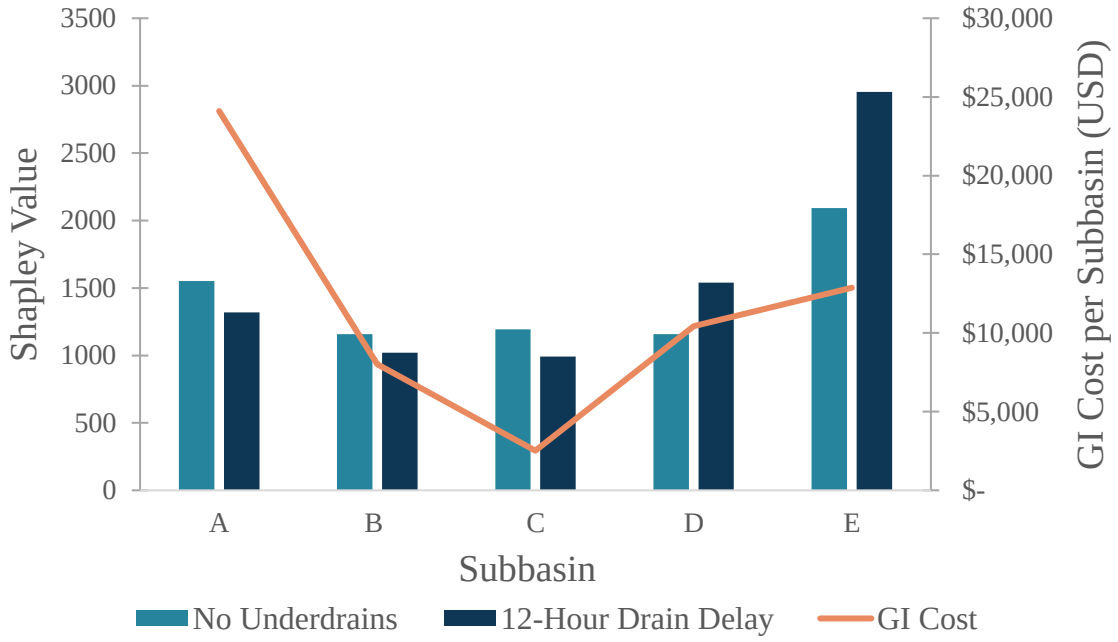

Figure 5.29: Game 6: Maxed, Rebate B Scenario, Subbasin Shapley Values and Total GI Costs

Maxed, Rebate B, No Underdrains	
Coalition	$ Spent / $ Saved
Empty	0
C	1.2
BC	2.8
CE	2.9
BCE	3.3
CD	3.4
BCD	3.7
E	3.8
CDE	3.9
BCDE	4.07
BE	4.08
B	4.11
DE	4.4
D	4.8
BD	4.88
BDE	4.88
ACE	5.3
ABC	5.4
ABCE	5.5
ACDE	5.7
ABCD	5.8
ABCDE	6.06
ACD	6.09
ABE	6.2
ABDE	6.4
AC	6.48
ADE	6.49
AE	6.6
ABD	6.7
AB	7.0
AD	8.1
A	10.0

Maxed, Rebate B, 12-Hour Drain Delay	
Coalition	$ Spent / $ Saved
Empty	0
C	0.6
BC	1.38
CE	1.42
CD	1.6
E	1.7
BCD	1.79
BCE	1.81
BE	1.9
CDE	1.96
DE	1.97
D	2.18
BDE	2.21
BD	2.27
B	2.30
BCDE	2.5
ABC	2.94
ACE	2.95
ACD	3.1
ADE	3.21
AE	3.23
AC	3.3
ABE	3.4
ABCE	3.5
ACDE	3.58
ABD	3.60
ABCD	3.61
ABDE	3.98
AD	3.998
AB	4.001
ABCDE	4.6
A	5.9

Figure 5.30: Game 6: Maxed, Rebate B Scenario Coalition GI Dollars Spent per TRC Dollars Saved (Spent/Saved Ratio)

cost savings for the Market Street watershed overall than any other subbasin, even though Subbasin C experienced the highest flood damage costs in the baseline scenario. Overwhelmingly, Coalition E also had the lowest SSR, saving more in repair dollars per GI dollars spent than any other coalition in every case aside from Games 5 and 6, in which rebates were considered in the cost efficiency metric. This is likely caused by several factors inherent to Subbasin E, including that it has the smallest subbasin area causing flood depth measurements over the subbasin to be higher than some of its neighboring subbasins which each received a uniform amount of rainfall. Additionally, Subbasin E has the lowest infiltration capacity, as it has the overall largest amount of impervious area and the highest percentage of high intensity developed land cover. From the digital elevation model, the majority of significant depression areas in the watershed are also in this subbasin, lining Market Street itself. Finally, Subbasin E is connected to Outfall 6.5 (Figure 4.10), one of two outfalls in the watershed that is tidally influenced, and which repeatedly had the highest inflow volume across all simulated games, therefore making the drainage network in the Subbasin E particularly vulnerable to backflow induced flooding.

The use of CGT in conjunction with PCSWMM allowed for consideration of other factors in addition to which subbasin experienced the most baseline flooding, which, considered alone, would have suggested GI be focused in Subbasin C. Shapley values, based on total flood damage costs, encompassed PCSWMM inputs and flooding results, which inherently consider other factors which were able to point to Subbasin E being the ideal location for GI focus, such as it consisting of the smallest pervious area, highest ratio of high intensity development land cover, and smallest subbasin area. The

games which instituted rebates are the only scenarios where Subbasin C is considered the most cost-efficient location for GI under Maxed conditions.

In both games which institute rebates, Subbasin C receives the same amount or more in rebates for GI than Subbasin E. Subbasin C saves an additional $7,000 under Rebate B conditions, even though Subbasin C is treating only an additional 4% of its IAT. However, under Equal Storage and spending conditions in Game 2, Subbasin E has higher Shapley values than Subbasin C in both drainage scenarios, and therefore higher AMCs to overall watershed flood damage savings. In every other game scenario explored, Subbasin E alone has been the most cost-effective option for GI placement, suggesting this would be the recommended area for GI and GI advocacy focus. From a policy standpoint, these results suggest that governing bodies offering GI spending assistance or rebates based solely on community or watershed IAT benchmarks fail to take into consideration things like total area, building GI capacity, and flood reduction need.

Coalition A provided the least cost reduction returns per GI dollar spent, and Subbasin A had the lowest Shapley value for both drainage scenarios in the Equal Storage and, expectedly, in the Maxed, 5,000-gallon Cisterns in Subbasin E games. In the other Maxed scenarios, Subbasin A consistently had the highest GI cost, due to it containing the highest number of buildings. Even in the 20% IAT scenario, Subbasin A had to spend double what Subbasins B and C spent on GI in order to reach the 20% IAT benchmark due to its relatively small average building sizes. These high cost, low return results led to the suggested scenario where Subbasin E received Subbasin A's Maxed cistern funding to install larger cisterns, and notably, this scenario saved the watershed

the most flood damage repair costs in both drainage scenarios out of all modeled games, the highest being the 12-hour drain delay scenario with a savings of approximately $17,200 for the watershed.

Finally, the drain scenario comparisons are valuable in their ability to show that while rainwater harvesting for the purpose of water recycling and cost savings within one's home or business can be beneficial, the drain delay scenarios unsurprisingly allow for more overall flood damage savings for the watershed as a whole. Additional analysis could be performed to determine more advantageous drain times and barrel locations, as the hydrographs provided in Appendices A through D give insight to how simultaneous draining of even Residential sized barrels, when distributed widely enough, can have an effect on downstream stormwater management capacity. Most notable is the Shapley value analysis which shows, unintuitively, that the watershed saves more in flood damage repair costs under coalitions other than the grand coalition when barrels and cisterns have 12-hour drain delays instituted in multiple games, including Coalition ADE in Game 1, ACDE in Game 2, and ABDE in Game 4.

CHAPTER 6

CONCLUSION

Game theory can be used to predict outcomes of human decision-making when self-interested parties are faced with conflict. Cooperative, and in this case, coalitional analysis, is used to predict how self-interested parties may form to better their individual outcomes. For this research, a coalitional game theory (CGT) solution concept, the Shapley value, was leveraged to observe how subgroups should work together to better serve the overall system, and by association, themselves. Results of this research serve to inform governing bodies, city planners, and relevant stakeholders by showing which subareas benefit the system most, through flood damage repair cost savings and cost efficiency. Even without the intention of government level green infrastructure (GI) project installation, these results serve to show where GI information campaigns should be focused to encourage individual property owners to participate in stormwater management strategies. Additionally, CGT shows which areas of the watershed working in conjunction is best for the watershed overall, so planners can strategically work within more than one community, neighborhood, or modeled subarea at a time. Overall, based on Shapley values and the utilized cost efficiency metric, results suggest GI spending, placement, and advocacy focus in Subbasin E, surrounding Market Street itself.

Of course, results would vary widely under a different set of modeling constraints and assumptions, for example if buildings could have more than one means of rainwater harvesting, if Homeowners Association restraints were considered for residential

properties, or if commercial buildings were additionally outfitted with underground cisterns. Regardless of the assumptions in place, the application of CGT to stormwater modeling and flood reduction practices allows for consideration of budget constraints, basin area, land cover, and drainage characteristics, rainfall-runoff processes, and both building and property size, type, and location simultaneously.

Additionally, the methods described here are highly versatile, as what the Shapley value measures is up to the discretion of the modeler, and PCSWMM can model any number of environmental conditions and storm events. If Shapley values measured not cost reductions, but overall flood volume reduction, there would be an entirely different analysis to be had. Leveraging PCSWMM results, Shapley values could be based on subcatchments' flood volume reduction, junction inflows, subbasin peak runoff values, or any number of other parameters, to compare any number of land development changes or GI choices, whose accuracy and insight could only stand to be improved through use of PCSWMM's 2D modeling capabilities. Additional suggestions for future work include the following:

- Use of a 2D hydrodynamic model to simulate compound flooding and dynamic boundary conditions for the Charleston Peninsula
- Development of a less computationally complex and time intensive simulation model capable of managing a larger number of both players and possible coalitions
- Consideration of stakeholder and water manager input when developing game scenarios

- Simulation of additional design storms, future storms, and flood events under projected climate conditions to develop stochastic games and estimate Shapley values
- Introduction of uncertainty in player behavior by combining game theory applications with hierarchical agent-based modeling strategies
- Development of additional human behavior studies concerning individual likelihood to partake in green stormwater management strategies and common barriers, as described for residents of South Carolina's coastal counties in (Ureta et al., 2021)
- Open dialogue with historic property owners and city managers to determine which adaptation strategies are appropriate for their sites in order to design feasible modeling institutions and flood adaption options for specific properties

As sea levels climb at accelerated rates and climate variations continue to alter storm intensity and frequency, the world's coastal communities will become increasingly vulnerable to the unequally distributed risks associated with the coupling of these events. Stakeholders and public alike will need novel approaches and nuanced responses to the combined effects of tide and stormwater induced flooding. Planners will be faced with increasingly difficult decisions regarding prioritization of infrastructure and related spending which can only stand to be improved by further exploration of human choices and consequent outcomes within the field of water resources management.

REFERENCES

Abebe, Y. A., Ghorbani, A., Nikolic, I., Manojlovic, N., Gruhn, A., & Vojinovic, Z. (2020). The role of household adaptation measures to reduce vulnerability to flooding: a coupled agent-based and flood modelling approach. *Hydrology and Earth System Sciences Discussions*, 1–40. https://doi.org/10.5194/hess-2020-272

Abebe, Y. A., Ghorbani, A., Nikolic, I., Vojinovic, Z., & Sanchez, A. (2019a). A coupled flood-agent-institution modelling (CLAIM) framework for urban flood risk management. *Environmental Modelling and Software*, *111*, 483–492. https://doi.org/10.1016/j.envsoft.2018.10.015

Abebe, Y. A., Ghorbani, A., Nikolic, I., Vojinovic, Z., & Sanchez, A. (2019b). Flood risk management in Sint Maarten – A coupled agent-based and flood modelling method. *Journal of Environmental Management*, *248*. https://doi.org/10.1016/j.jenvman.2019.109317

Ahern, J. (2011). From fail-safe to safe-to-fail: Sustainability and resilience in the new urban world. *Landscape and Urban Planning*, *100*(4), 341–343. https://doi.org/10.1016/j.landurbplan.2011.02.021

Ahiablame, L., & Shakya, R. (2016). Modeling flood reduction effects of low impact development at a watershed scale. *Journal of Environmental Management*, *171*, 81–91. https://doi.org/10.1016/j.jenvman.2016.01.036

An, L., Linderman, M., Qi, J., Shortridge, A., & Liu, J. (2005). Exploring complexity in a human-environment system: An agent-based spatial model for multidisciplinary and multiscale integration. *Annals of the Association of American Geographers*, *95*(1), 54–79.

Bai, Y., Zhao, N., Zhang, R., & Zeng, X. (2018). Storm water management of low impact development in urban areas based on SWMM. *Water (Switzerland)*, *11*(1). https://doi.org/10.3390/w11010033

Bandini, S., Manzoni, S., & Vizzari, G. (2009). Agent Based Modeling and Simulation: An Informatics Perspective. *Computational Complexity: Theory, Techniques, and Applications*, 105–117. https://doi.org/10.1007/978-1-4614-1800-9_7

Baptiste, A. K., Foley, C., & Smardon, R. (2015). Understanding urban neighborhood differences in willingness to implement green infrastructure measures: A case study of Syracuse, NY. *Landscape and Urban Planning*, *136*, 1–12. https://doi.org/10.1016/j.landurbplan.2014.11.012

Berglund, E. Z. (2015). Using Agent-Based Modeling for Water Resources Planning and Management. *Journal of Water Resources Planning and Management*, *141*(11). https://doi.org/10.1061/(ASCE)WR.1943-5452.0000544

Bonsteel, F. E., & Carr, E. P. (1904). *Charleston, 1904*. Soil Survey of Charleston County, South Carolina. https://digital.tcl.sc.edu/digital/collection/HSSM/id/7

Braden, J., Eheart, J., & Saleth, R. (1991). Bargaining Rules for a Thin Spot Water Market. *Land Economics*, *67*(3), 326–339.

Carter, T., & Fowler, L. (2008). Establishing Green Roof Infrastructure Through Environmental Policy Instruments. *Environmental Management*, *42*, 151–164. https://doi.org/10.1007/s00267-008-9095-5

Center for Emergency Management and Homeland Security. (2020). *The Spatial Hazard Events and Losses Database for the United States, Version 17.0 [Online Database]*. http://www.sheldus.org

Cerini, M. (2019). *Venice is flooding -- what's the future of its historical sites?* CNN Style. https://www.cnn.com/style/article/venice-flooding-st-mark-damages/index.html

Chaffin, B. C., Shuster, W. D., Garmestani, A. S., Furio, B., Albro, S. L., Gardiner, M., Spring, M., & Green, O. O. (2016). A tale of two rain gardens: Barriers and bridges to adaptive management of urban stormwater in Cleveland, Ohio. *Journal of Environmental Management*, *183*, 431–441. https://doi.org/10.1016/J.JENVMAN.2016.06.025

Charleston County. (1999). *High Tides Affect Drainage Systems*. Charleston, SC Official Website. https://www.charleston-sc.gov/1999/High-Tides-Affect-Drainage-Systems

Charleston County. (2010). *History*. Charleston, SC Official Website. https://www.charleston-sc.gov/2010/History

Chow, V. Te. (1959). *Open-Channel Hydraulics* (H. E. Davis (ed.); Internatio). McGraw-Hill Book Compnay.

Chow, V. Te, Maidment, D. R., & Mays, L. W. (1988). *Applied Hydrology*. McGraw-Hill. http://ponce.sdsu.edu/Applied_Hydrology_Chow_1988.pdf

City of Charleston. (2015). *Sea Level Rise Strategy: Charleston, South Carolina*.

City of Charleston. (2021). *City of Charleston GIS*. https://gis.charleston-sc.gov/

Coleman, S., Hurley, S., Rizzo, D., Koliba, C., & Zia, A. (2018). From the household to watershed: A cross-scale analysis of residential intention to adopt green stormwater infrastructure. *Landscape and Urban Planning*, *180*, 195–206. https://doi.org/10.1016/j.landurbplan.2018.09.005

Cotti-Rausch, B. E., Majidzadeh, H., & DeVoe, M. R. (2019). *Stormwater Ponds in Coastal South Carolina: 2019 State of Knowledge Full Report*. https://www.scseagrant.org/wp-content/uploads/Stormwater-Ponds-State-of-Knowledge-Report.pdf

Dawson, R. J., Peppe, R., & Wang, M. (2011). An agent-based model for risk-based flood incident management. *Natural Hazards*, *59*, 167–189. https://doi.org/10.1007/s11069-011-9745-4

Eckart, K., McPhee, Z., & Bolisetti, T. (2018). Multiobjective optimization of low impact development stormwater controls. *Journal of Hydrology*, *562*, 564–576. https://doi.org/10.1016/j.jhydrol.2018.04.068

Ellis, K., Whiteside, S., Smith, E., Berg, C., Caraco, D., Drescher, S., Hoffmann, G., Keppler, B., LaRocco, M., & Turner, A. (2014). *Low Impact Development in Coastal South Carolina: A Planning and Design Guide*. http://www.northinlet.sc.edu/LID

Farooqui, A. D., & Niazi, M. A. (2016). Game theory models for communication between agents: a review. *Complex Adaptive Systems Modeling*, *4*(13). https://doi.org/10.1186/s40294-016-0026-7

FEMA. (2022). *National Risk Index: Census tract 45019005100, Charleston County, South Carolina*. National Risk Index. https://hazards.fema.gov/nri/map

Gately, D. (1974). Sharing the Gains from Regional Cooperation: a Game Theoretic Application to Planning Investment in Electric Power. *International Economic Review*, *15*(1), 195–208.

Ghodsi, S. H., Zahmatkesh, Z., Goharian, E., Kerachian, R., & Zhu, Z. (2020). Optimal design of low impact development practices in response to climate change. *Journal of Hydrology*, *580*. https://doi.org/10.1016/j.jhydrol.2019.124266

Hamers, H. J. M., Miquel, S., Norde, H. W., & van Velzen, S. (2003). *Fixed Tree Game with Repeated Players*.

Howe, G. M. (1950). *Map of Drainage System Charleston S.C.* https://data-charleston-sc.opendata.arcgis.com/documents/168deb460f4e444fbbab2a676f56097d/about

Hyun, J. Y., Huang, S. Y., Yang, Y. C. E., Tidwell, V., & Macknick, J. (2019). Using a coupled agent-based modeling approach to analyze the role of risk perception in water management decisions. *Hydrology and Earth System Sciences*, *23*(5), 2261–2278. https://doi.org/10.5194/HESS-23-2261-2019

Ichihara, K., & Cohen, J. P. (2010). New York City property values: what is the impact of green roofs on rental pricing? *Letters in Spatial and Resource Sciences*, *4*(1), 21–30. https://doi.org/10.1007/S12076-010-0046-4

Insurance Journal. (2019). *Venice Hotels Suffer Nearly $34M in Damages from November's Floods*. Insurance Journal. https://www.insurancejournal.com/news/international/2019/12/23/552711.htm

Just, R. E., & Netanyahu, S. (2004). Implications of "Victim Pays" Infeasibilities for Interconnected Games with an Illustration for Aquifer Sharing under Unequal Access Costs. *Water Resources Research*, *40*(5).

Kilgour, D. M., Nishikori, A., & Okada, N. (1988). Control Regulation of Water Pollution: An Analysis Using Game Theory. *Journal of Environmental Management*, *27*, 179–194.

Kim, J., Lee, J., Song, Y., Han, H., & Joo, J. (2018). Modeling the runoffreduction effect of low impact development installations in an industrial area, South Korea. *Water (Switzerland)*, *10*(8). https://doi.org/10.3390/w10080967

Lawyer, C., & Goharian, E. (2021). Protecting Cultural Identity and Tourism Against Flooding in Charleston, South Carolina's Old Historic District. *EWRI Congress*.

Lawyer, C., & Goharian, E. (2020). Developing Resilient Optimal Flood Control Portfolios for Low Country Flooding: Charleston, South Carolina. *AGU Fall Meeting*, H164-0005.

Loucks, D. P., & Beek, E. van. (2017). Water Resources Planning and Management: An Overview. In *Water Resource Systems Planning and Management*. Springer, Cham. https://doi.org/10.1007/978-3-319-44234-1_1

Macal, C. M., & North, M. J. (2010). Tutorial on agent-based modelling and simulation. *Journal of Simulation*, *4*, 151–162. https://doi.org/10.1057/jos.2010.3

Macro, K., Matott, L. S., Rabideau, A., Ghodsi, H., & Zhu, Z. (2019). OSTRICH-SWMM: A new multi-objective optimization tool for green infrastructure planning with SWMM. *Environmental Modelling and Software*, *113*, 42–47. https://doi.org/10.1016/j.envsoft.2018.12.004

Madani, K. (2010). Game theory and water resources. *Journal of Hydrology*, *381*, 225–238. https://doi.org/10.1016/j.jhydrol.2009.11.045

Manson, S. M. (2001). Calibration, Verification, and Validation. In Dawn C. Parker, T. Berger, & S. M. Manson (Eds.), *Meeting the Challenge of Complexity: Proceedings of a Special Workshop on Land-Use/Land-Cover Change* (pp. 42–46). Center for Spatially Integrated Social Science at University of California at Santa Barbara.

Mein, R.G, & Larson, C. L. (1973). Modeling Infiltration during a Steady Rain. *Water Resources Research*, *9*(2), 384–394.

Meney, K. A., & Pantelic, L. (2022). Decentralized Water and Wastewater Systems for Resilient Societies: A Shift Towards a Green Infrastructure-Based Alternate Economy. In *The Palgrave Handbook of Climate Resilient Societies* (pp. 157–184). Springer International Publishing.

Michaelis, T., Brandimarte, L., Mazzoleni, M., Archfield, S., & Pande, S. (2020). Capturing flood-risk dynamics with a coupled agent-based and hydraulic modelling framework. *Hydrological Sciences Journal*, *65*(9), 1458–1473. https://doi.org/10.1080/02626667.2020.1750617

Milly, P. C. D., Betancourt, J., Falkenmark, M., Hirsch, R. M., Kundzewicz, Z. W., Lettenmaier, D. P., & Stouffer, R. J. (2008). Stationarity Is Dead: Whither Water Management? *New Series*, *319*(5863), 573–574. https://doi.org/10.1126/science.ll51915

Montalto, F. A., Bartrand, T. A., Waldman, A. M., Travaline, K. A., Loomis, C. H., McAfee, C., Geldi, J. M., Riggall, G. J., & Boles, L. M. (2013). Decentralised green infrastructure: The importance of stakeholder behaviour in determining spatial and temporal outcomes. *Structure and Infrastructure Engineering*, *9*(12), 1187–1205. https://doi.org/10.1080/15732479.2012.671834

Morbidelli, R., Corradini, C., Saltalippi, C., Flammini, A., Dari, J., & Govindaraju, R. S. (2018). Rainfall infiltration modeling: A review. *Water (Switzerland), 10*(12). https://doi.org/10.3390/w10121873

Morris, J. T., & Renken, K. A. (2020). Past, present, and future nuisance flooding on the Charleston peninsula. *PLoS ONE*, *15*(9). https://doi.org/10.1371/journal.pone.0238770

Myerson, R. B. (1991). *Game Theory: Analysis of Conflict*. Harvard University Press.

Niazi, M. A., & Hussain, A. (2012). *Cognitive Agent-based Computing-I: A Unified Framework for Modeling Complex Adaptive Systems using Agent-based & Complex Network-based Methods*. Springer Netherlands. http://www.springer.com/series/10374

NOAA. (2016). The Historic South Carolina Floods of October 1-5, 2015. In *Service Assessment*. https://www.weather.gov/media/publications/assessments/SCFlooding_072216_Signed_Final.pdf

NOAA. (2019). *Sea Level Rise: Charleston, Berkeley, Dorchester*. Sea Level Rise Data Download. https://coast.noaa.gov/slrdata/

NOAA. (2022). *U.S. coastline to see up to a foot of sea level rise by 2050*. https://www.noaa.gov/news-release/us-coastline-to-see-up-to-foot-of-sea-level-rise-by-2050

NOAA, & National Weather Service. (2022). *Coastal Flood Event Database Charleston Harbor*. Coastal Flood Database; NOAA's National Weather Service. https://doi.org/10.2/JQUERY.MIN.JS

Office of Tourism Analysis. (2018). *2017-2018 Office of Tourism Analysis Annual Report*.

Parker, D. C., Manson, S. M., Janssen, M. A., Hoffmann, M. J., & Deadman, P. (2003). Multi-agent systems for the simulation of land-use and land-cover change: A review. *Annals of the Association of American Geographers*, *93*(2), 310–320.

Parrachino, I., Dinar, A., & Patrone, F. (2006). *Cooperative Game Theory and Its Application to Natural, Environmental and Water Resource Issues: 3. Application to Water Resources* (No. 4074; The Policy Research Working Paper Series). http://econ.worldbank.org.

Patt, A., & Siebenhüner, B. (2005). Agent Based Modeling and Adaptation to Climate Change. *Quarterly Journal of Economic Research*, *74*(2), 310–320. https://doi.org/10.3790/vjh.74.2.310

Peterson, B., & Porter, M. (2020, January 3). Charleston and the South Carolina coast ooded record 89 times in 2019. *Post and Courier*. https://www.postandcourier.com/news/charleston-and-the-south-carolina-coast-flooded-record-times-in/article_7c18ee5e-2e3b-11ea-8784-23ddbc8d4e0c.html

Platt, S. E. (2020). Urban Dialectics, Misrememberings, and Memory-Work: The Halsey Map of Charleston, South Carolina. *International Journal of Historical Archaeology*, *24*(4), 989–1014. https://doi.org/10.1007/S10761-019-00533-8

Qin, H. peng, Li, Z. xi, & Fu, G. (2013). The effects of low impact development on urban flooding under different rainfall characteristics. *Journal of Environmental Management*, *129*, 577–585. https://doi.org/10.1016/j.jenvman.2013.08.026

Raei, E., Reza Alizadeh, M., Reza Nikoo, M., & Adamowski, J. (2019). Multi-objective decision-making for green infrastructure planning (LID-BMPs) in urban storm water management under uncertainty. *Journal of Hydrology*, *579*. https://doi.org/10.1016/j.jhydrol.2019.124091

Simpson, M. G. (2010). *Low Impact Development Modeling to Manage Urban Storm Water Runoff and Restore Predevelopment Site Hydrology*. Colorado State University.

South Carolina Climatology Office. (2013). *South Carolina Climate*. https://www.dnr.sc.gov/climate/sco/ClimateData/cli_sc_climate.php#precipitation

Spanger-Siegfried, E., Fitzpatrick, M., & Dahl, K. (2014). *Encroaching Tides: How Sea Level Rise and Tidal Flooding Threaten U.S. East and Gulf Coast Communities over the Next 30 Years*. https://www.ucsusa.org/sites/default/files/attach/2014/10/encroaching-tides-full-report.pdf

Stormwater Ponds Research and Management Collaborative. (2014). *Inventory of Stormwater Ponds in the Eight Coastal Counties of South Carolina*.

Tavakol-Davani, H. E., Tavakol-Davani, H., Burian, S. J., Mcpherson, B. J., & Barber, M. E. (2019). Green infrastructure optimization to achieve pre-development conditions of a semiarid urban catchment. *Environmental Science: Water Research & Technology*, *5*, 1157. https://doi.org/10.1039/c8ew00789f

Ureta, J., Motallebi, M., Scaroni, A. E., Lovelace, S., & Ureta, J. C. (2021). Understanding the public's behavior in adopting green stormwater infrastructure. *Sustainable Cities and Society*, *69*(February), 102815. https://doi.org/10.1016/j.scs.2021.102815

USDA, & NRCS. (2017). *National Elevation Dataset 3 Meter, 15 maps*. GeoSpatial Data Gateway. https://datagateway.nrcs.usda.gov/GDGHome.aspx

USDA, & NRCS. (2019). *LiDAR Elevation Dataset - Bare Earth DEM - 1 Meter, 15 maps*. GeoSpatial Data Gateway. https://datagateway.nrcs.usda.gov/

Van De Meene, S. J., Brown, R. R., & Farrelly, M. A. (2009). Exploring sustainable urban water governance: A case study of institutional capacity. *Water Science and Technology*, *59*(10), 1921–1928. https://doi.org/10.2166/wst.2009.190

Vandiver, L., & Hernandez, D. (2010). *Assessment of Stormwater Management in Coastal South Carolina: A Focus on Stormwater Ponds and Low Impact Development (LID) Practices*. https://www.scseagrant.org/assessment-of-stormwater-management-in-coastal-south-carolina-a-focus-on-stormwater-ponds-and-low-impact-development-lid-practices/

Voicu, I., & Been, V. (2008). The Effect of Community Gardens on Neighboring Property Values. *Real Estate Economics*, *36*(2), 241–283.

Weather Underground. (2015). *Charleston Air Force Base, SC Weather History*. Weather Underground. https://www.wunderground.com/history/daily/us/sc/charleston-air-force-base/KCHS/date/2015-10-1

William, R., Garg, J., & Stillwell, A. S. (2017). A game theory analysis of green infrastructure stormwater management policies. *Water Resources Research*, *53*(9), 8003–8019. https://doi.org/10.1002/2017WR021024

Williams, E., & Moore, T. (2020, October 19). Rising tides take Charleston to the brim, threatening businesses. *The Post and Courier*. https://www.postandcourier.com/rising-waters/rising-tides-take-charleston-to-the-brim-threatening-businesses/article_4282b1be-fc28-11ea-891d-07e663e3afed.html

Xu, T., Jia, H., Wang, Z., Mao, X., & Xu, C. (2017). SWMM-based methodology for block-scale LID-BMPs planning based on site-scale multi-objective optimization: a case study in Tianjin. *Frontiers of Environmental Science and Engineering*, *11*(4). https://doi.org/10.1007/s11783-017-0934-6

Yang, L. E., Scheffran, J., Süsser, D., Dawson, R., & Chen, Y. D. (2018). Assessment of Flood Losses with Household Responses: Agent-Based Simulation in an Urban Catchment Area. *Environmental Modeling and Assessment*, *23*(4), 369–388. https://doi.org/10.1007/s10666-018-9597-3

York, C., Goharian, E., & Burian, S. J. (2015). Impacts of Large-Scale Stormwater Green Infrastructure Implementation and Climate Variability on Receiving Water Response in the Salt Lake City Area. *American Journal of Environmental Sciences*, *11*(4), 278–292. https://doi.org/10.3844/ajessp.2015.278.292

Zahmatkesh, Z., Steven, J. B., Karamouz, M., Tavakol-Davani, H., & Goharian, E. (2014). Low-Impact Development Practices to Mitigate Climate Change Effects on Urban Stormwater Runoff: Case Study of New York City. *Journal of Irrigation and Drainage Engineering*, *14*(1). https://doi.org/10.1061/(ASCE)IR.1943-4774.0000770

APPENDIX A

GAME SCENARIO HYDROGRAPHS

The following are PCSWMM hydrographs which illustrate changes in hydrological processes observed during the modeled historic South Carolina 2015 flood event in Charleston's Market Street watershed. Comparisons highlight notable differences in system flood and runoff volumes, subbasin runoff volumes, and junction flood volumes between the no underdrain and drain scenarios and also between the most flood damage cost saving coalitions for each game. Because the hydrographs are taken directly from PCSWMM results, some model components are labeled differently. On some of the graphs provided, Subbasins A, B, C, D, E are referred to as Subbasins 6.1, 6.2, 6.3, 6.4, and 6.5, respectively. Additionally, the words node and junction are used interchangeably. Node locations within each subbasin can be referred to in Figure 4.10.

A.1 Game 1 System Flooding

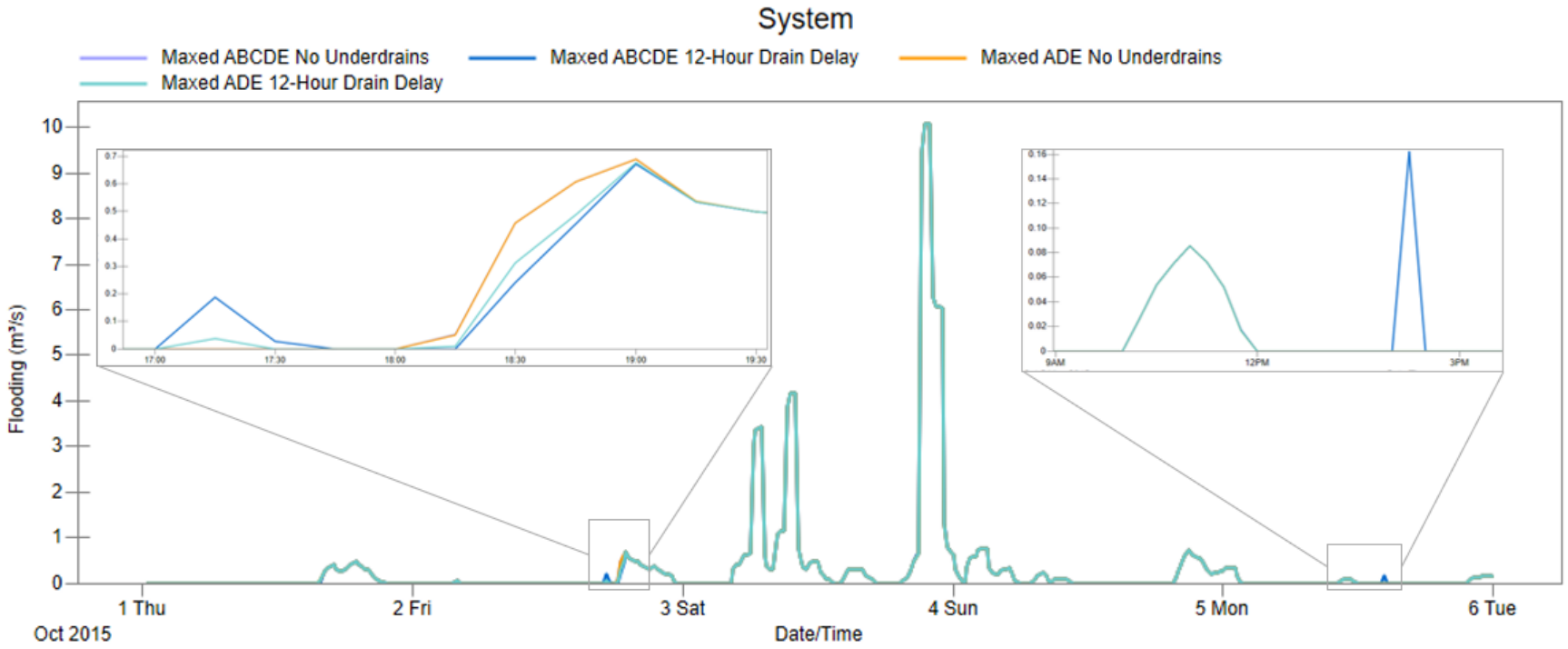

Figure A.1: Game 1 “Maxed” System Flooding

A.2 Game 1 System Runoff

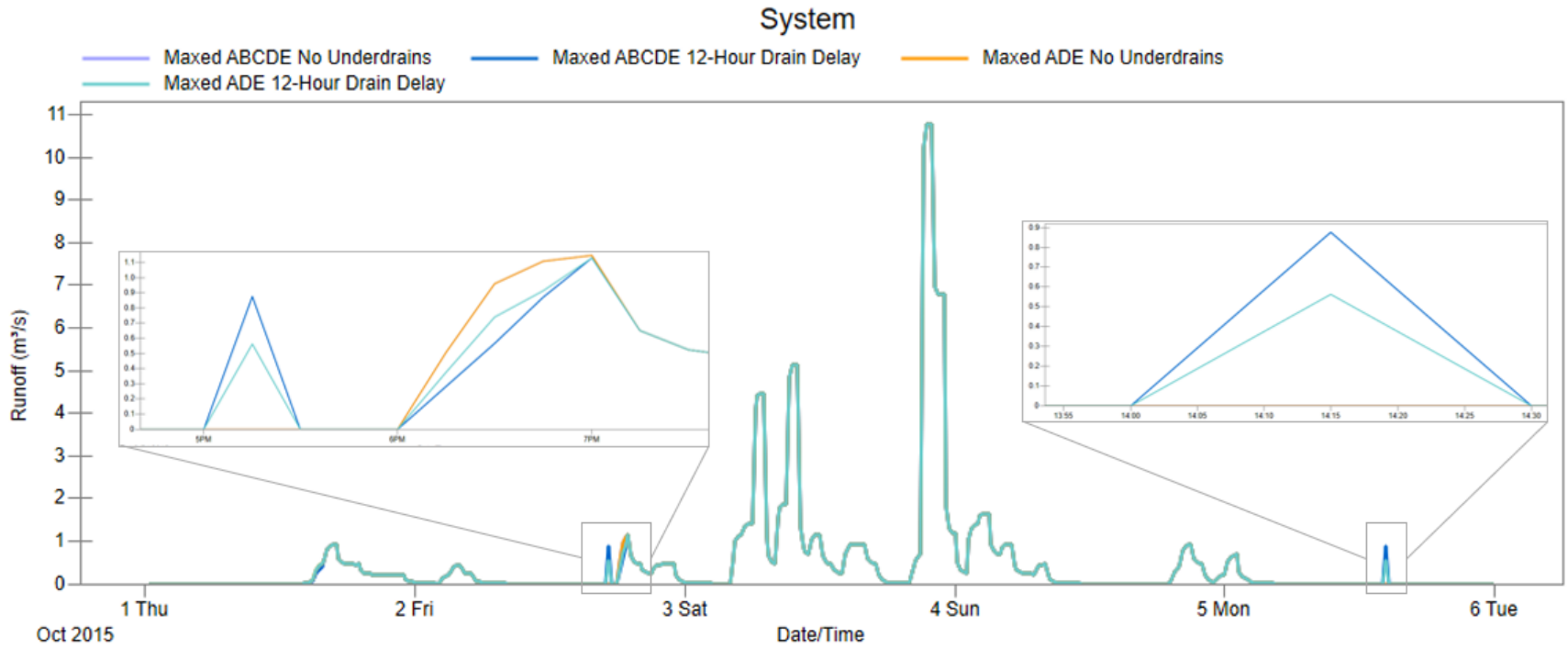

Figure A.2: Game 1 System Runoff

A.3 Game 1 Subbasin A Runoff

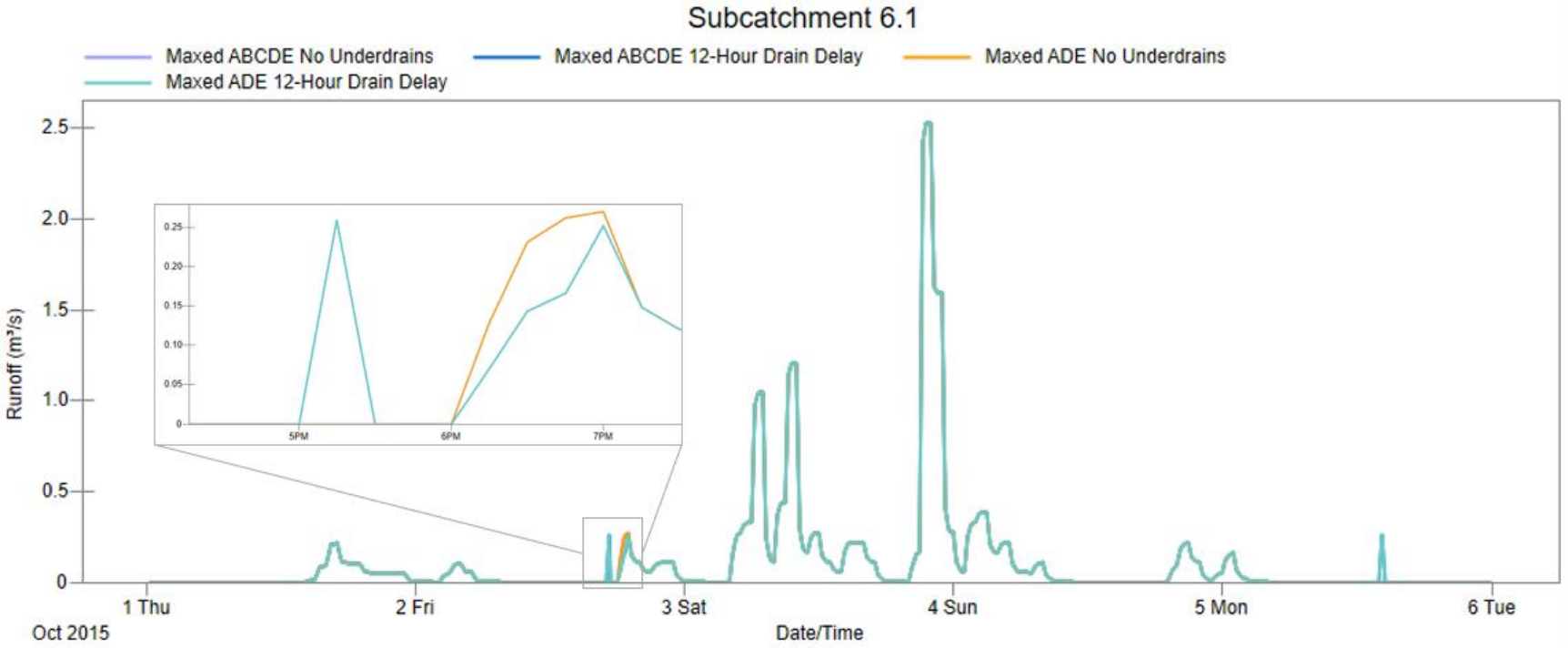

Figure A.3: Game 1 Subbasin A Runoff

A.4 Game 1 Subbasin B Runoff

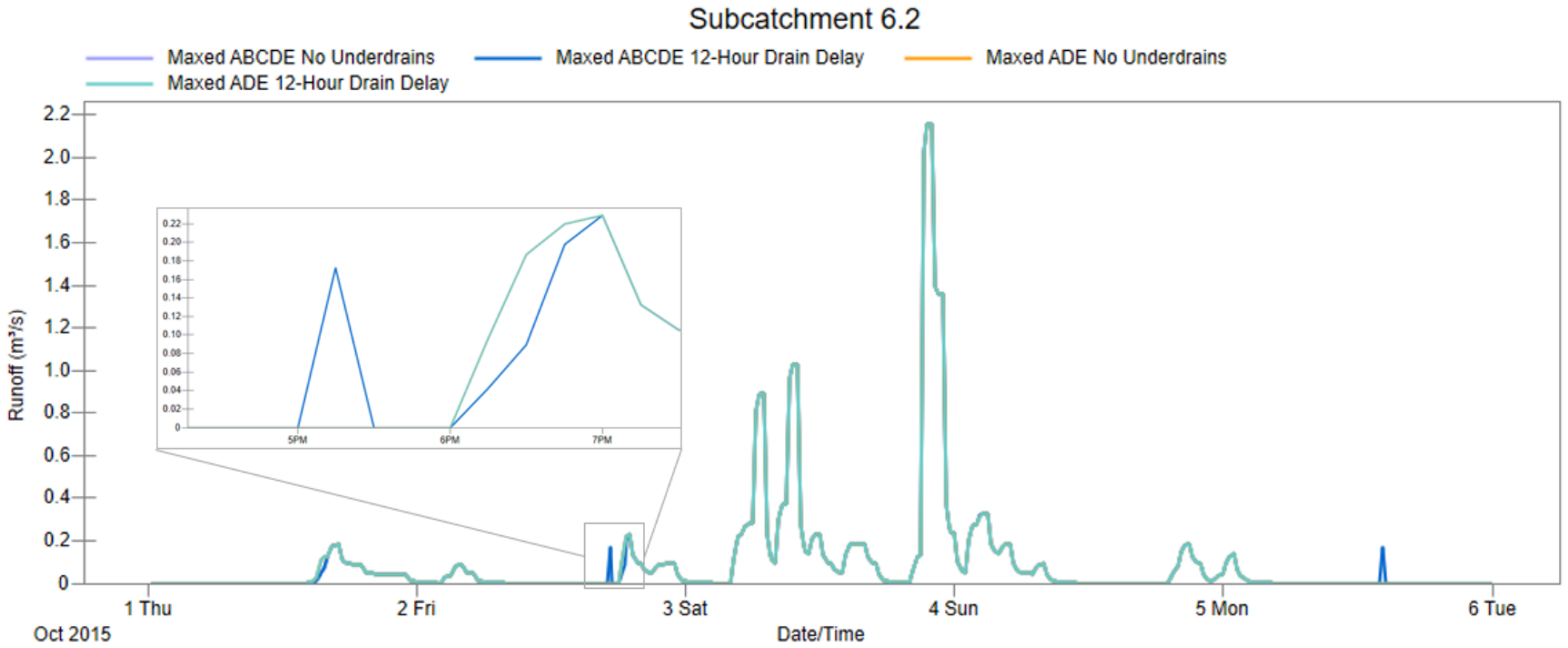

Figure A.3: Game 1 Subbasin B Runoff

A.5 Game 1 Subbasin C Runoff

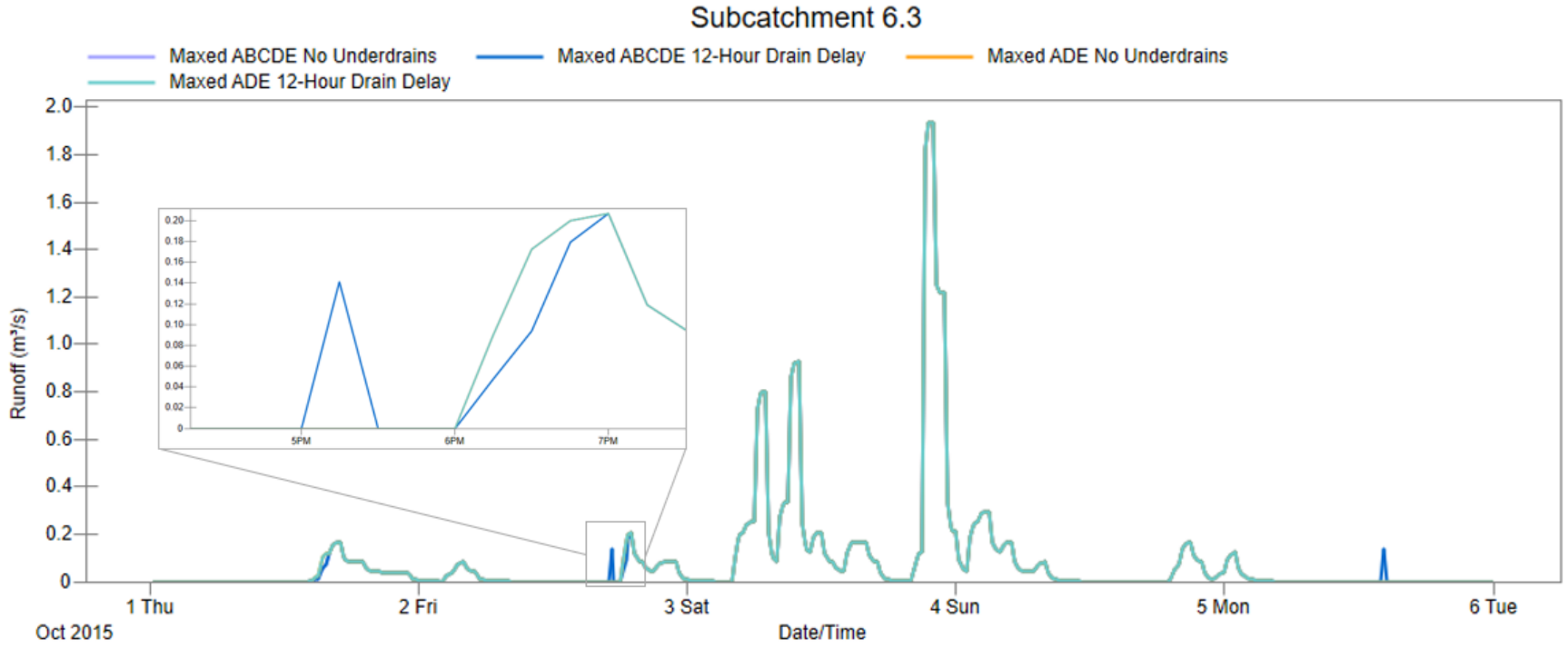

Figure A.5: Game 1 Subbasin C Runoff

A.6 Game 1 Subbasin D Runoff

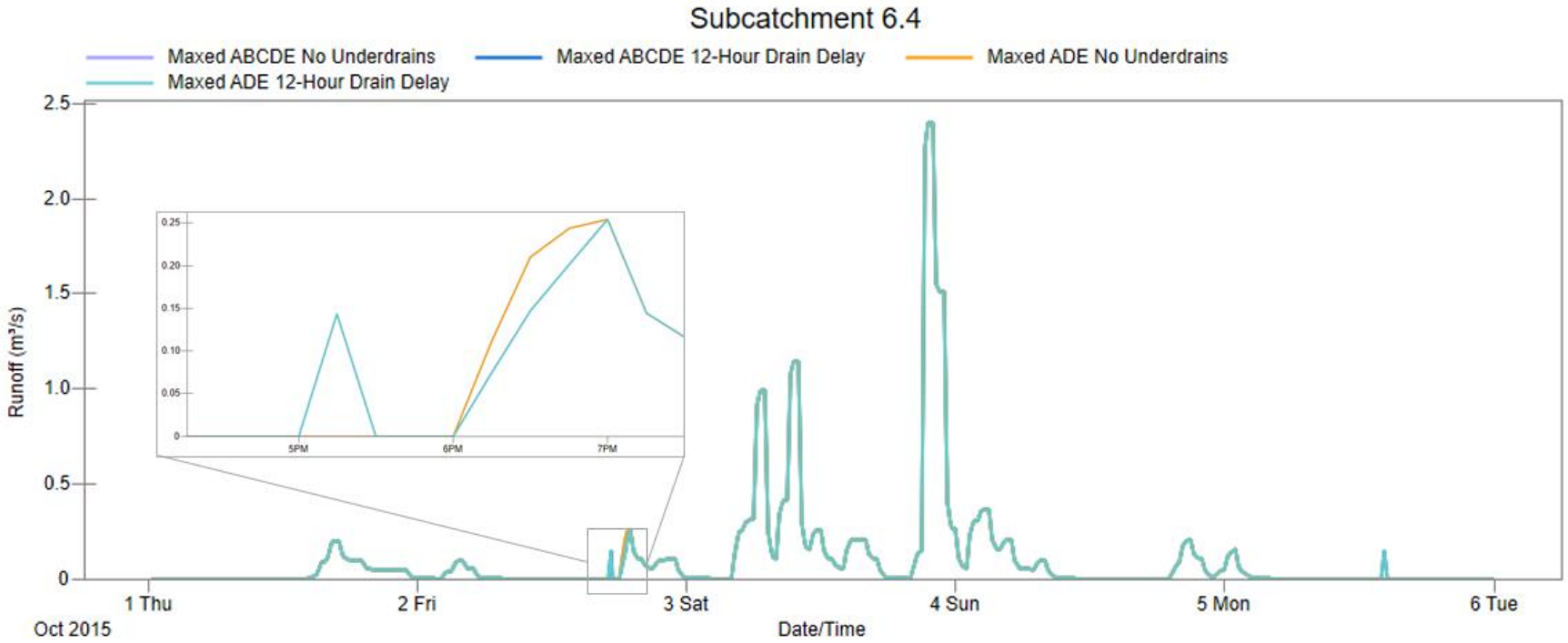

Figure A.6: Game 1 Subbasin D Runoff

A.7 Game 1 Subbasin E Runoff

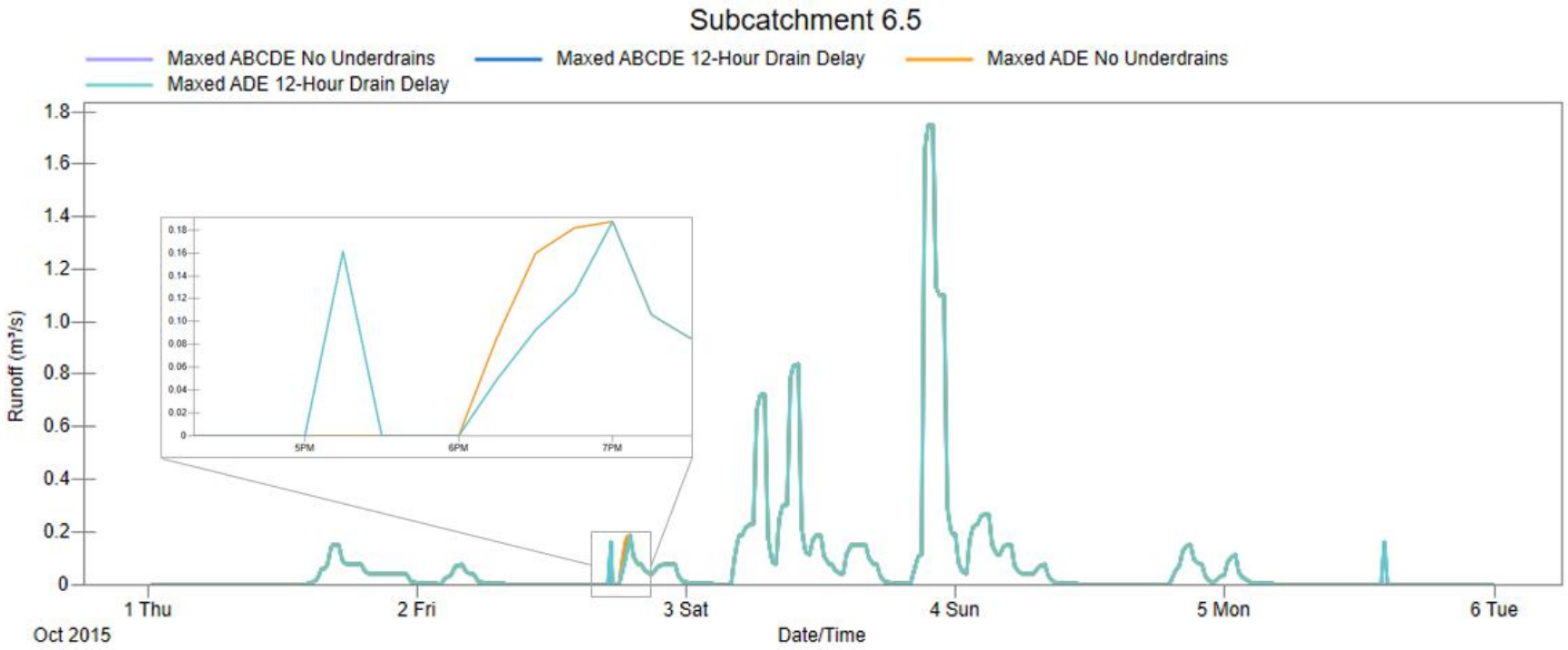

Figure A.7: Game 1 Subbasin E Runoff

A.8 Game 1 Junction 6.3.4 Flooding

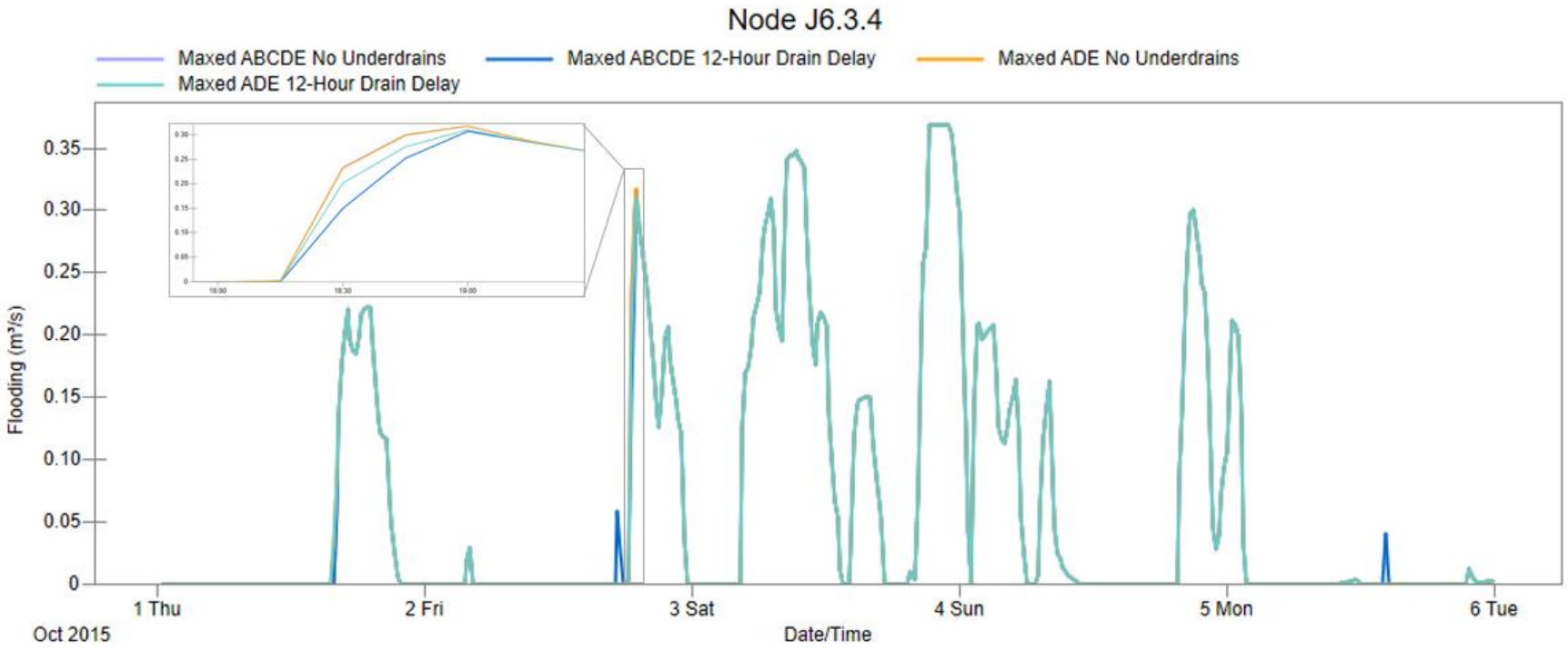

Figure A.8: Game 1 Junction 6.3.4 Flooding

Figure A.9 Game 1 Junction 6.4.2 Flooding

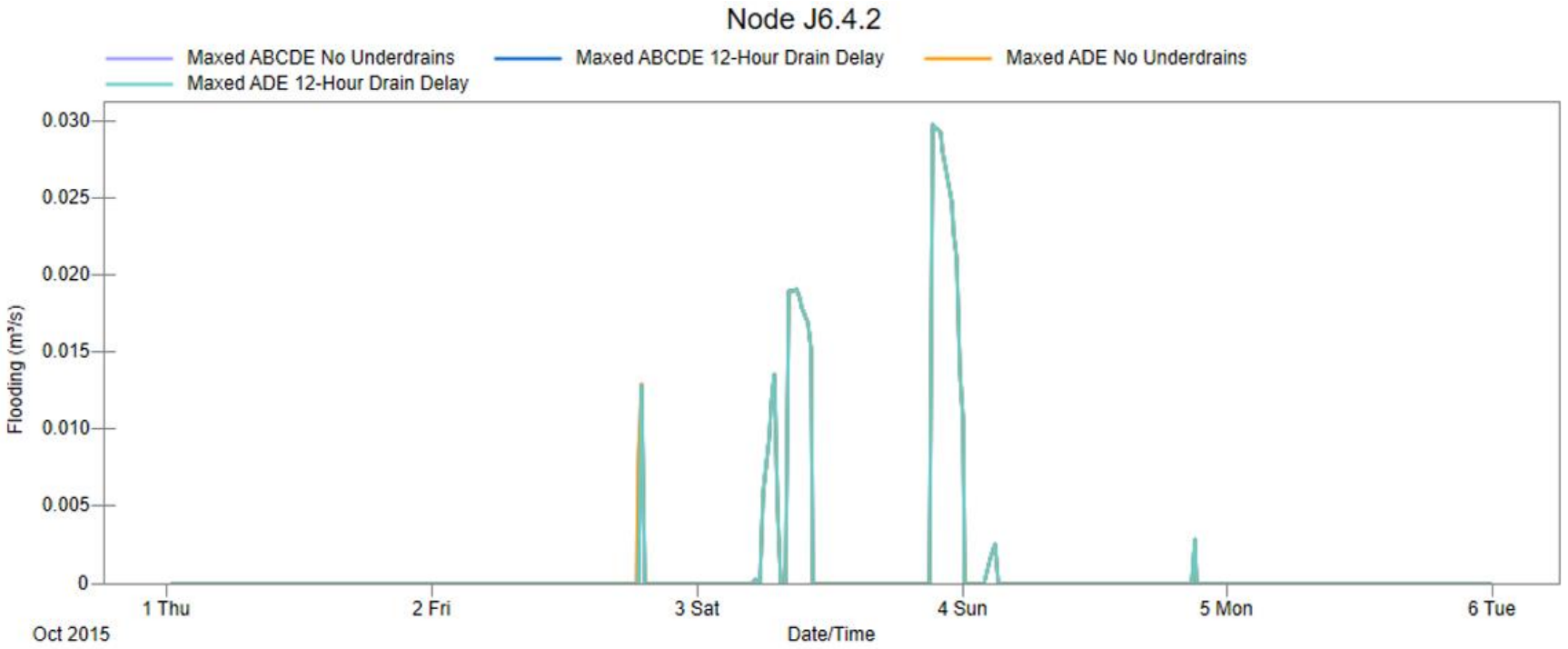

Figure A.9: Game 1 Junction 6.4.2 Flooding

Figure A.10: Game 1 Junction 6.4.4 Flooding

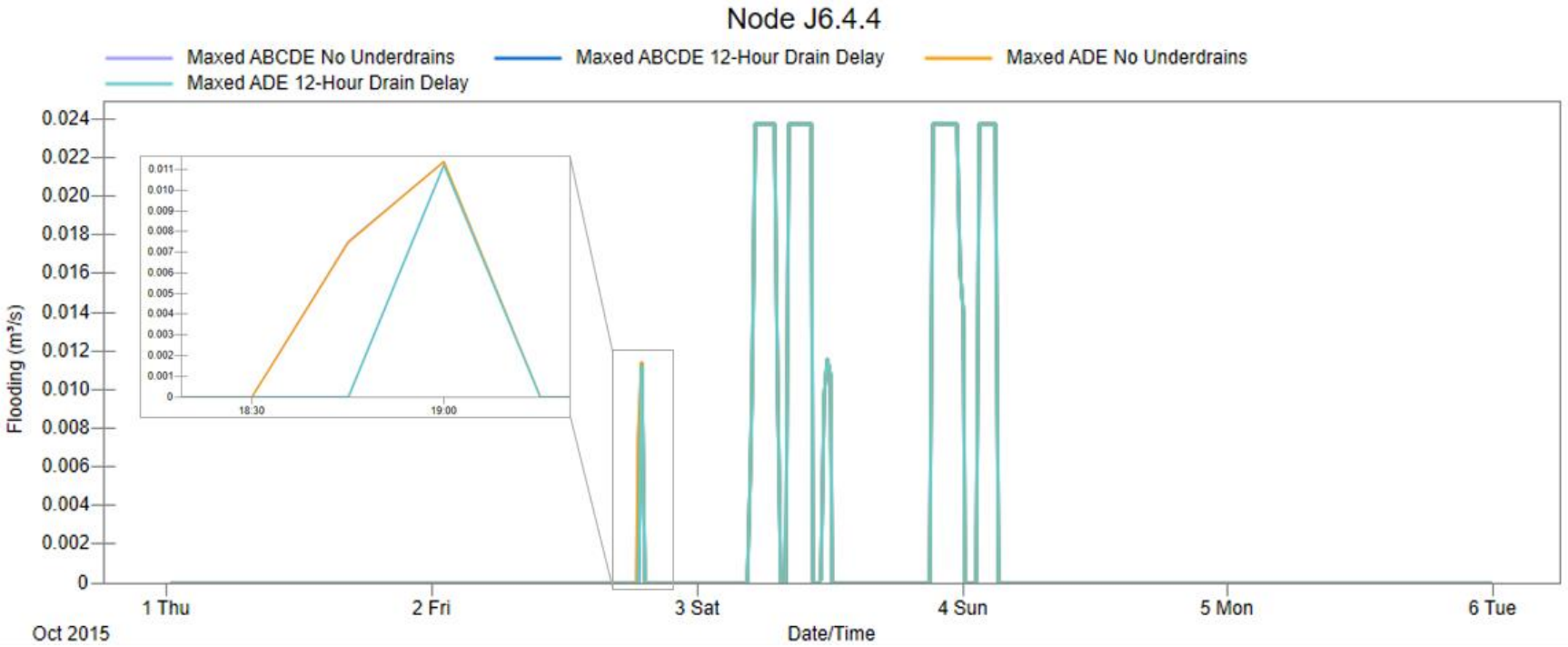

Figure A.10: Game 1 Junction 6.4.4 Flooding

A.11 Game 1 Junction 6.4.5 Flooding

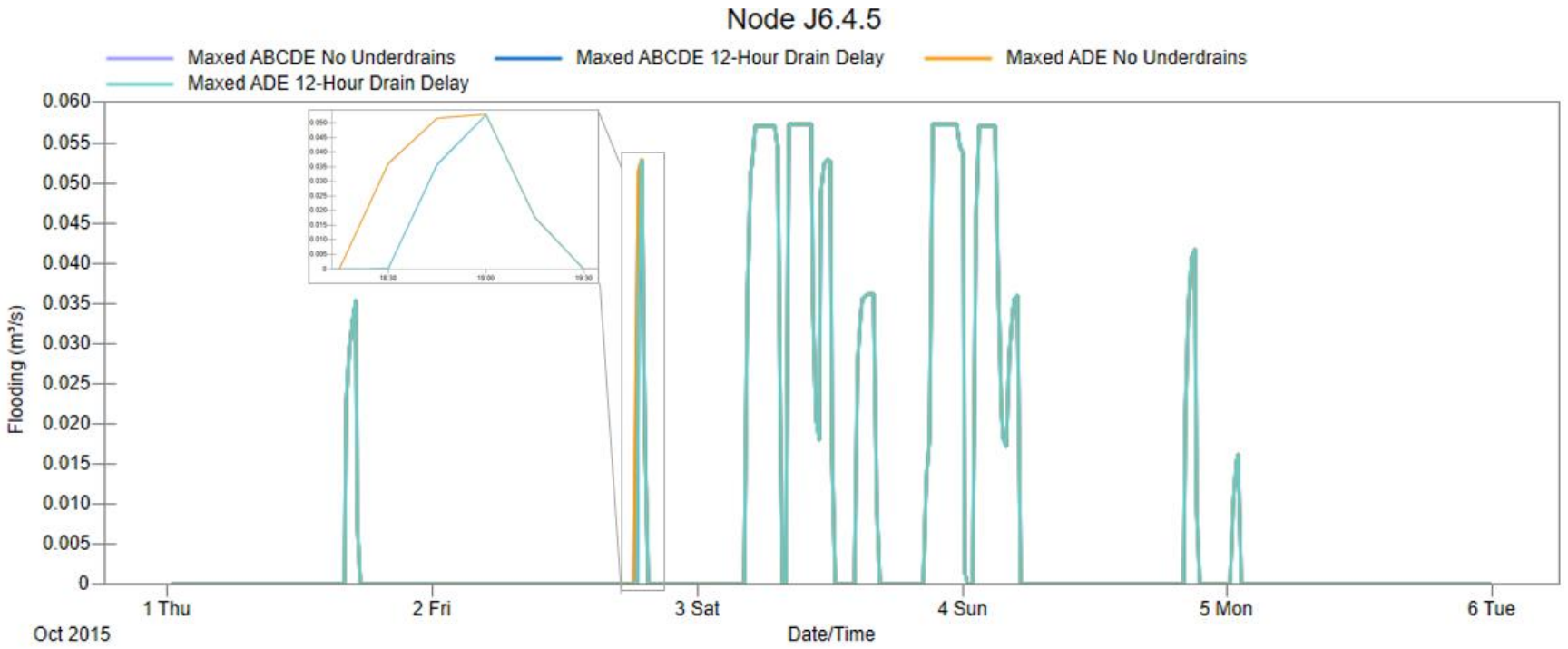

Figure A.11: Game 1 Junction 6.4.5 Flooding

Figure A.12 Game 1 Junction 6.5.1 Flooding

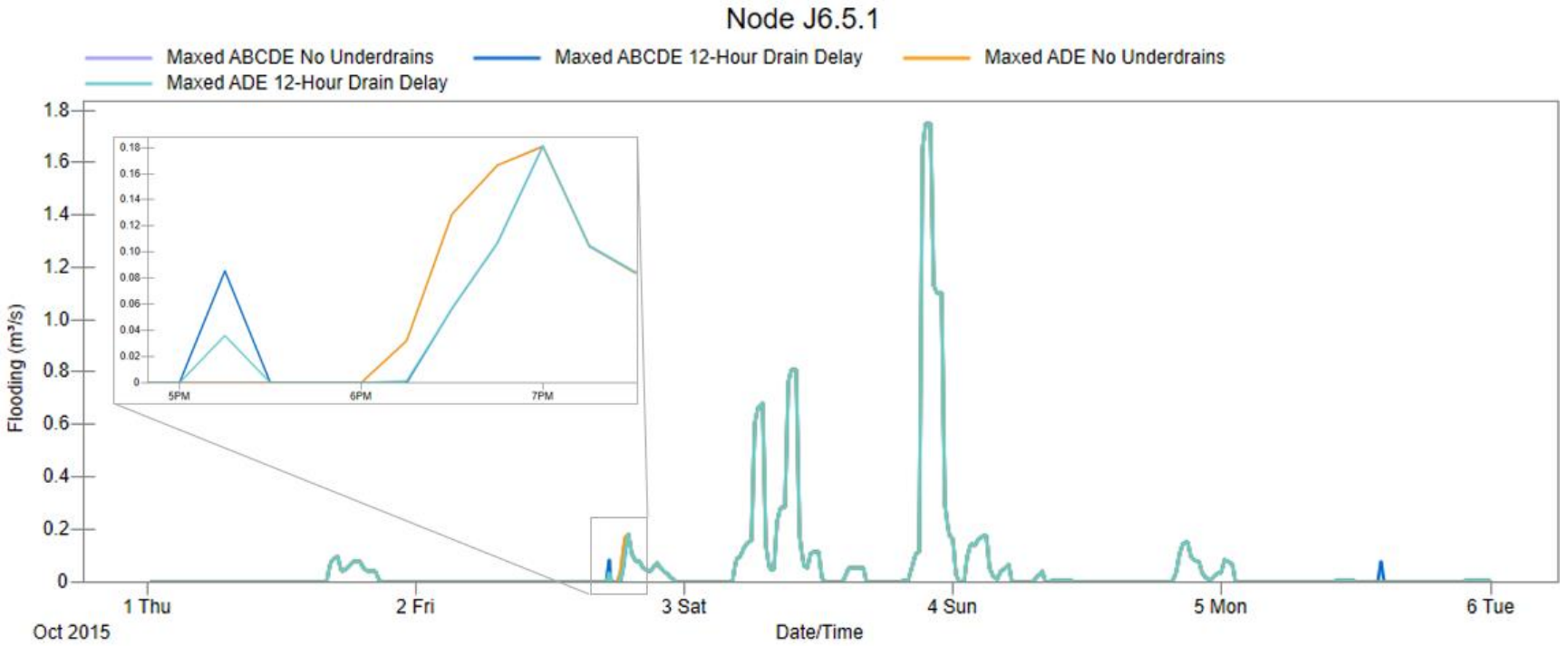

Figure A.12: Game 1 Junction 6.5.1 Flooding

A.13 Game 1 Junction 6.5.5 Flooding

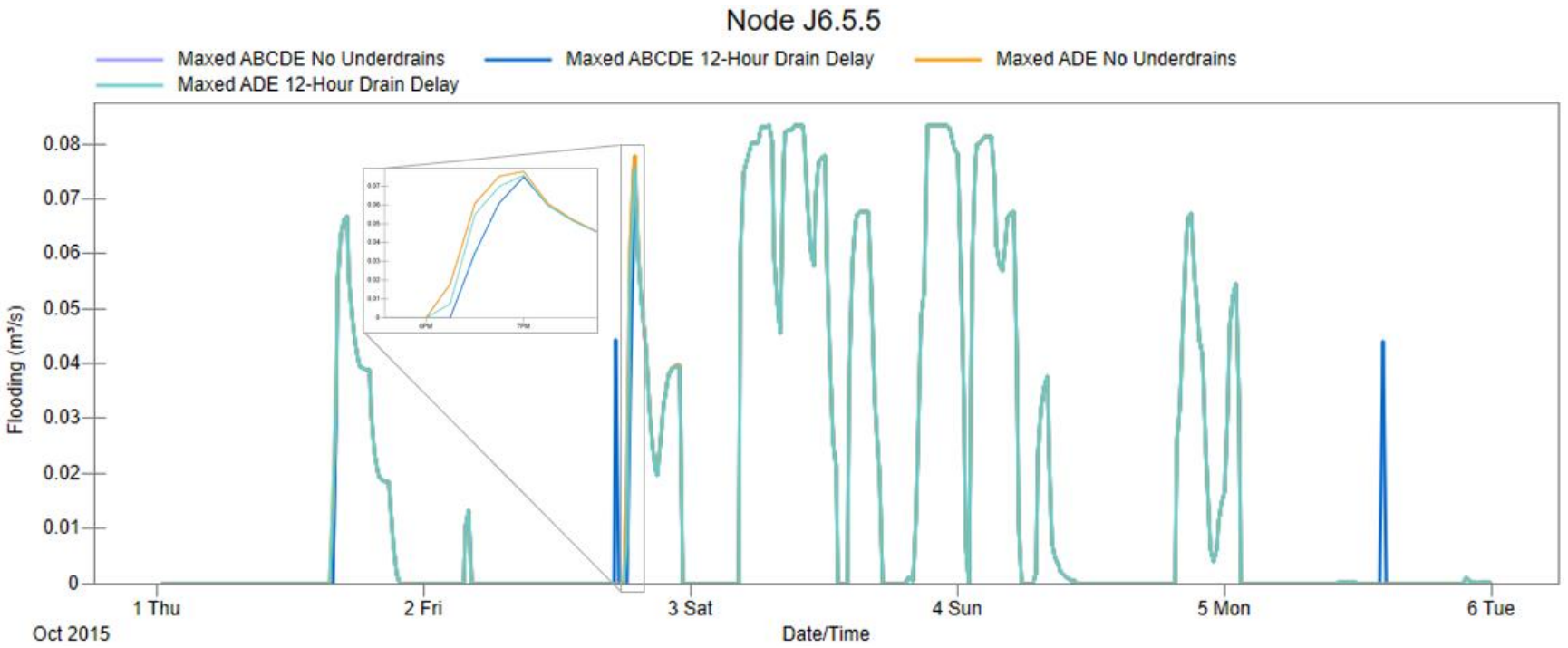

Figure A.13: Game 1 Junction 6.5.5 Flooding

APPENDIX B

GAME 2 HYDROGRAPHS

B.1 Game 2 System Flooding

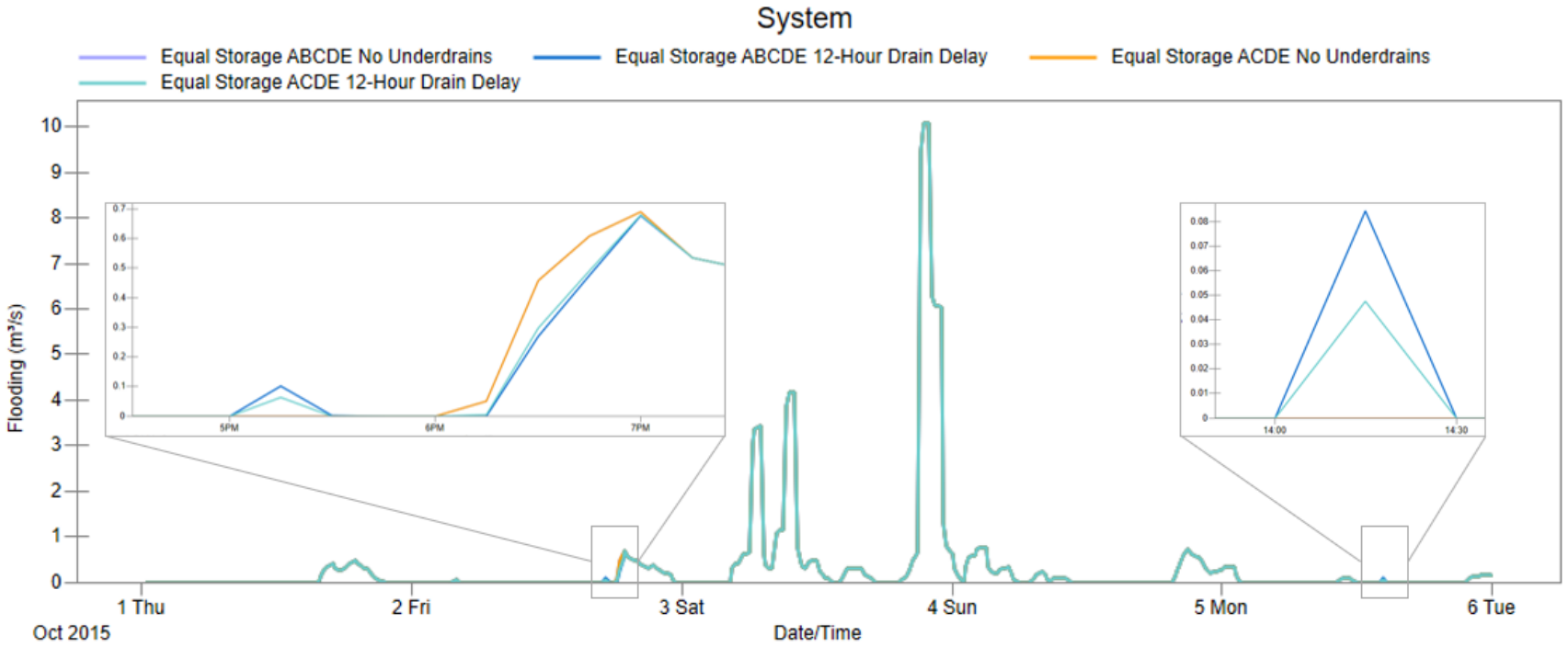

Figure B.1: Game 2 System Flooding

B.2 Game 2 System Runoff

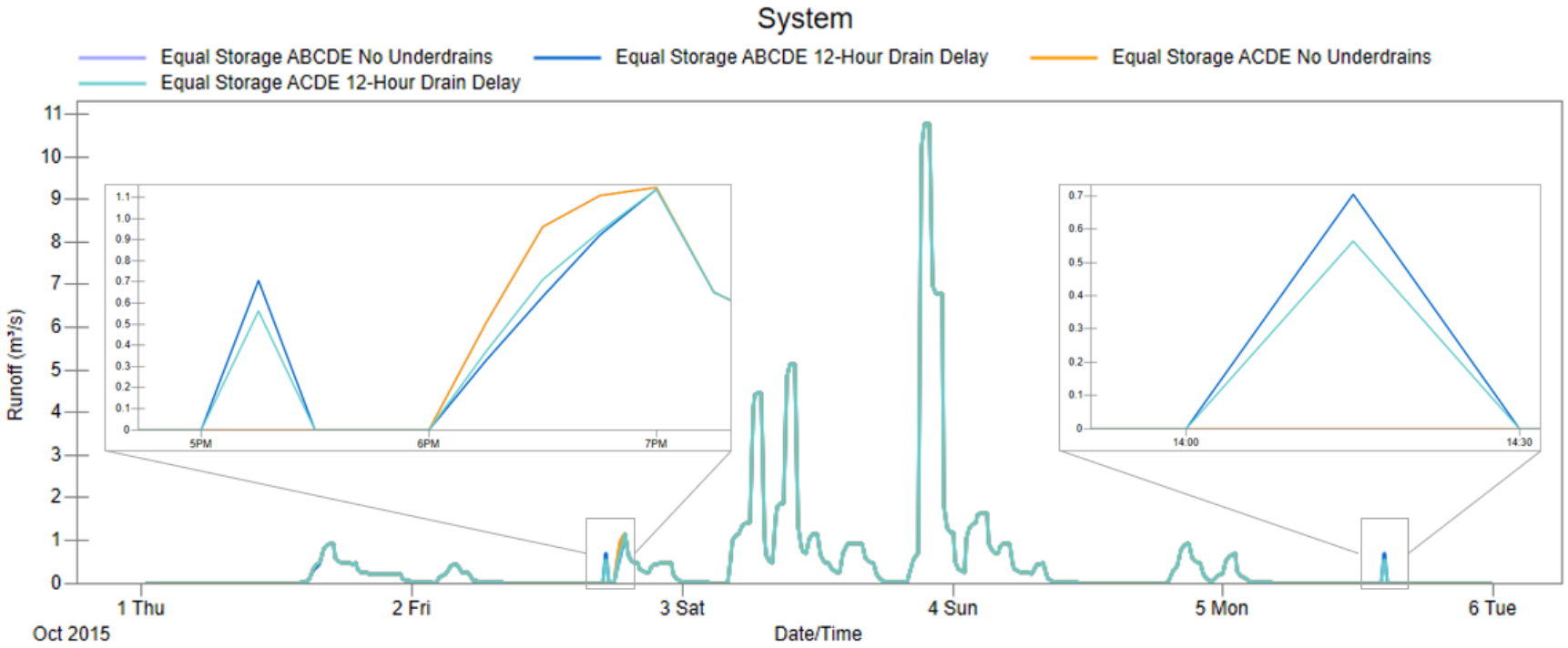

Figure B.2: Game 2 System Runoff

B.3 Game 2 Subbasin A Runoff

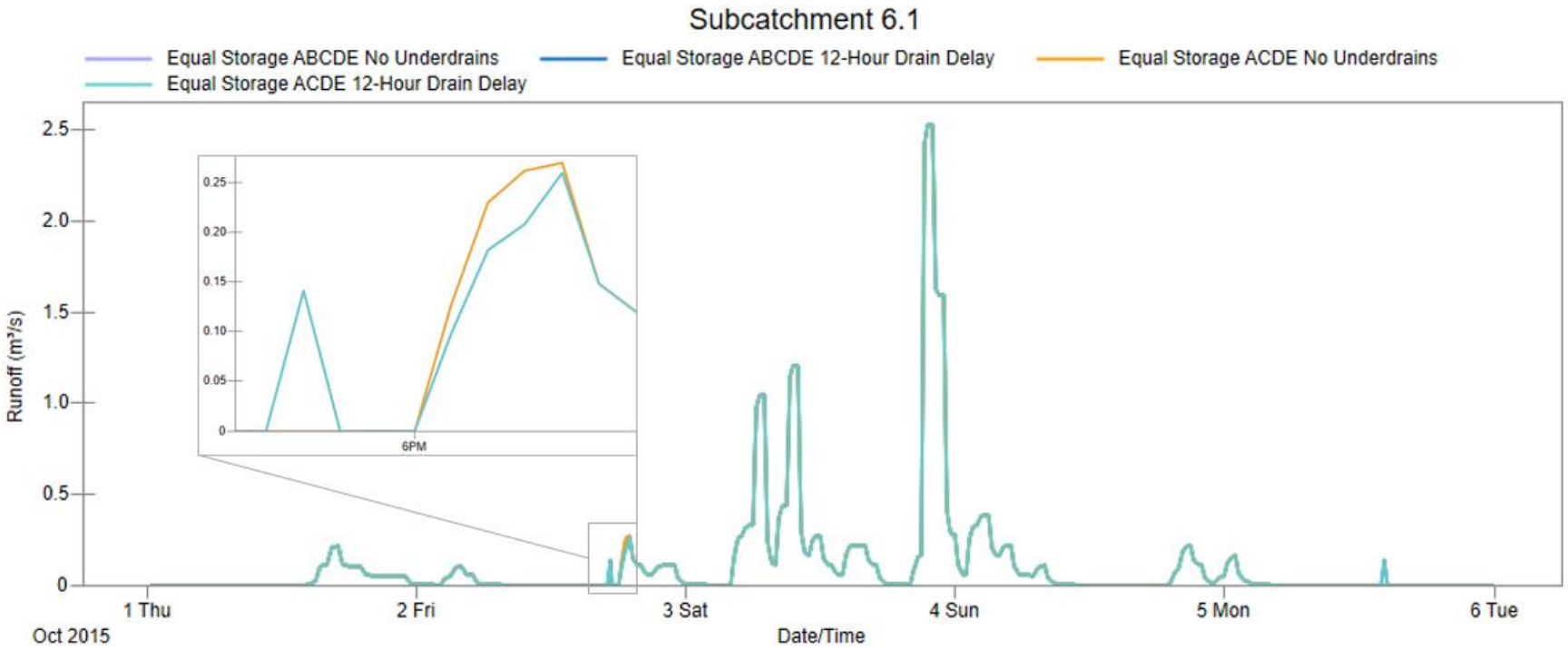

Figure B.3: Game 2 Subbasin A Runoff

B.4 Game 2 Subbasin B Runoff

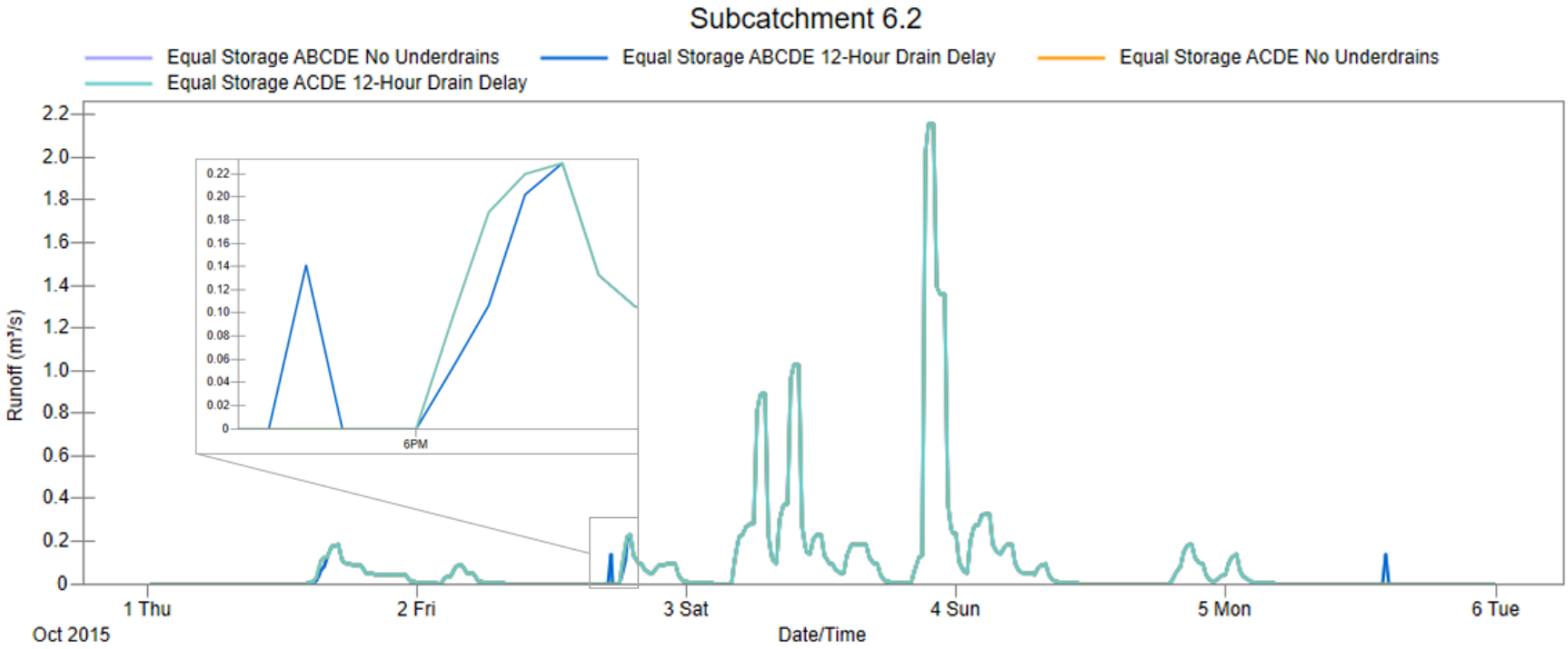

Figure B.4: Game 2 Subbasin B Runoff

B.5 Game 2 Subbasin C Runoff

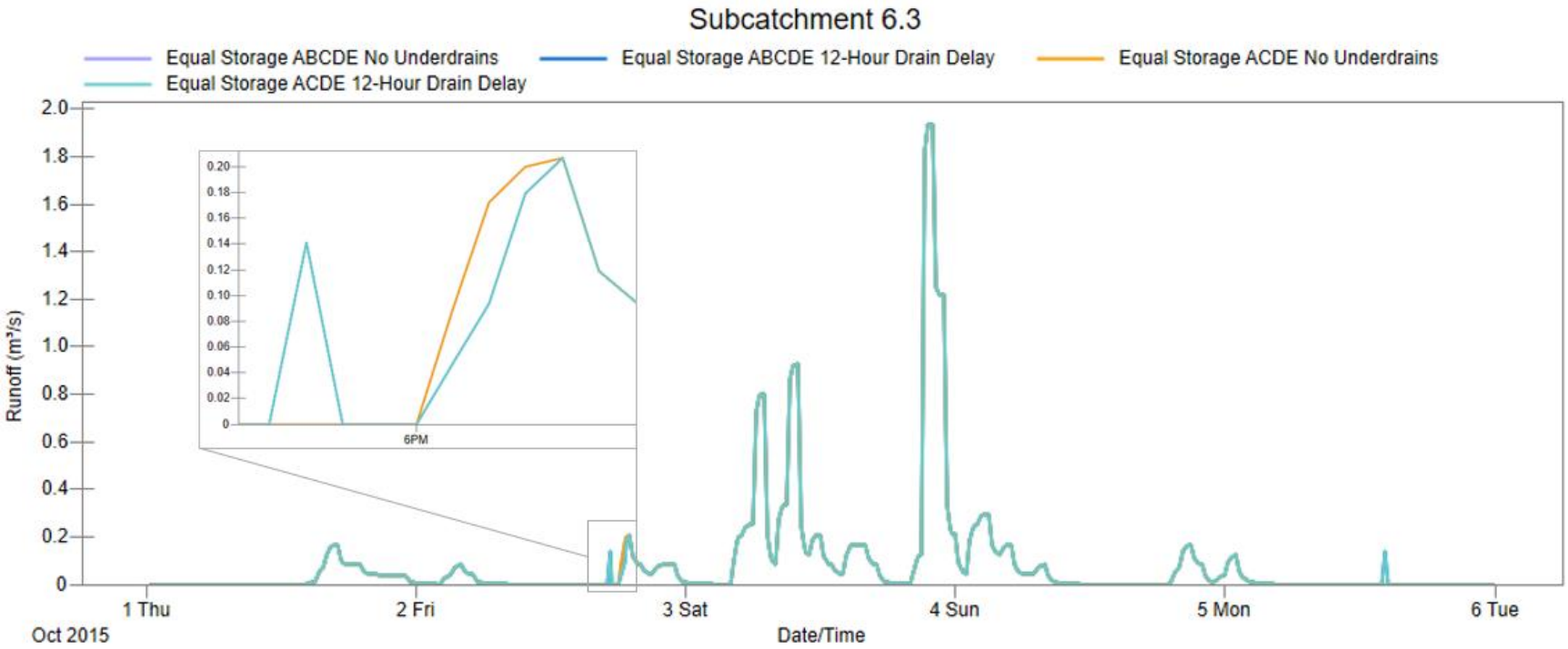

Figure B.5: Game 2 Subbasin C Runoff

B.6 Game 2 Subbasin D Runoff

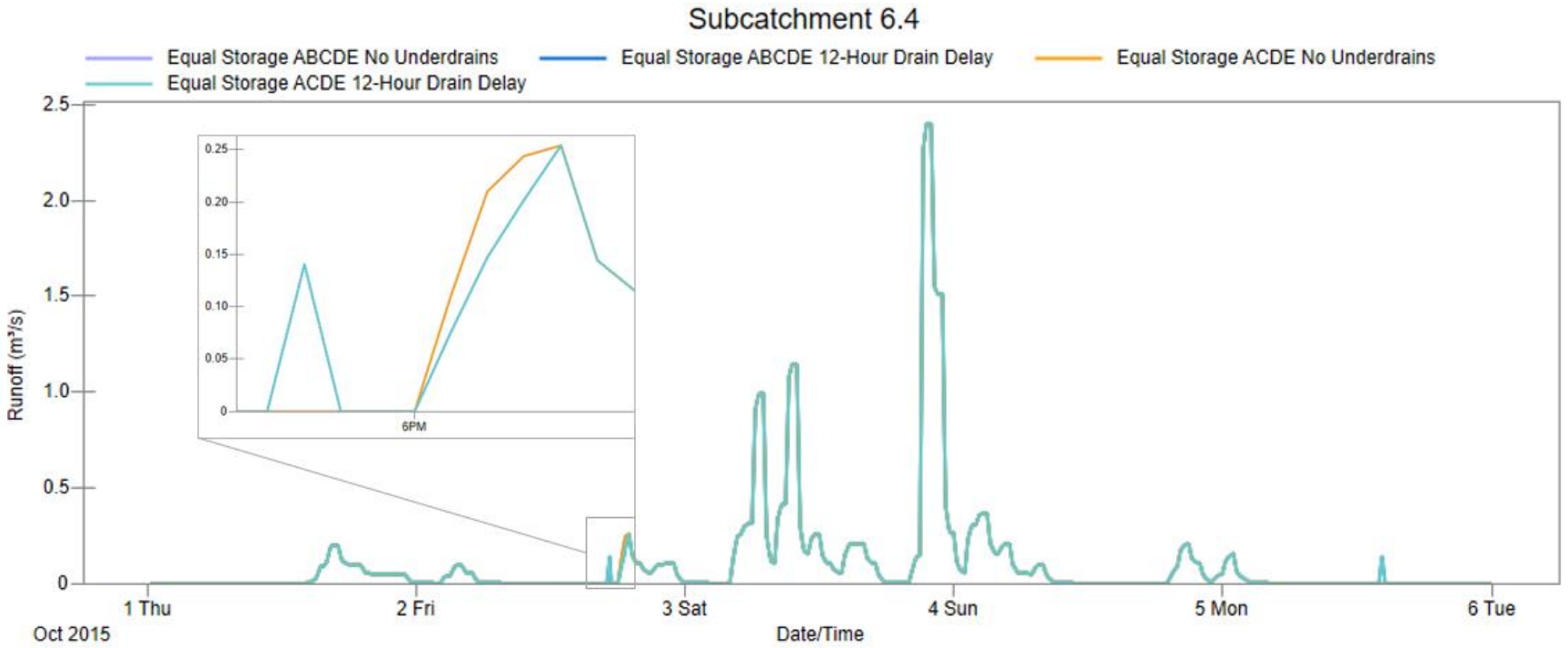

Figure B.6: Game 2 Subbasin D Runoff

B.7 Game 2 Subbasin E Runoff

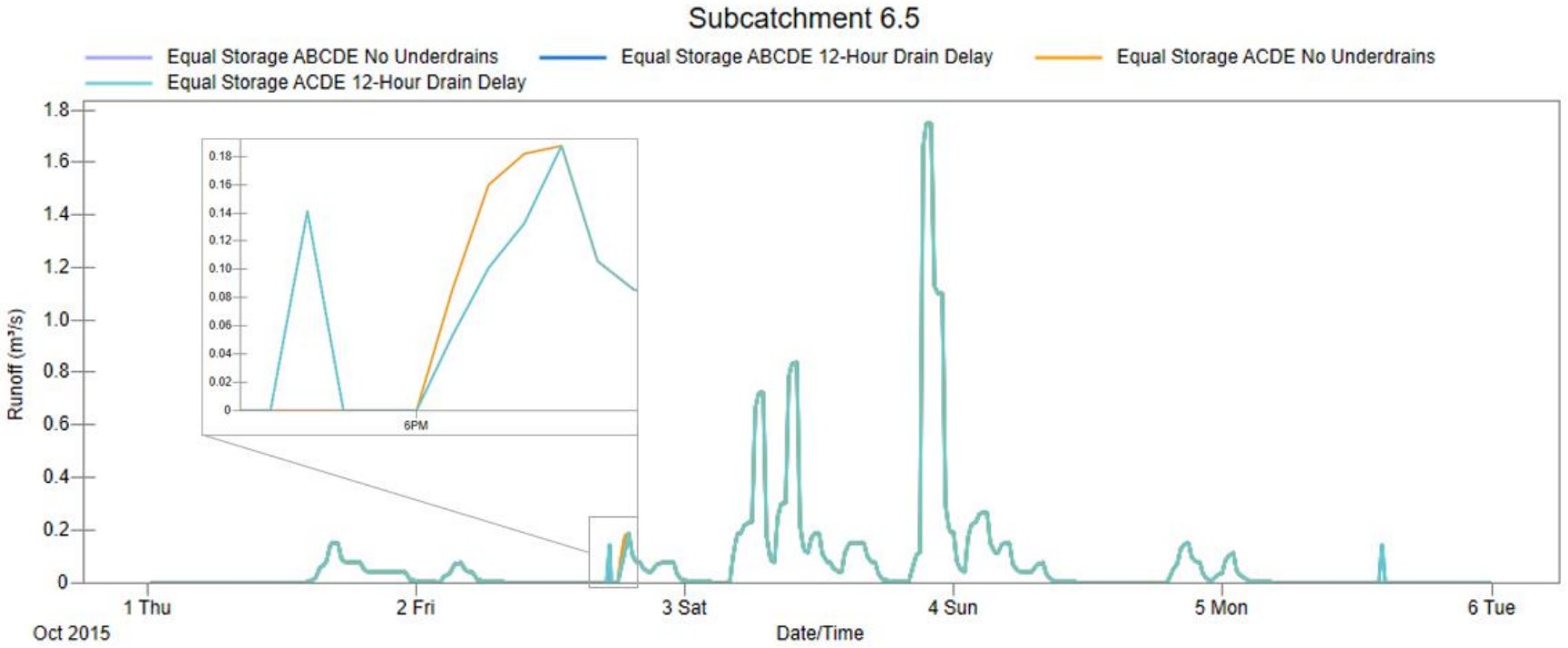

Figure B.7: Game 2 Subbasin E Runoff

B.8 Game 2 Junction 6.3.4 Flooding

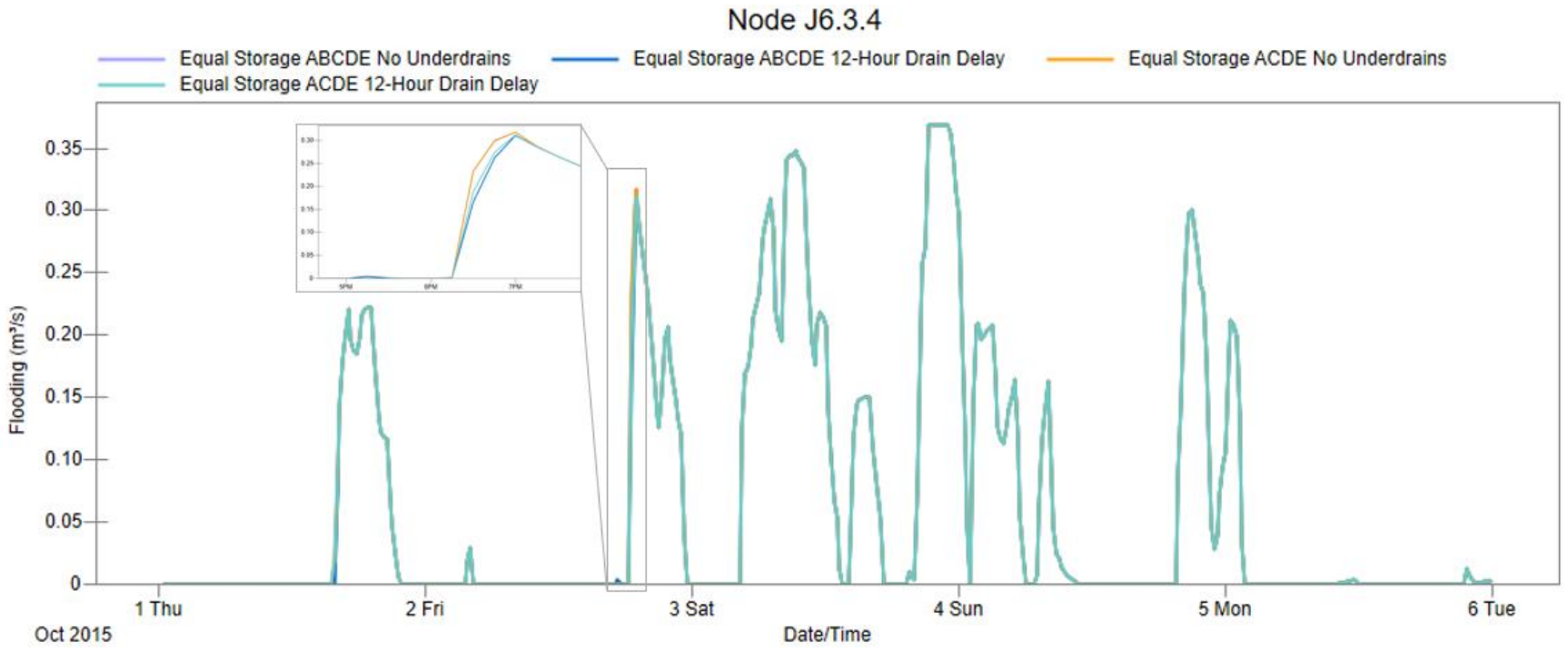

Figure B.8: Game 2 Junction 6.3.4 Flooding

B.9 Game 2 Junction 6.4.2 Flooding

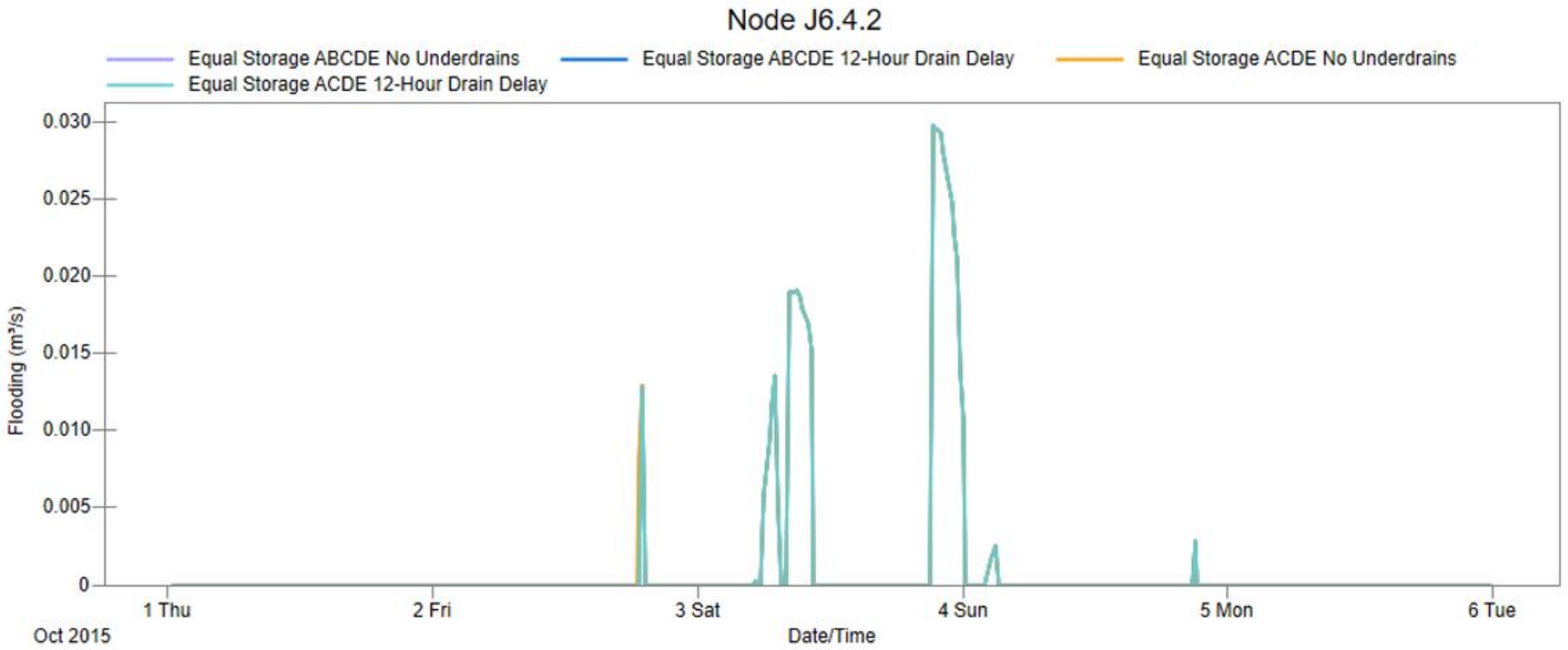

Figure B.9: Game 2 Junction 6.4.2 Flooding

B.10 Game 2 Junction 6.4.4 Flooding

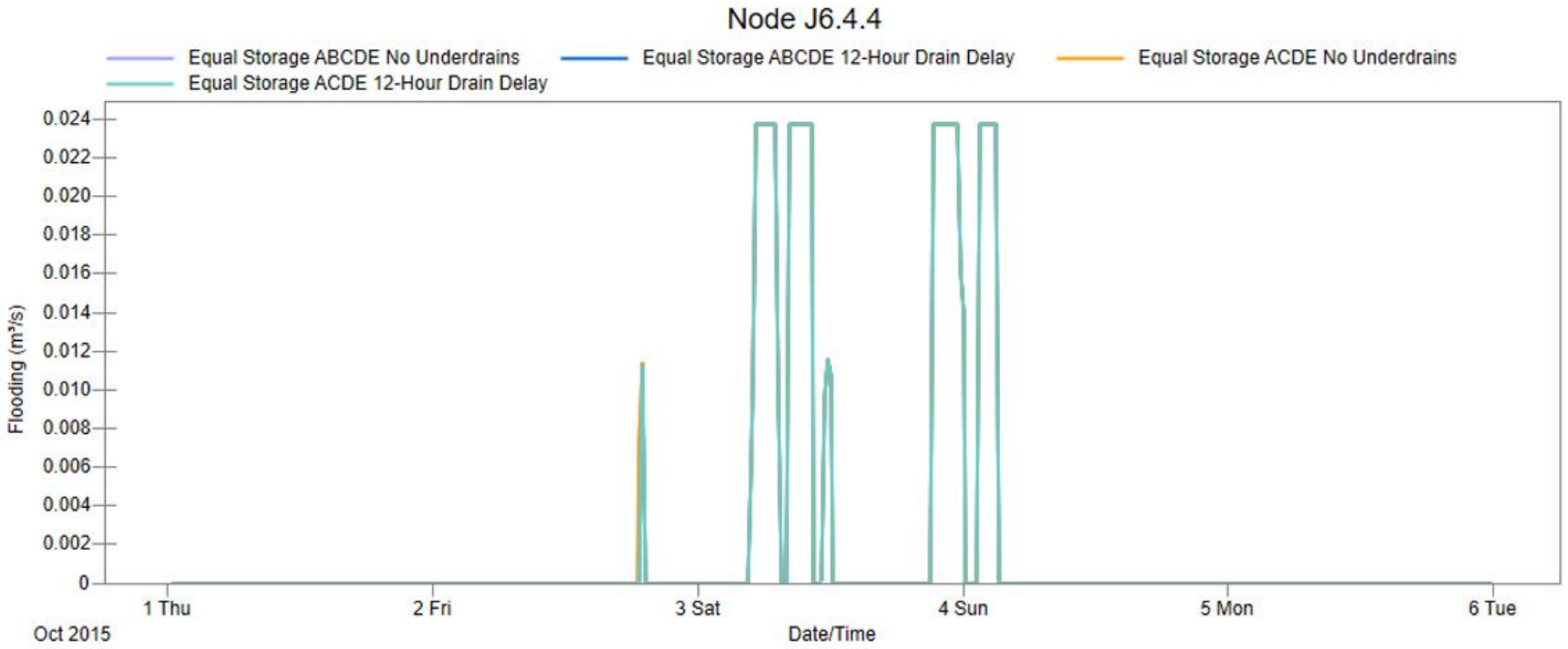

Figure B.10: Game 2 Junction 6.4.4 Flooding

B.11 Game 2 Junction 6.4.5 Flooding

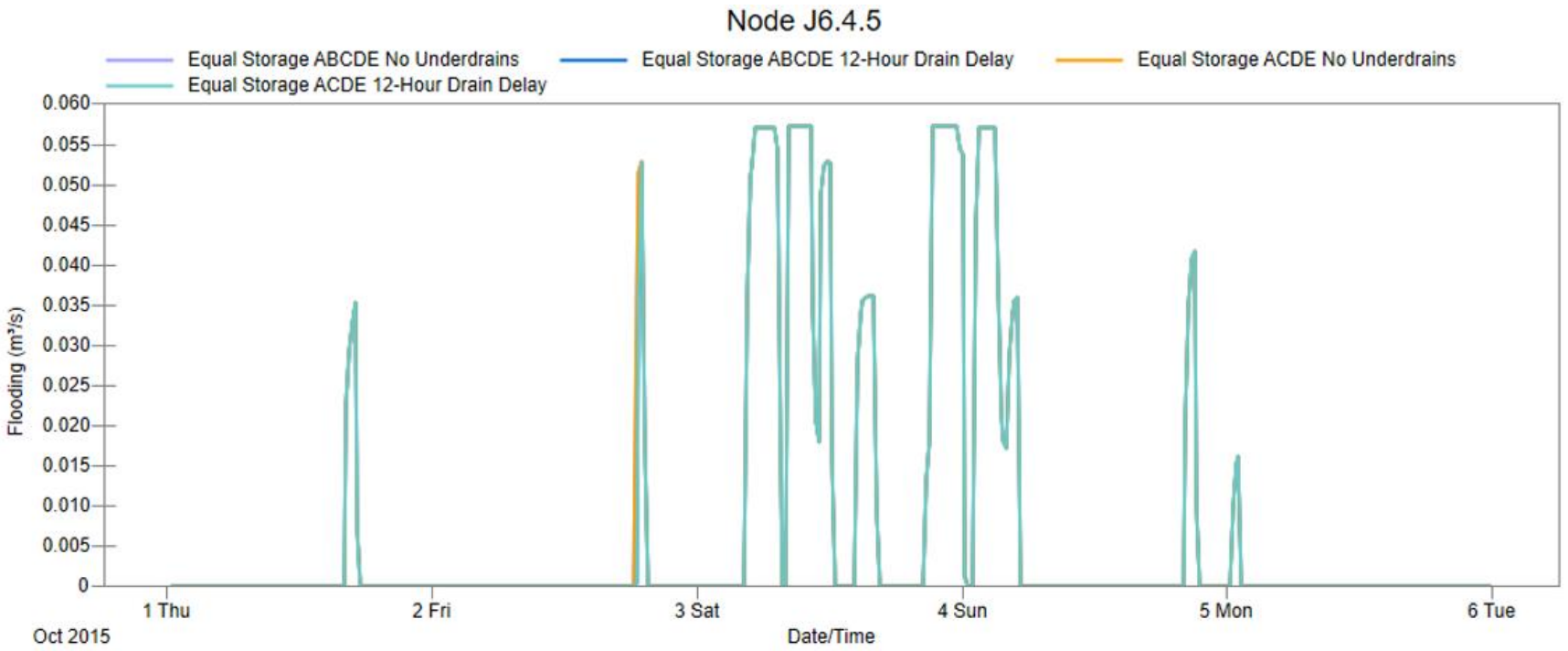

Figure B.11: Game 2 Junction 6.4.5 Flooding

B.12 Game 2 Junction 6.5.1 Flooding

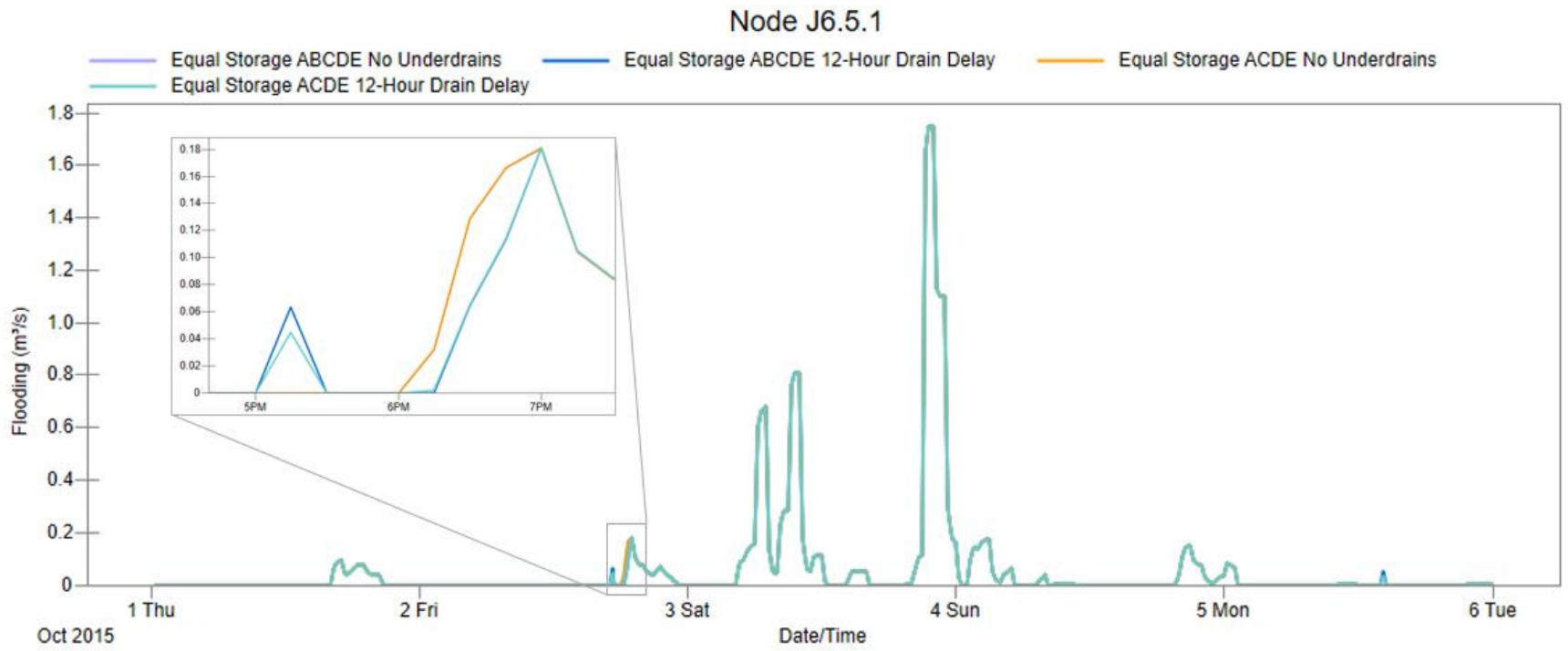

Figure B.12: Game 2 Junction 6.5.1 Flooding

B.13 Game 2 Junction 6.5.5 Flooding

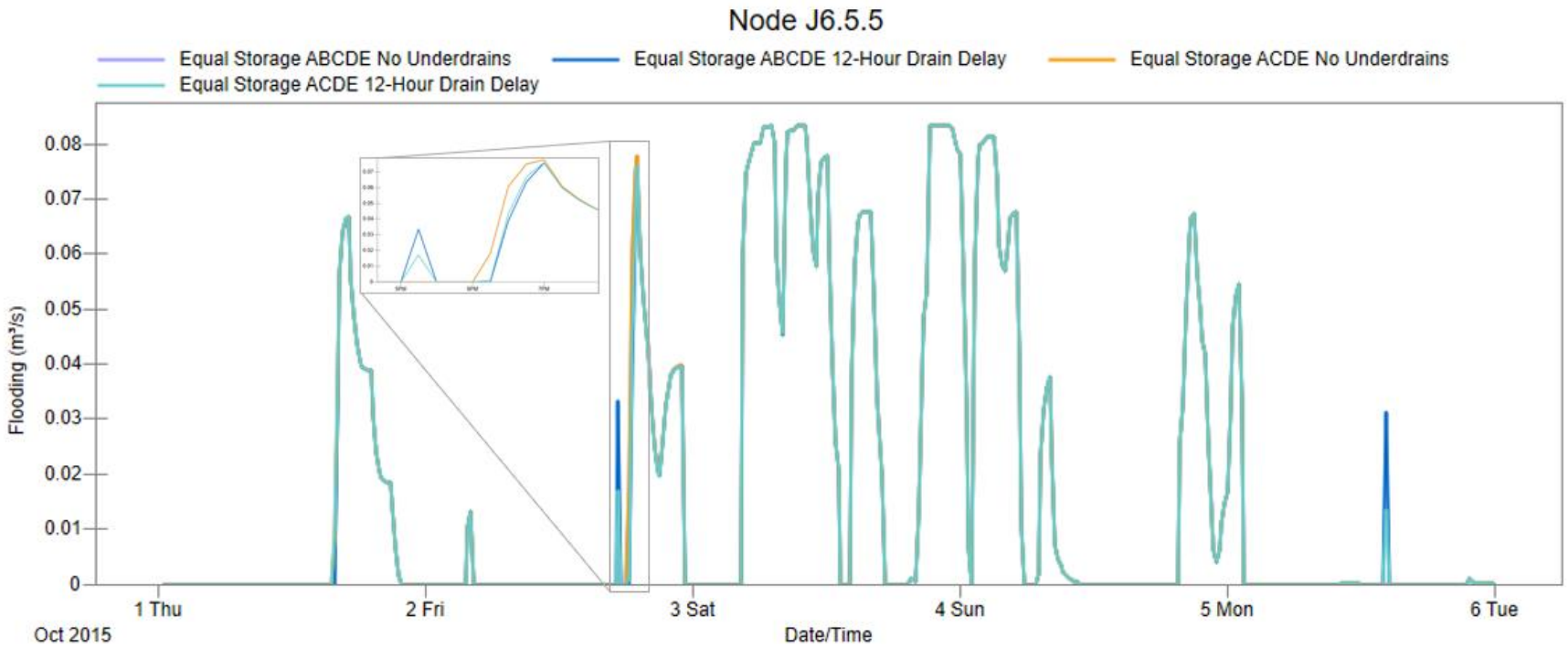

Figure B.13: Game 2 Junction 6.5.5 Flooding

APPENDIX C

GAME 3 HYDROGRAPHS

C.1 Game 3 System Flooding

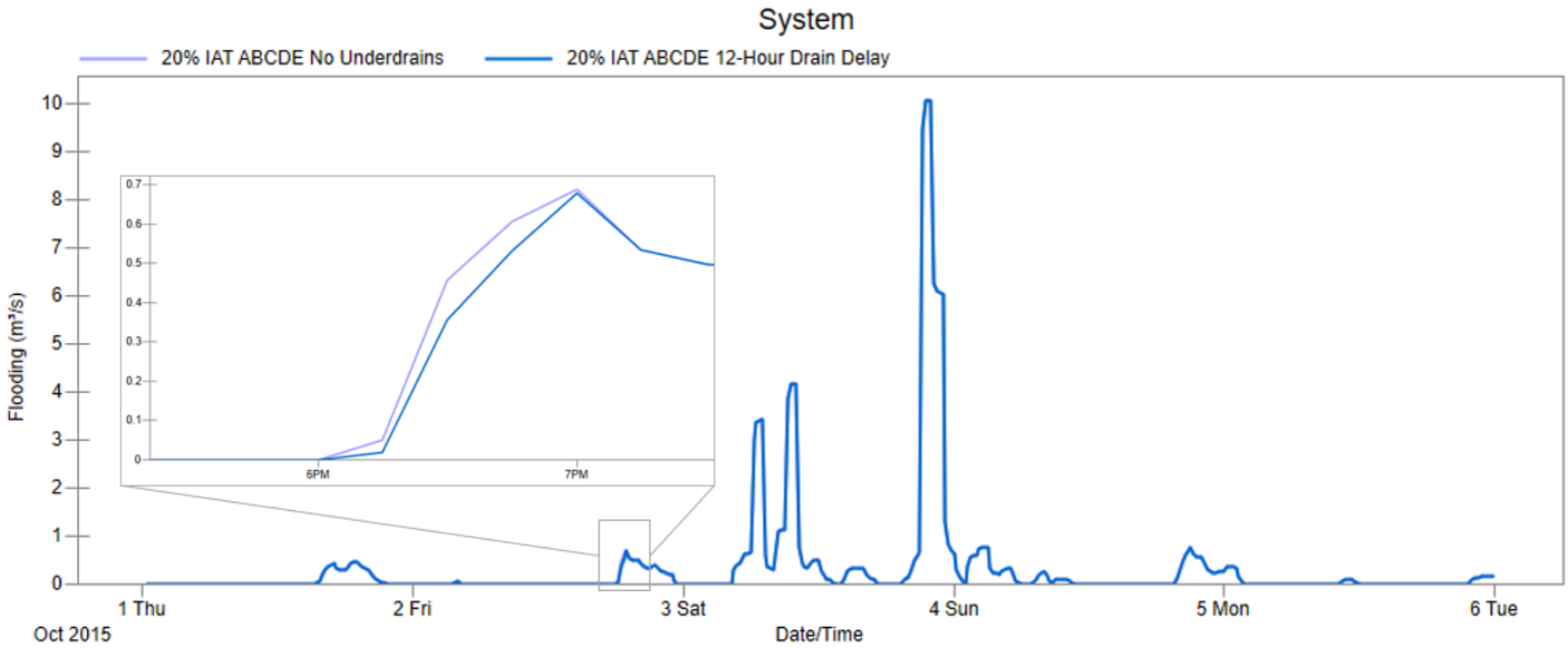

Figure C.1: Game 3 System Flooding

C.2 Game 3 System Runoff

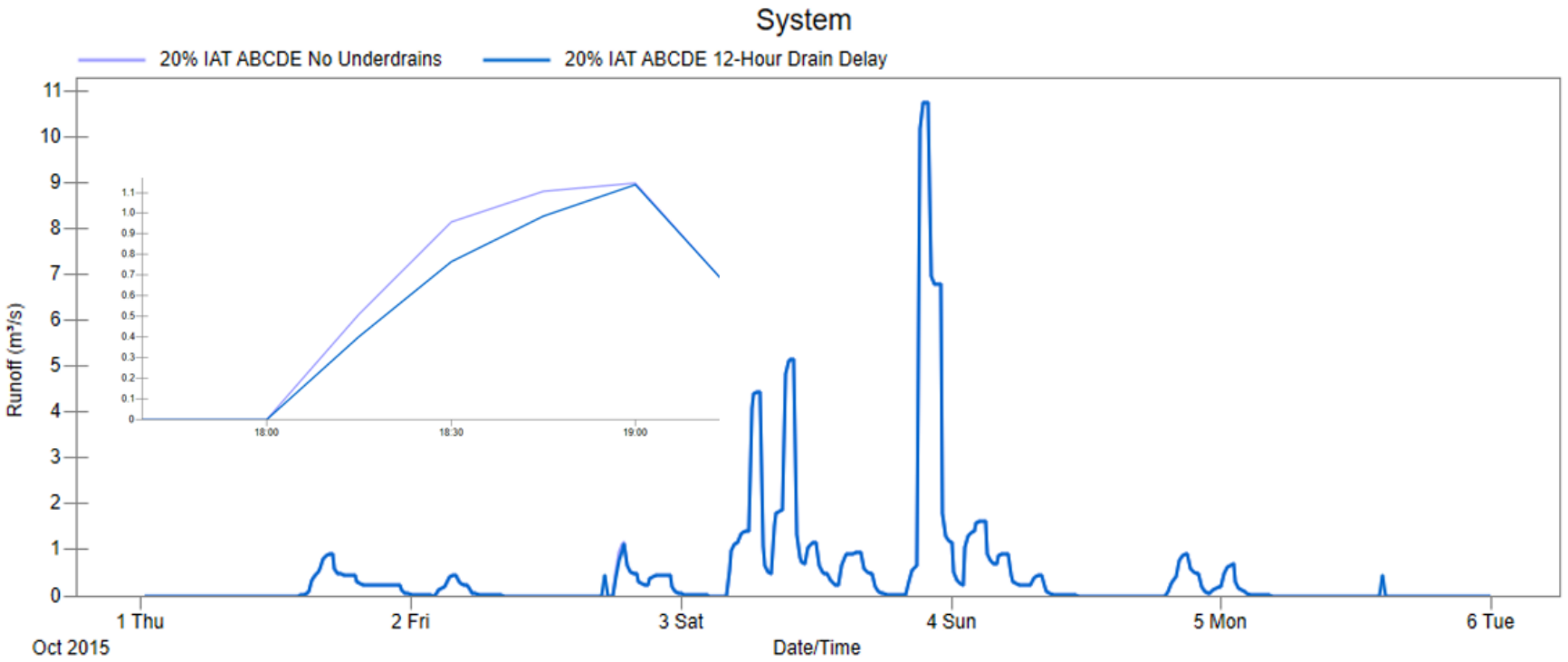

Figure C.2: Game 3 System Runoff

C.3 Game 3 Subbasin A Runoff

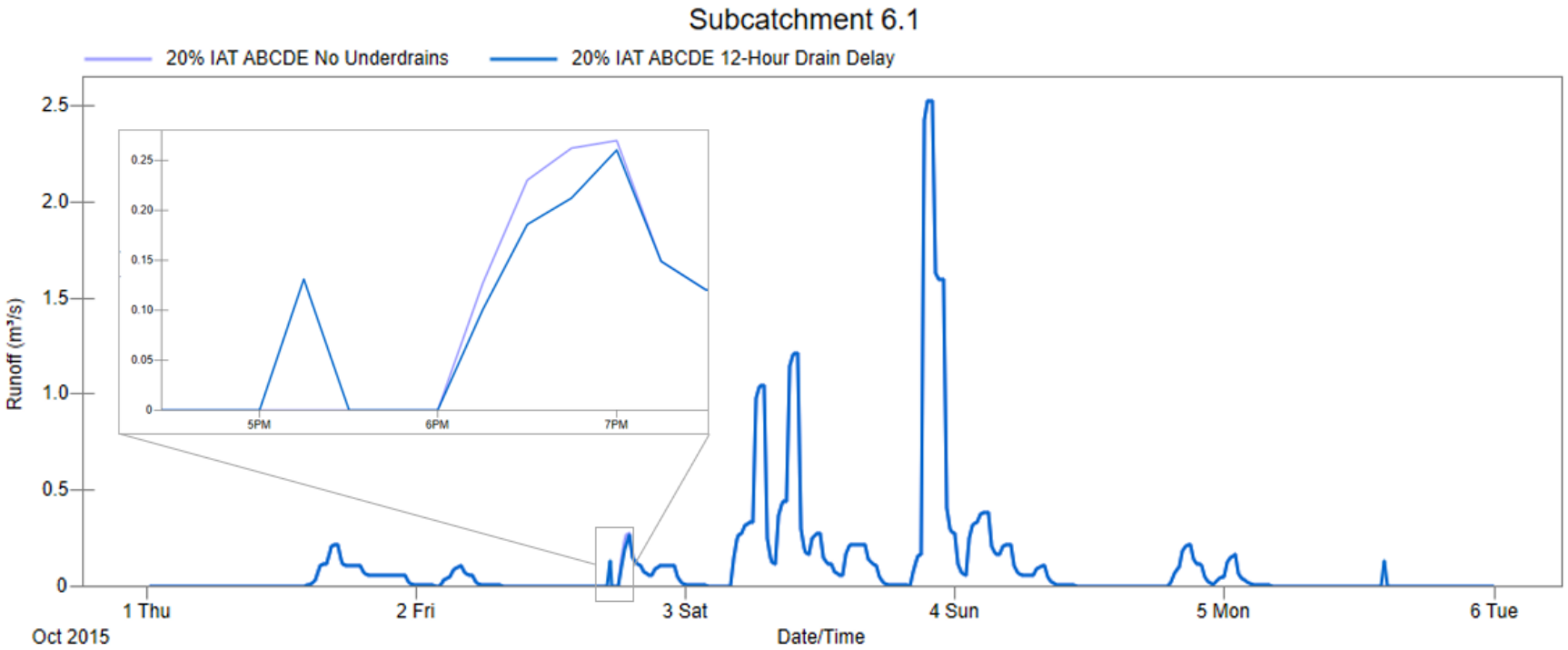

Figure C.3: Game 3 Subbasin A Runoff

C.4 Game 3 Subbasin B Runoff

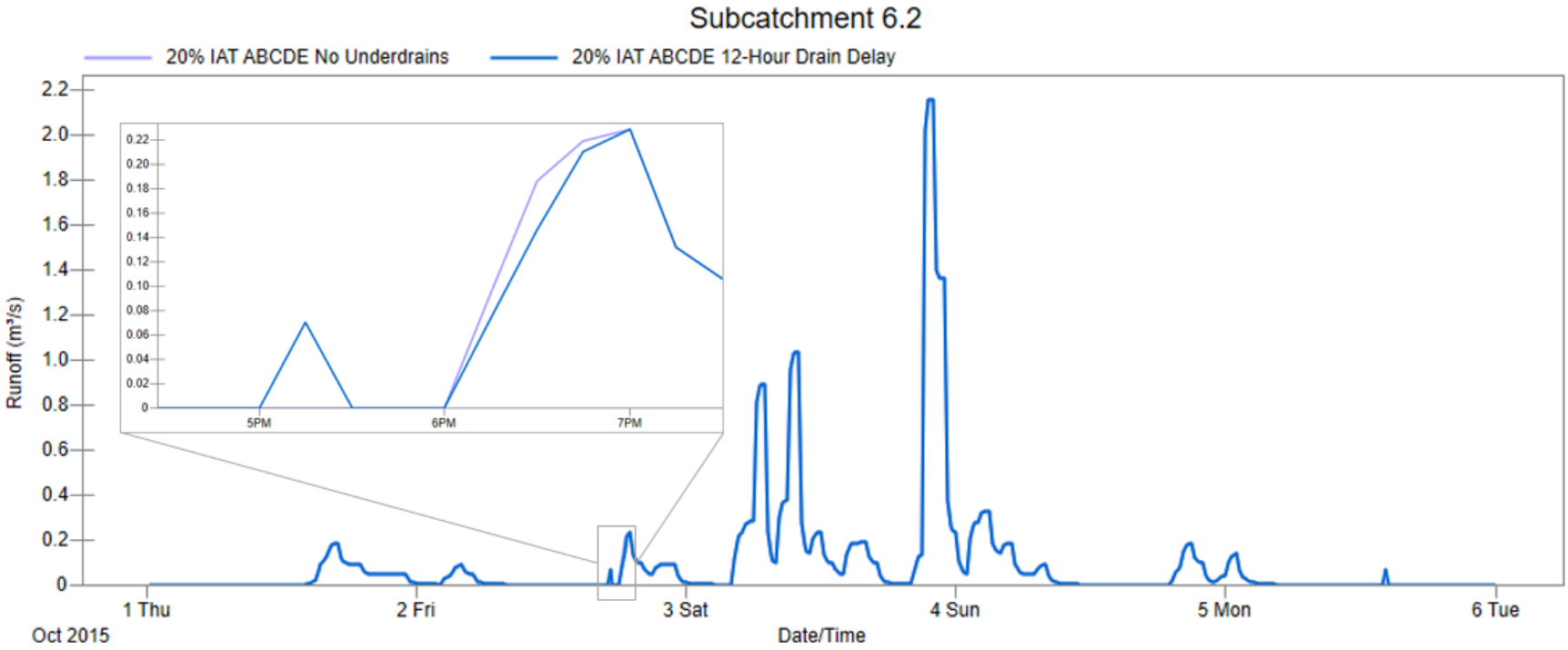

Figure C.4: Game 3 Subbasin B Runoff

C.5 Game 3 Subbasin C Runoff

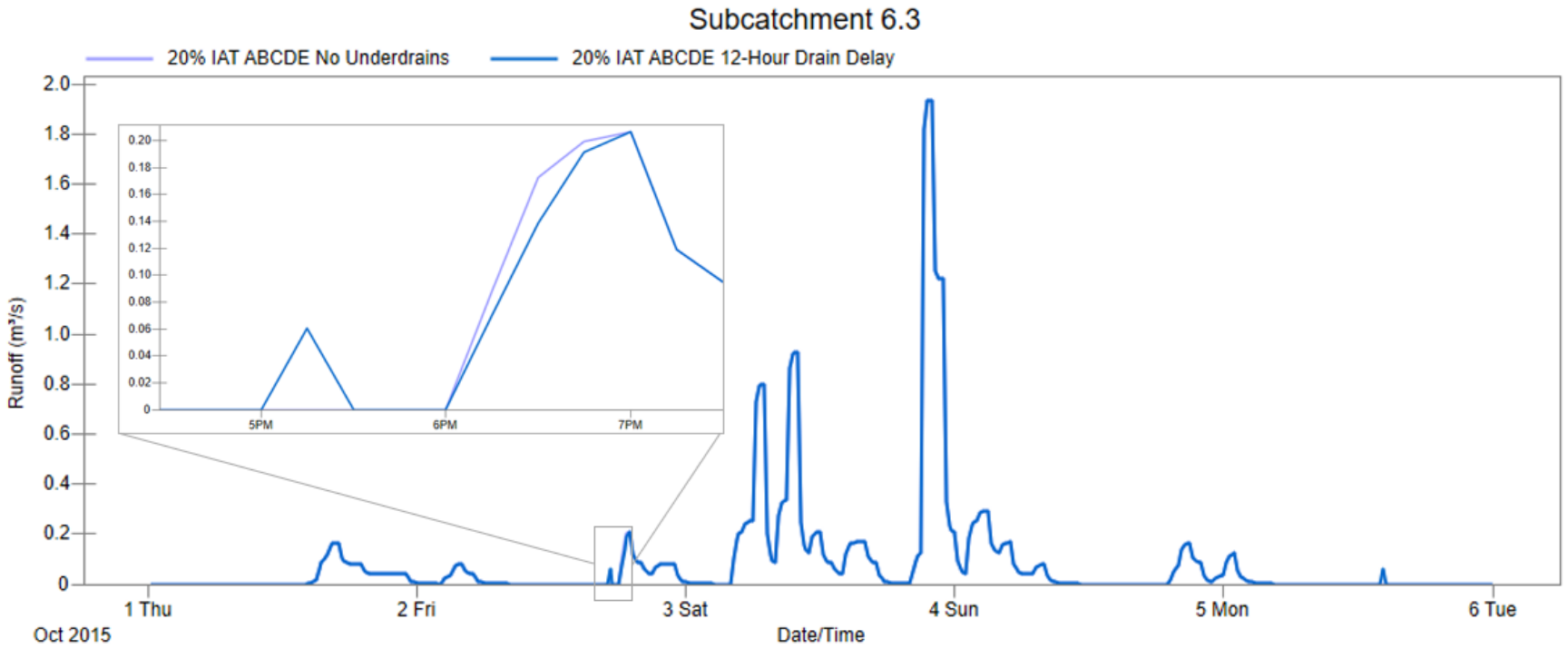

Figure C.5: Game 3 Subbasin C Runoff

C.6 Game 3 Subbasin D Runoff

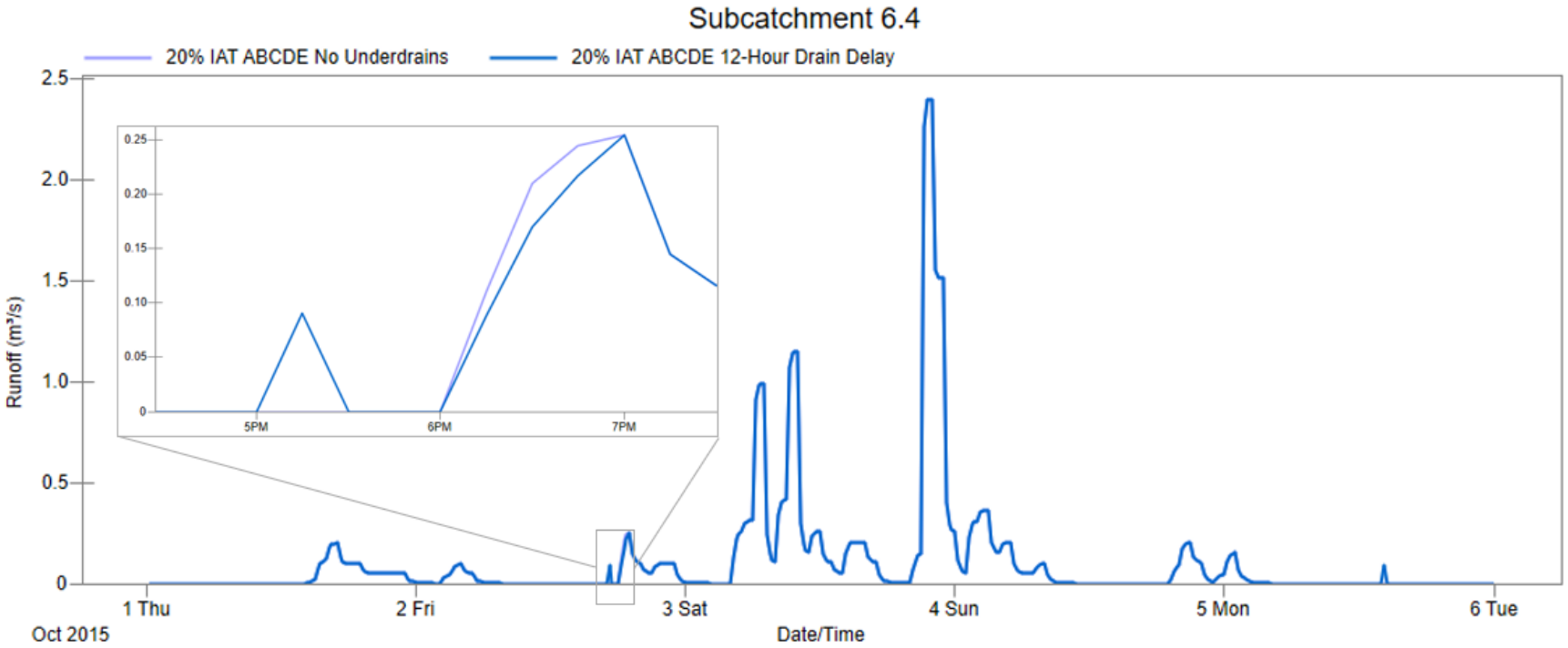

Figure C.6: Game 3 Subbasin D Runoff

C.7 Game 3 Subbasin E Runoff

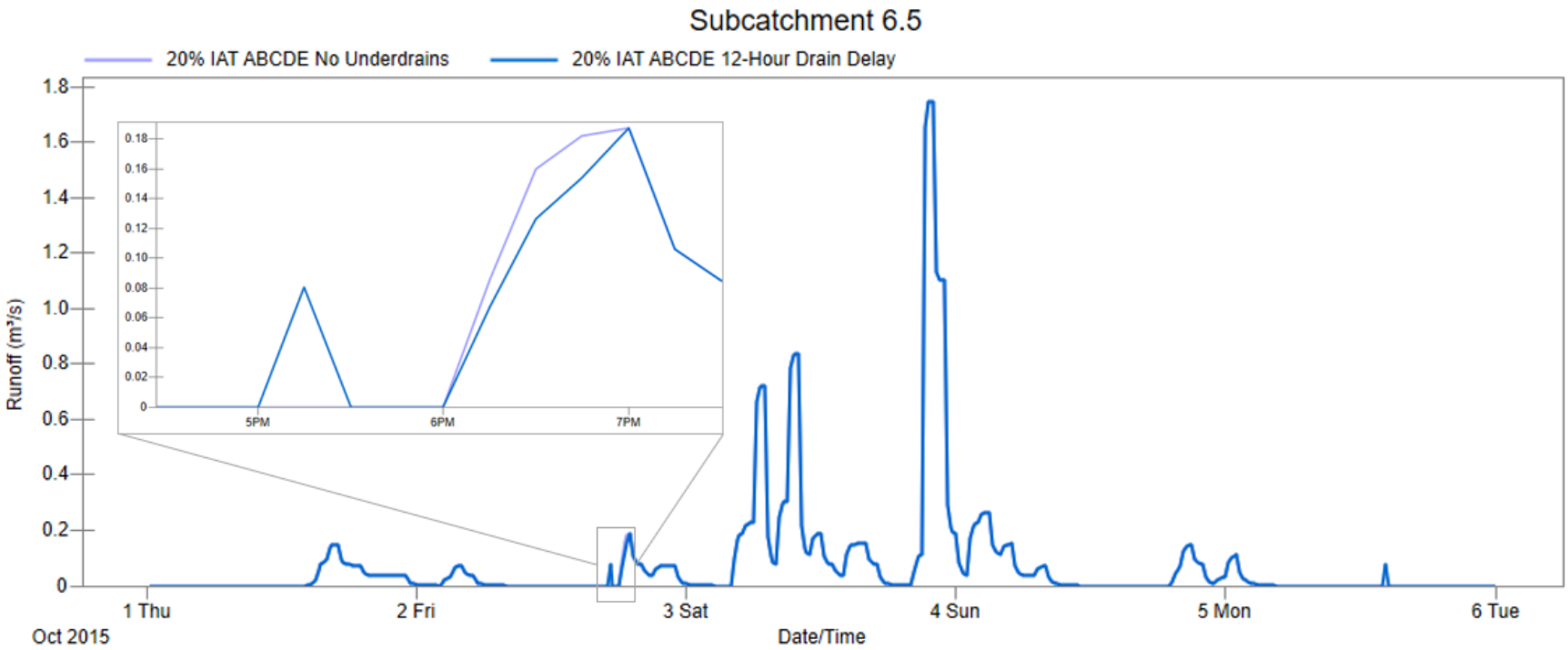

Figure C.7: Game 3 Subbasin E Runoff

C.8 Game 3 Junction 6.3.4 Flooding

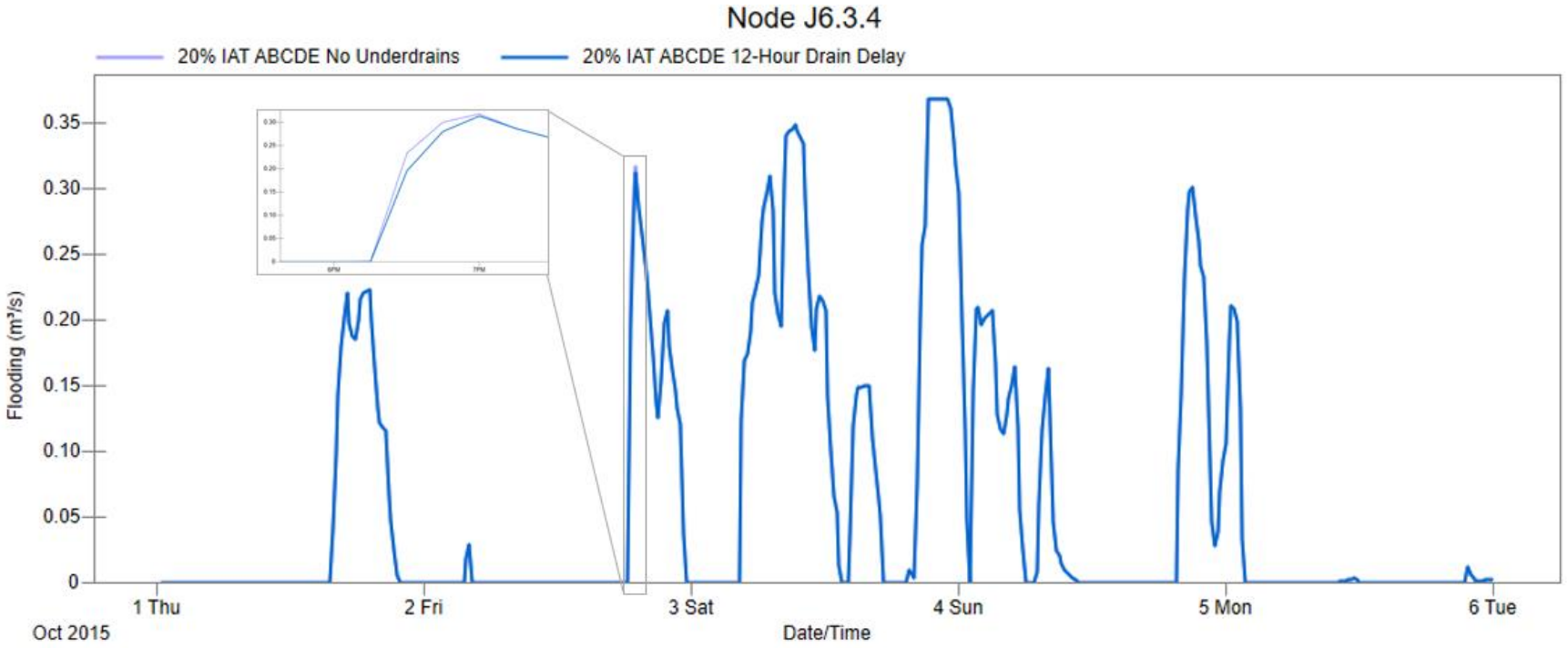

Figure C.8: Game 3 Junction 6.3.4 Flooding

C.9 Game 3 Junction 6.4.2 Flooding

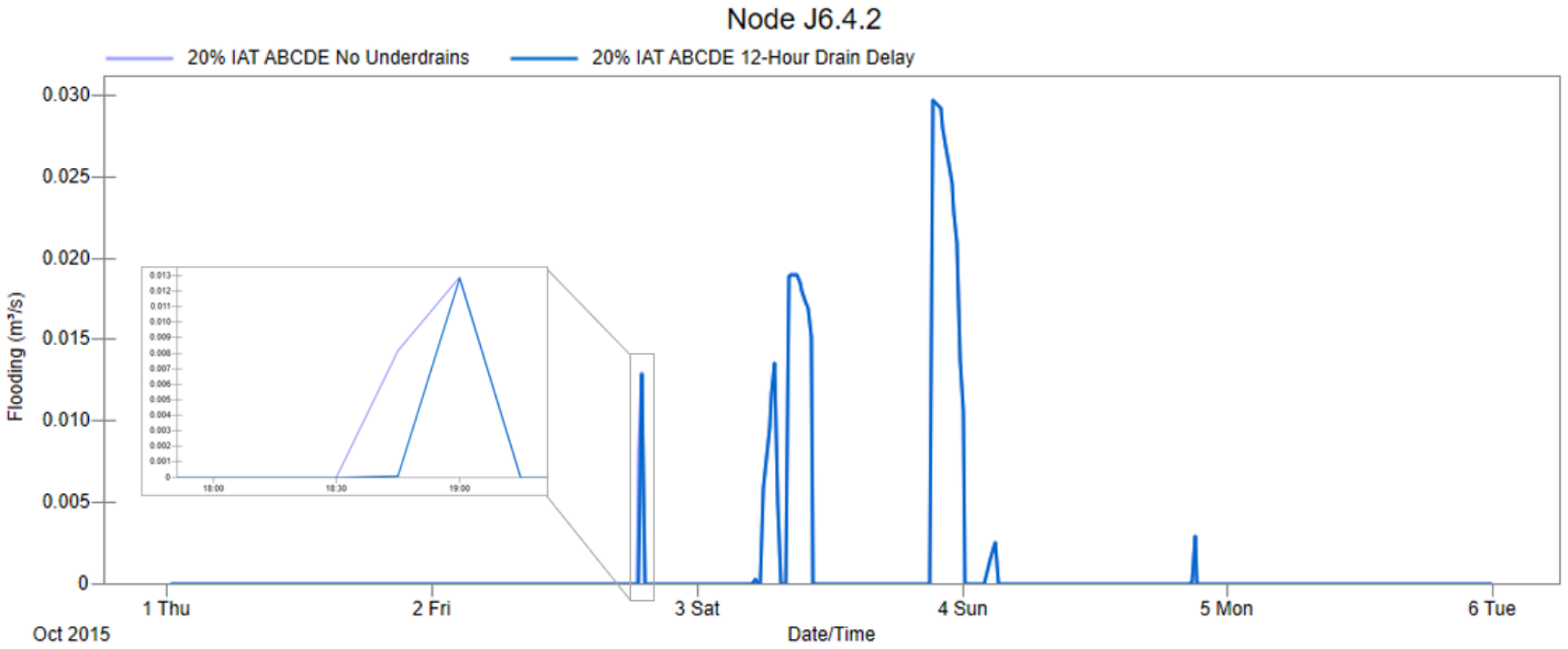

Figure C.9: Game 3 Junction 6.4.2 Flooding

C.10 Game 3 Junction 6.4.4 Flooding

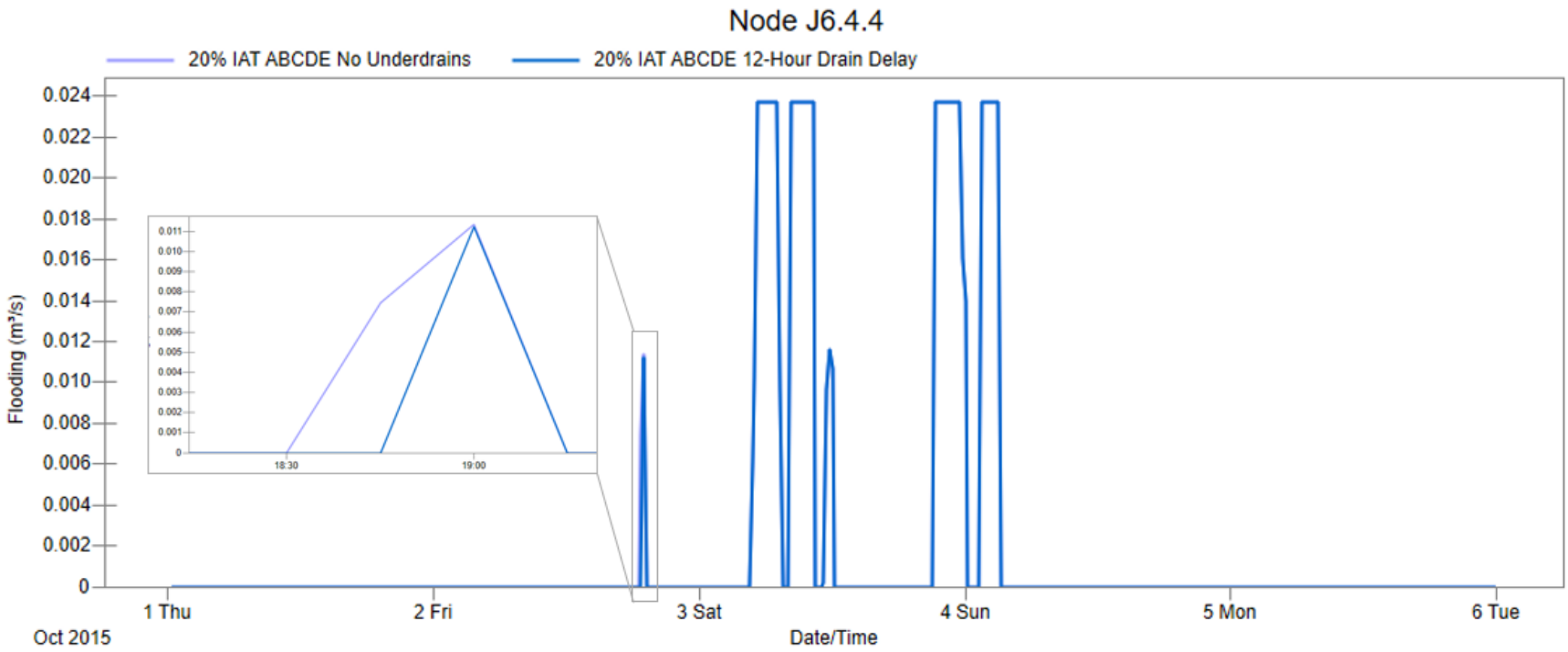

Figure C.10: Game 3 Junction 6.4.4 Flooding

C.11 Game 3 Junction 6.4.5 Flooding

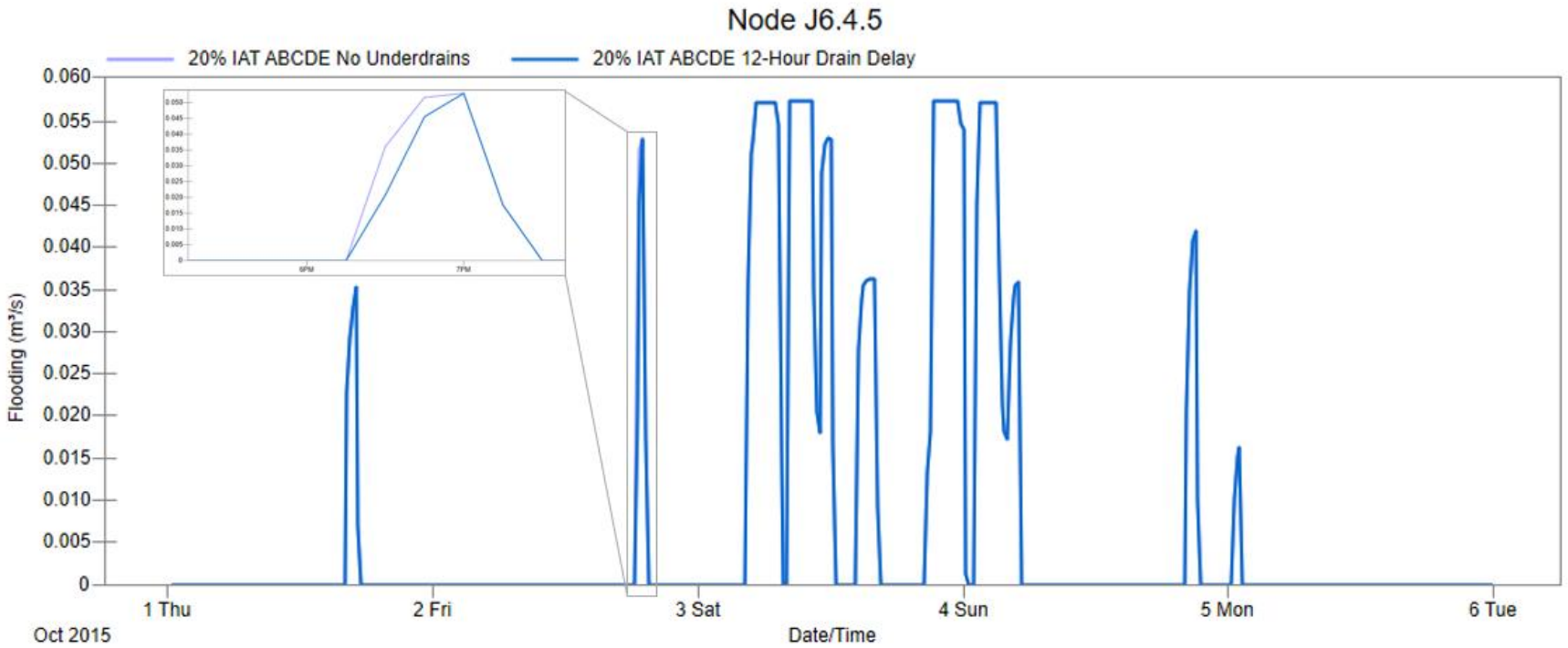

Figure C.11: Game 3 Junction 6.4.5 Flooding

C.12 Game 3 Junction 6.5.1 Flooding

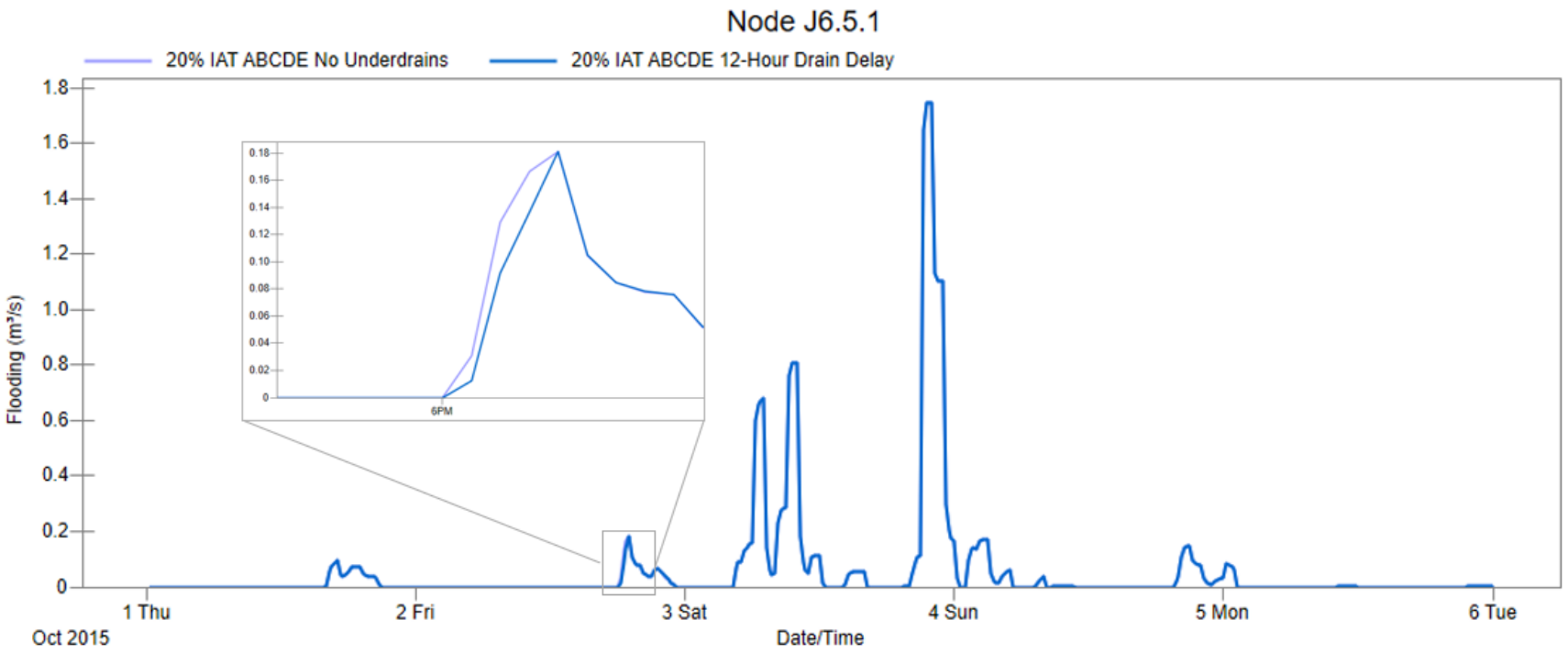

Figure C.12: Game 3 Junction 6.5.1 Flooding

C.13 Game 3 Junction 6.5.5 Flooding

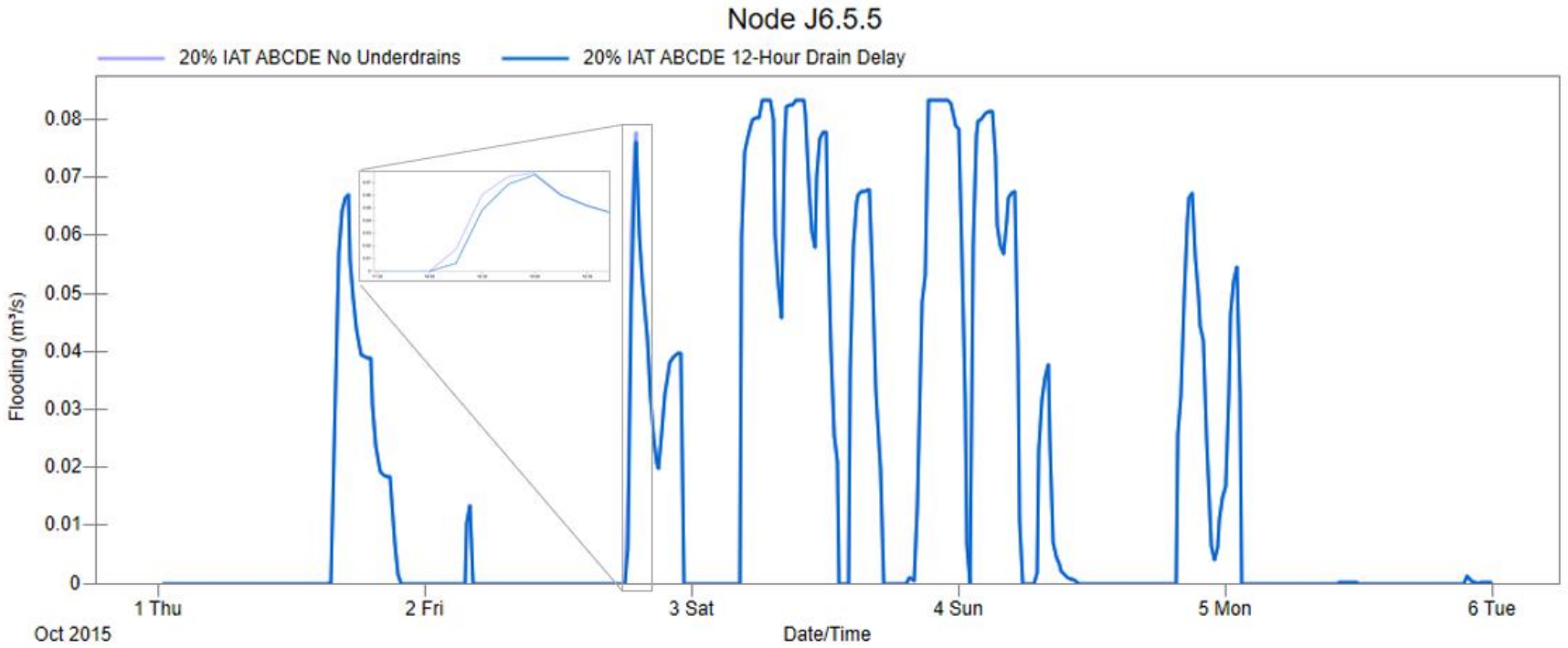

Figure C.13: Game 3 Junction 6.5.5 Flooding

APPENDIX D

GAME 4 HYDROGRAPHS

D.1 Game 4 System Flooding

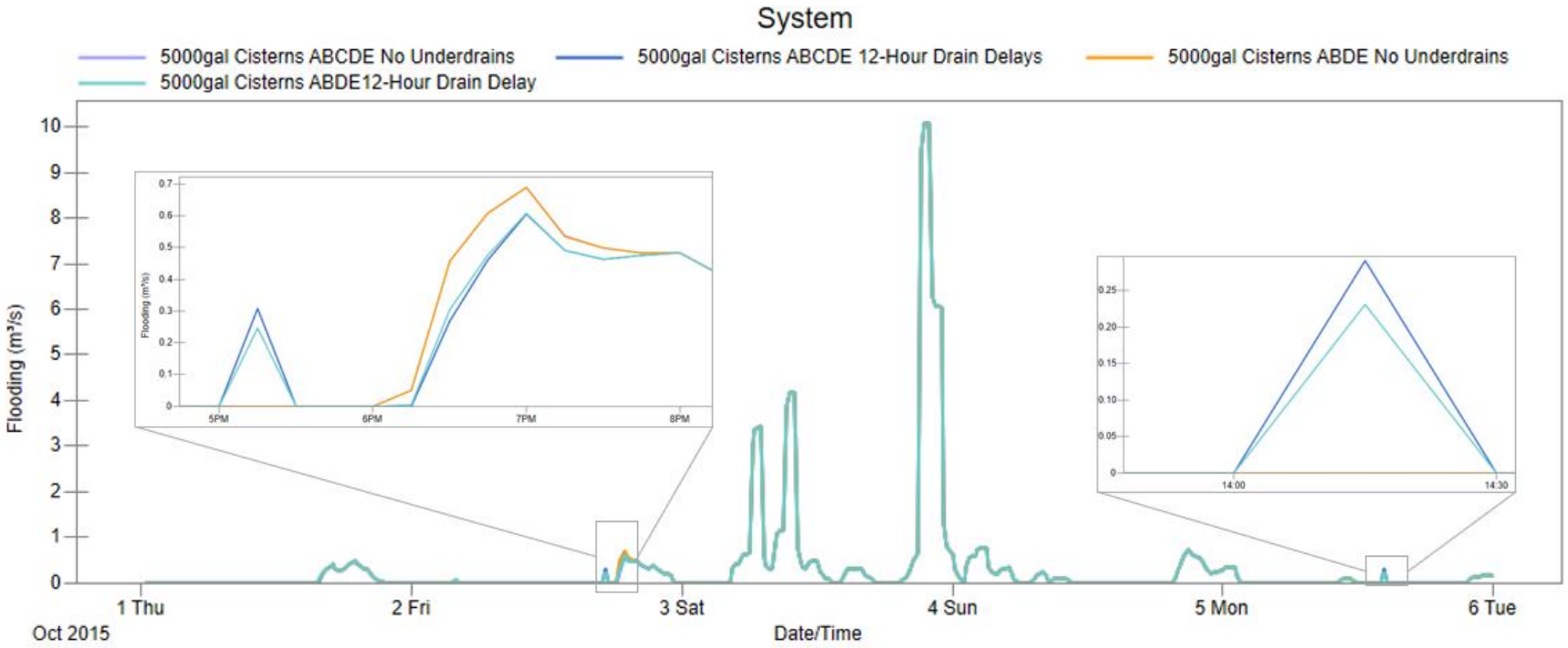

Figure D.1: Game 4 System Flooding

D.2 Game 4 System Runoff

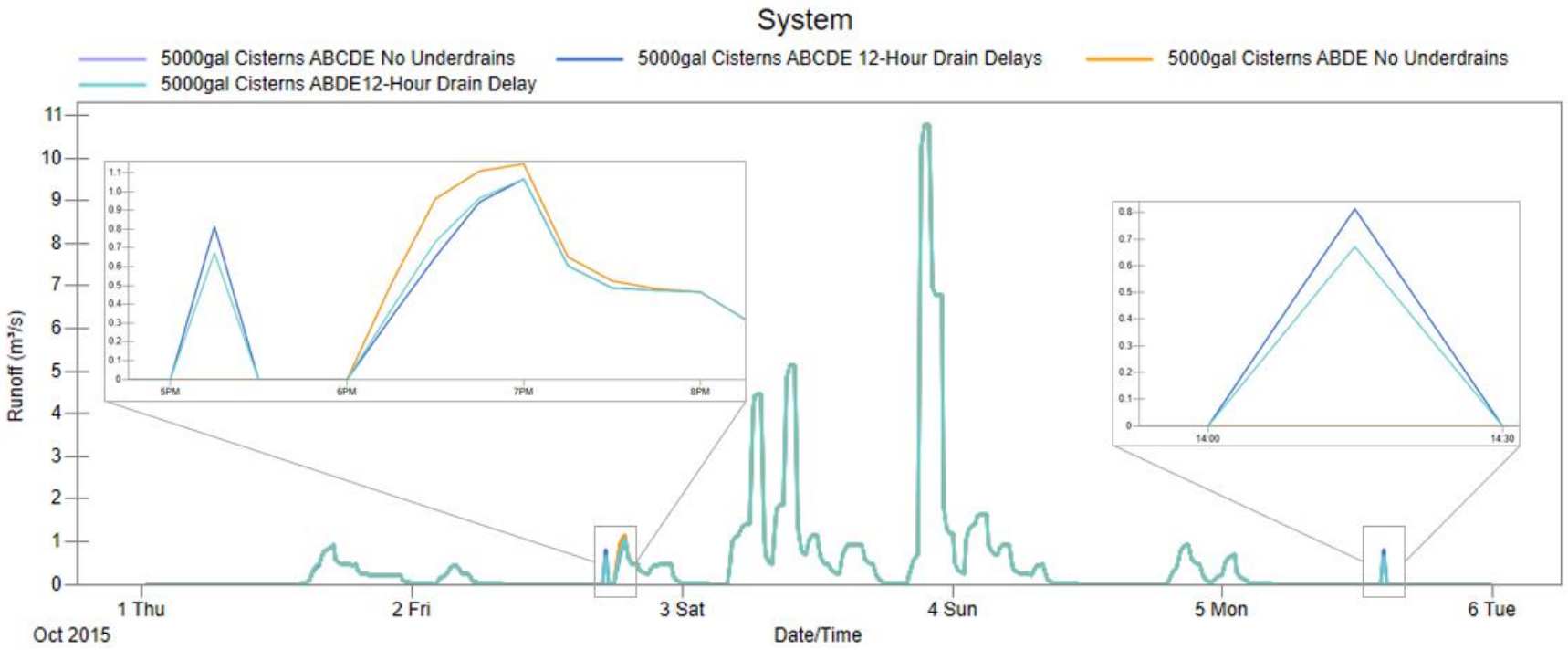

Figure D.2: Game 4 System Runoff

D.3 Game 4 Subbasin A Runoff

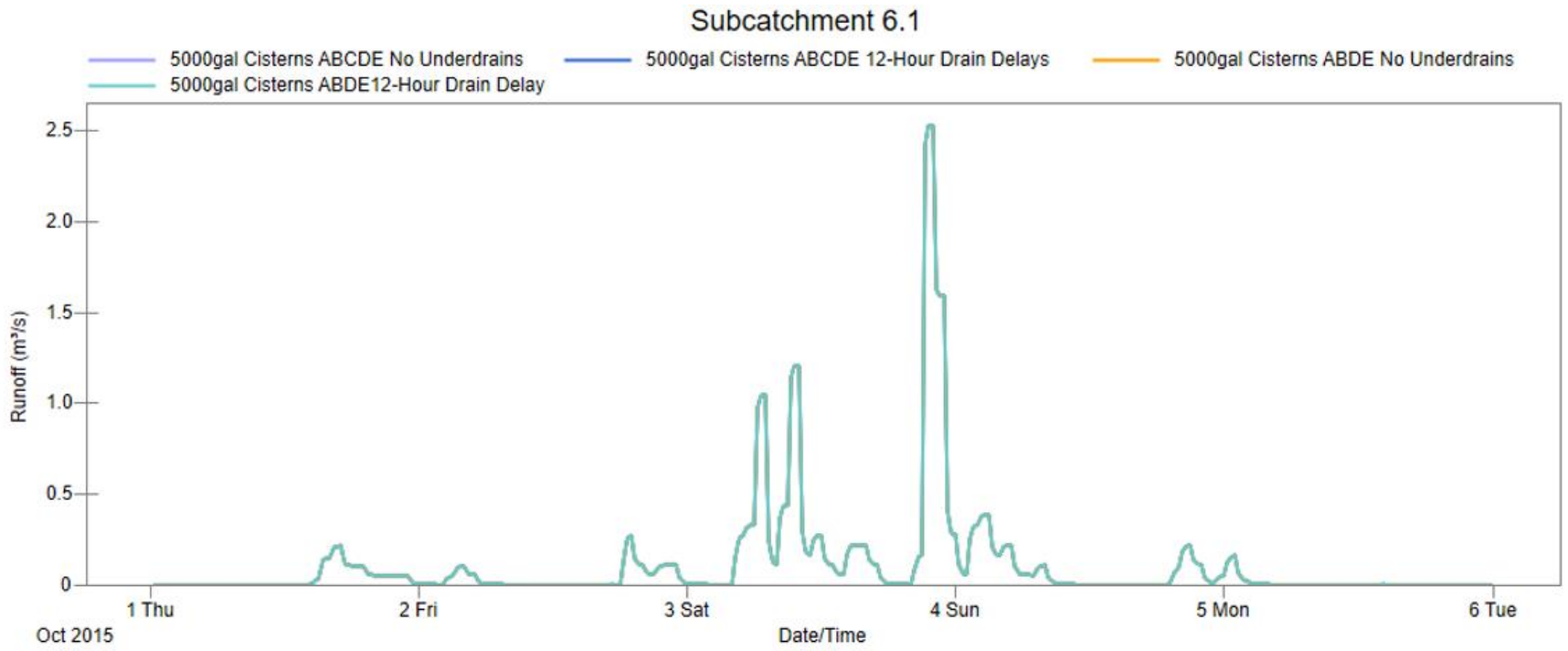

Figure D.3: Game 4 Subbasin A Runoff

D.4 Game 4 Subbasin B Runoff

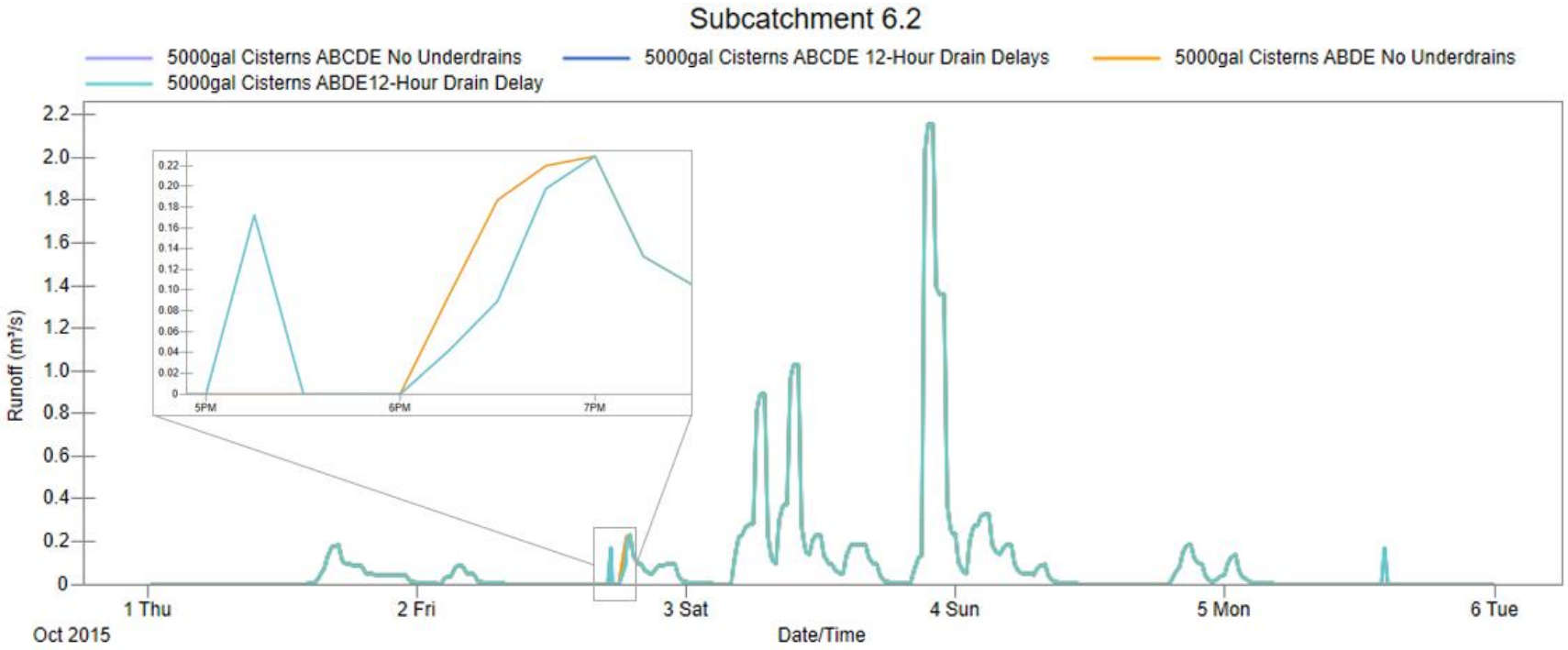

Figure D.4: Game 4 Subbasin B Runoff

D.5 Game 4 Subbasin C Runoff

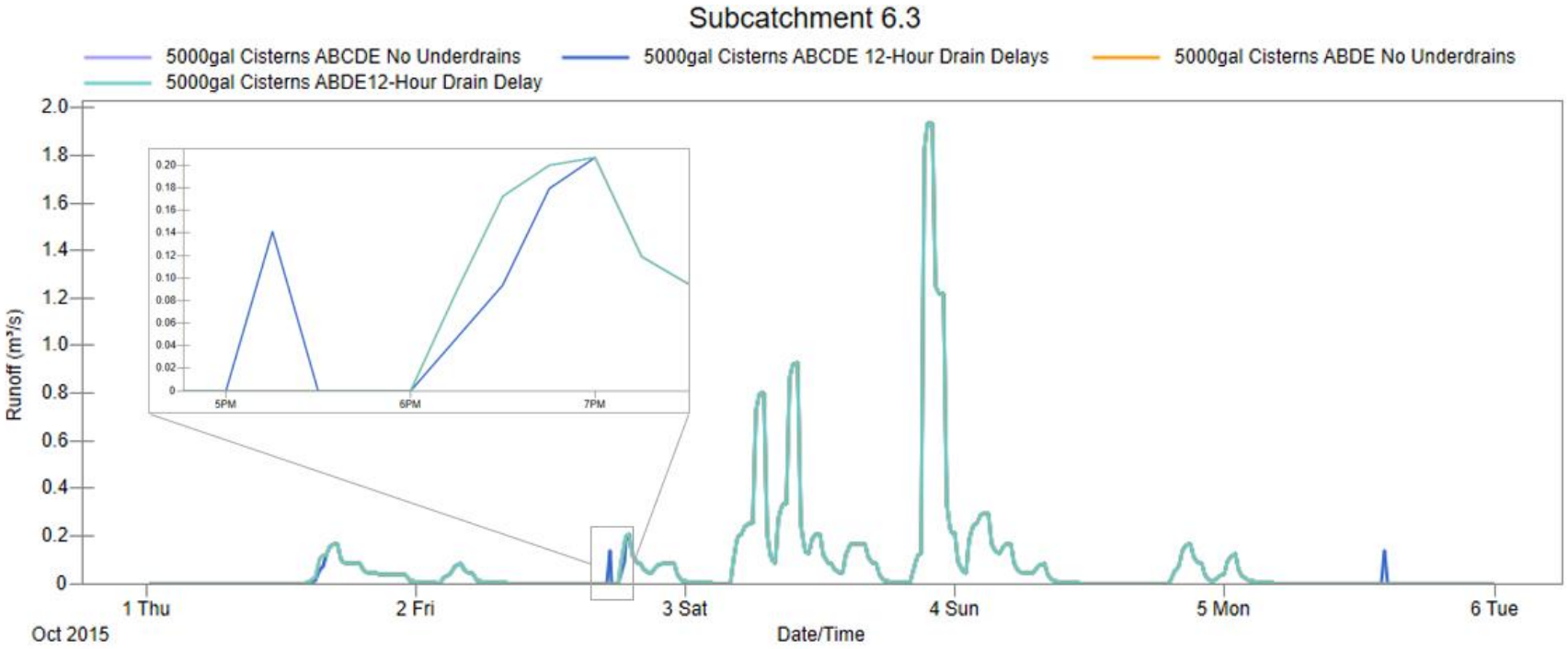

Figure D.5: Game 4 Subbasin C Runoff

D.6 Game 4 Subbasin D Runoff

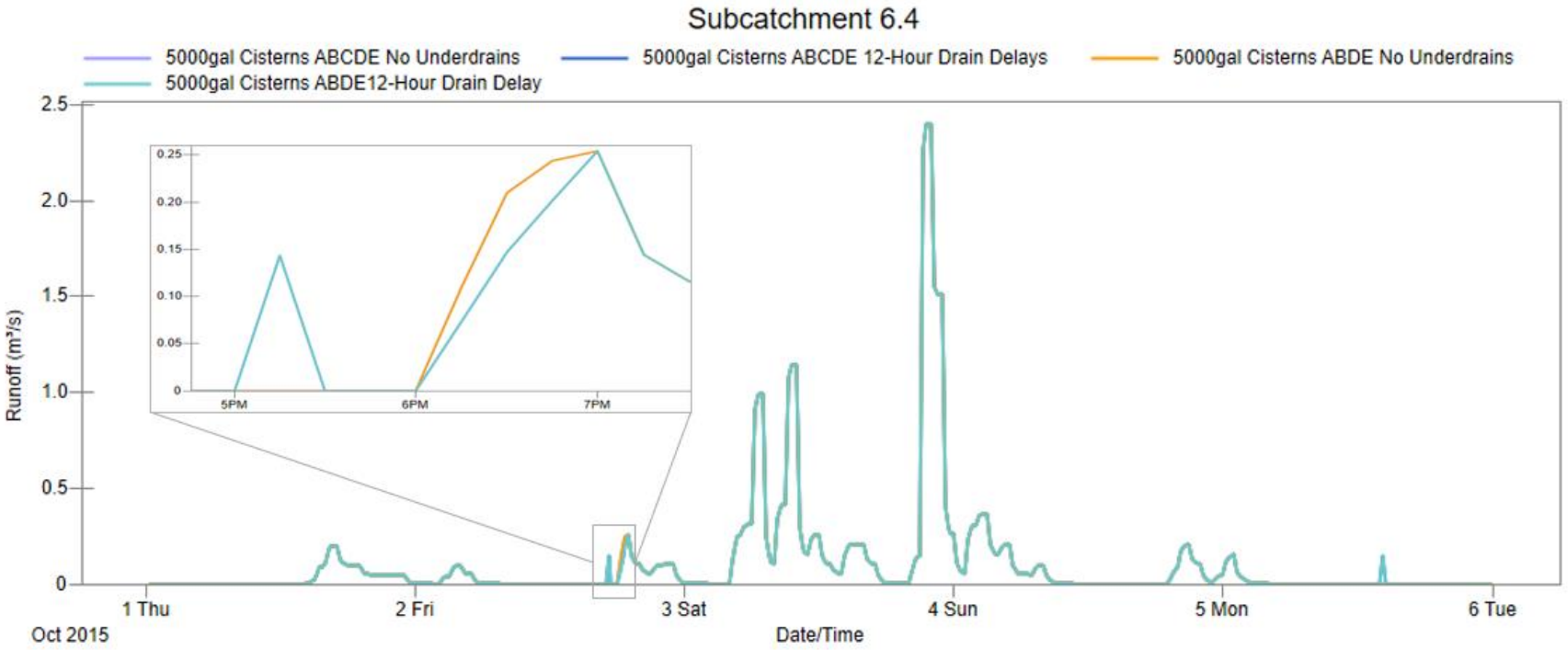

Figure D.6 Game 4 Subbasin D Runoff

D.7 Game 4 Subbasin E Runoff

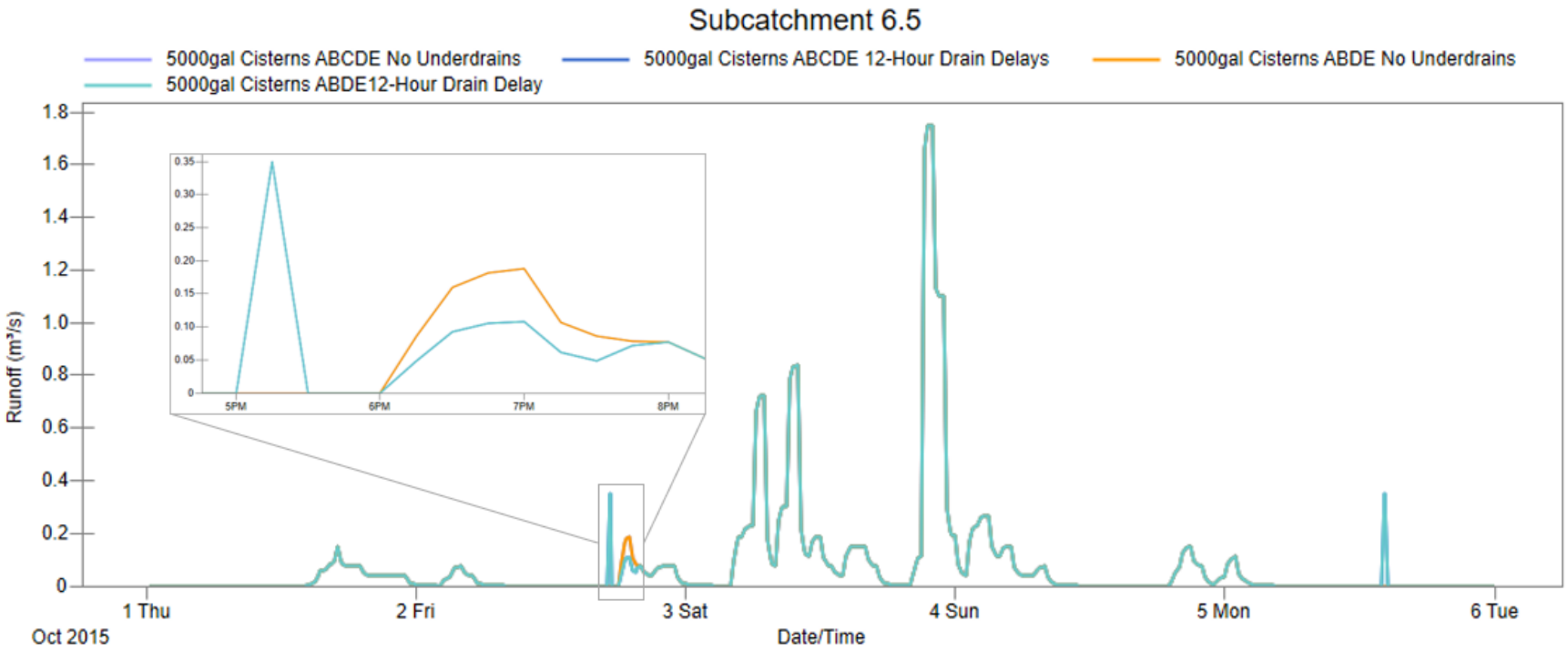

Figure D.7: Game 4 Subbasin E Runoff

D.8 Game 4 Junction 6.3.4 Flooding

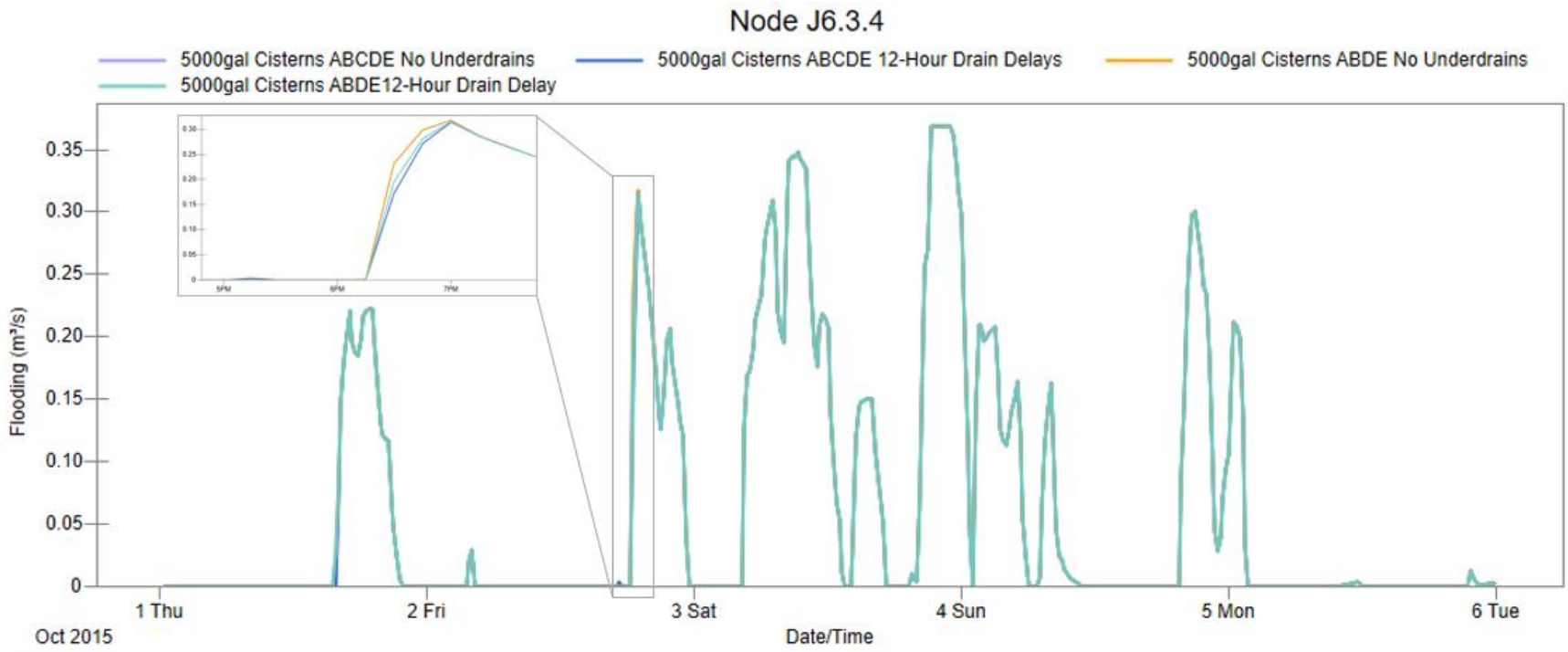

Figure D.8: Game 4 Junction 6.3.4 Flooding

D.9 Game 4 Junction 6.4.2

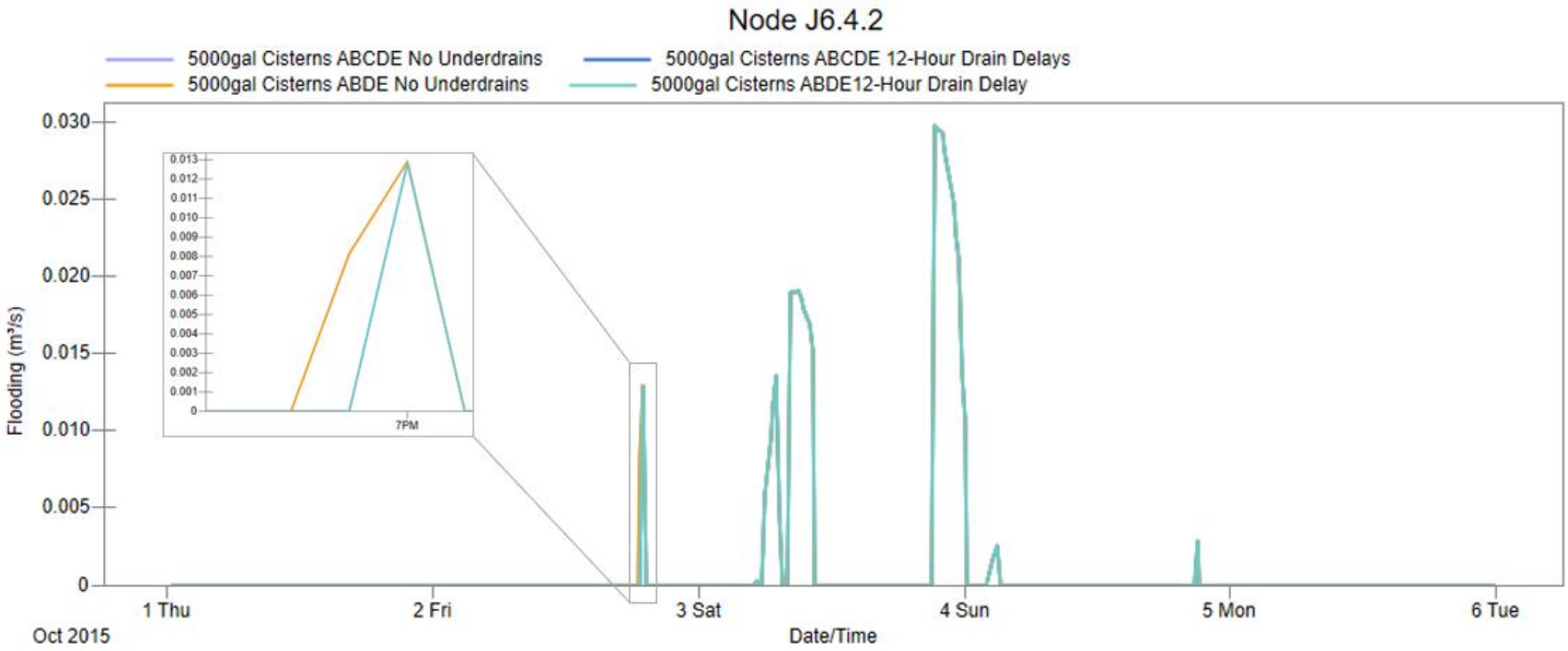

Figure D.9: Game 4 Junction 6.4.2

D.10 Game 4 Junction 6.4.4 Flooding

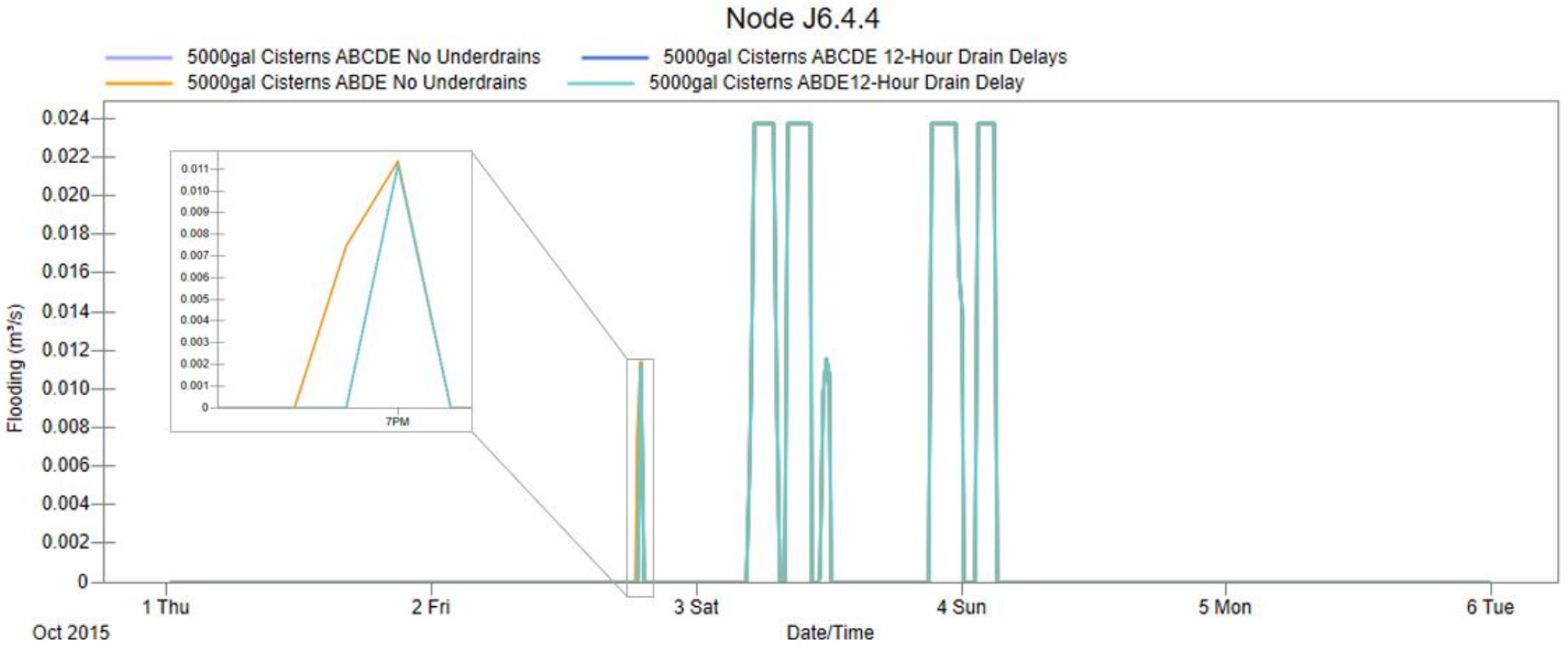

Figure D.10: Game 4 Junction 6.4.4 Flooding

D.11 Game 4 Junction 6.4.5 Flooding

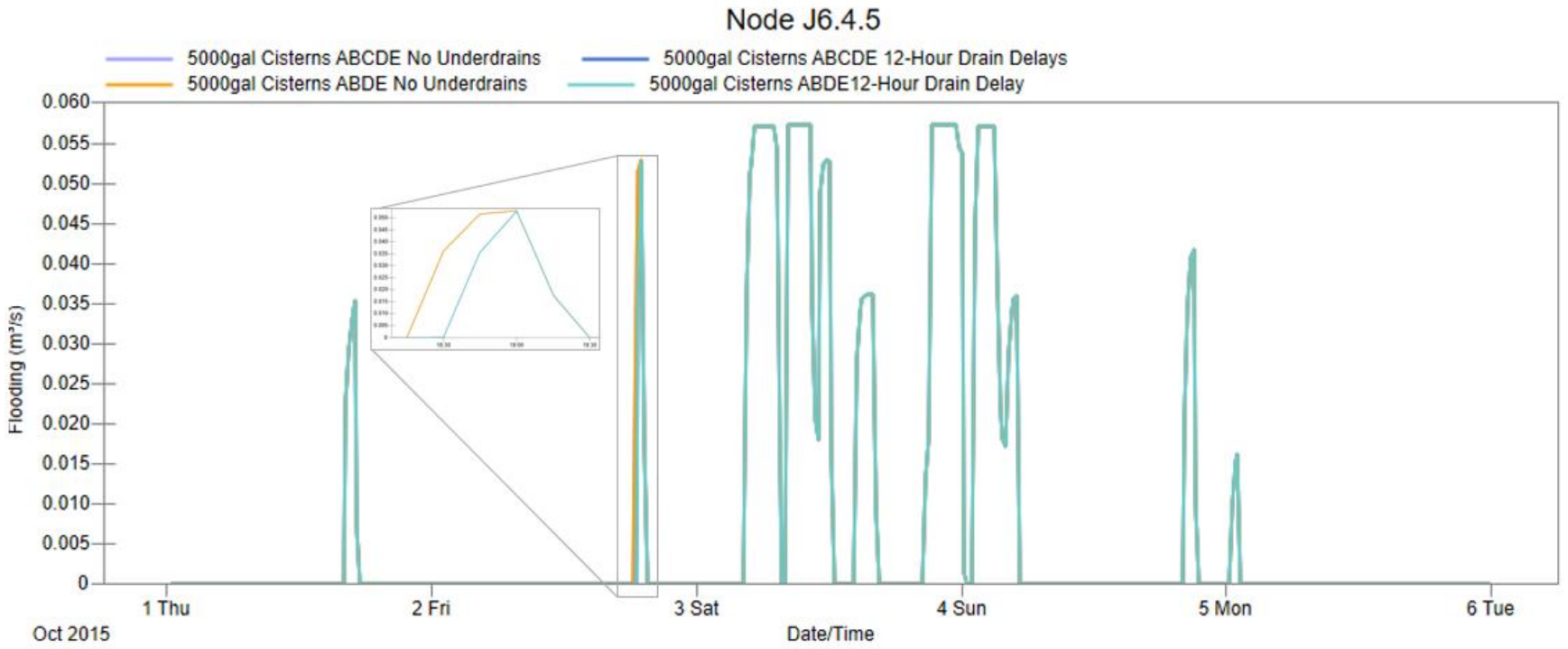

Figure D.11: Game 4 Junction 6.4.5 Flooding

D.12: Game 4 Junction 6.5.1 Flooding

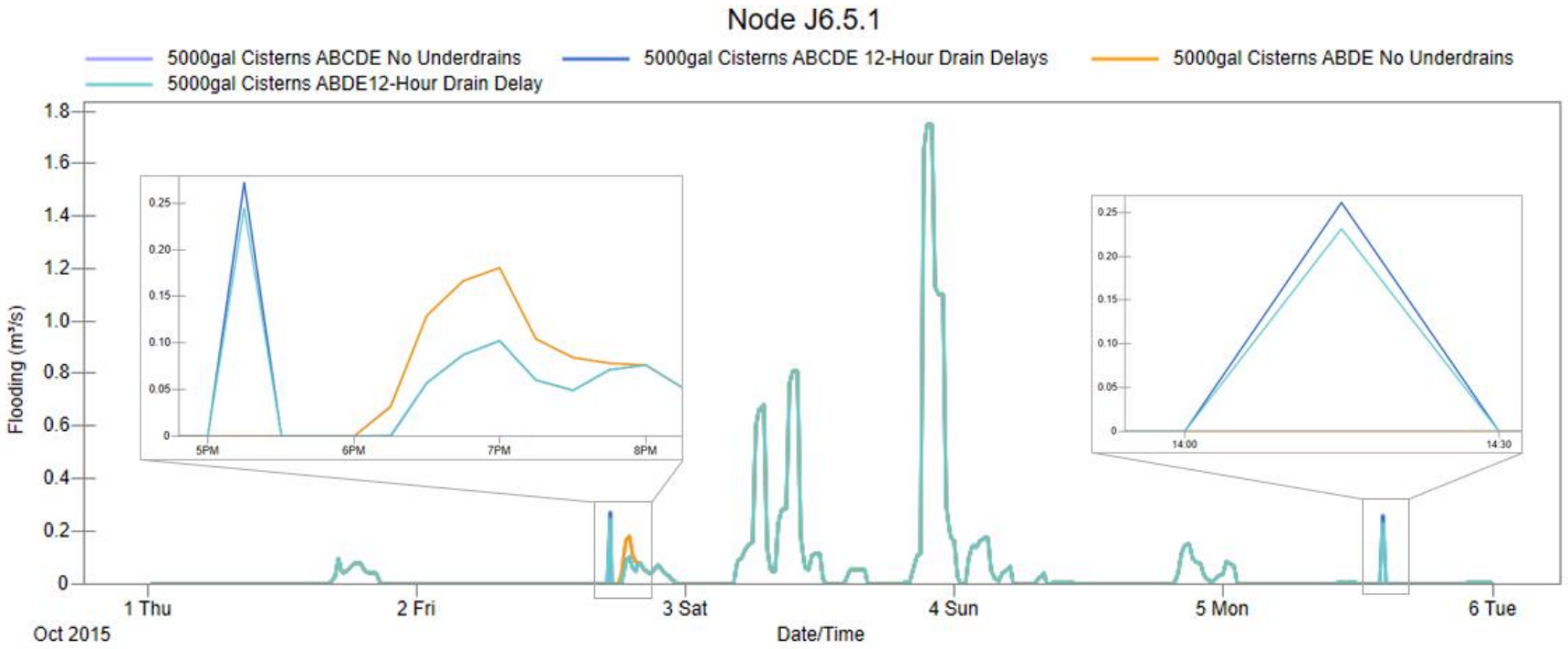

Figure D.12: Game 4 Junction 6.5.1 Flooding

D.13 Game 4 Junction 6.5.5 Flooding

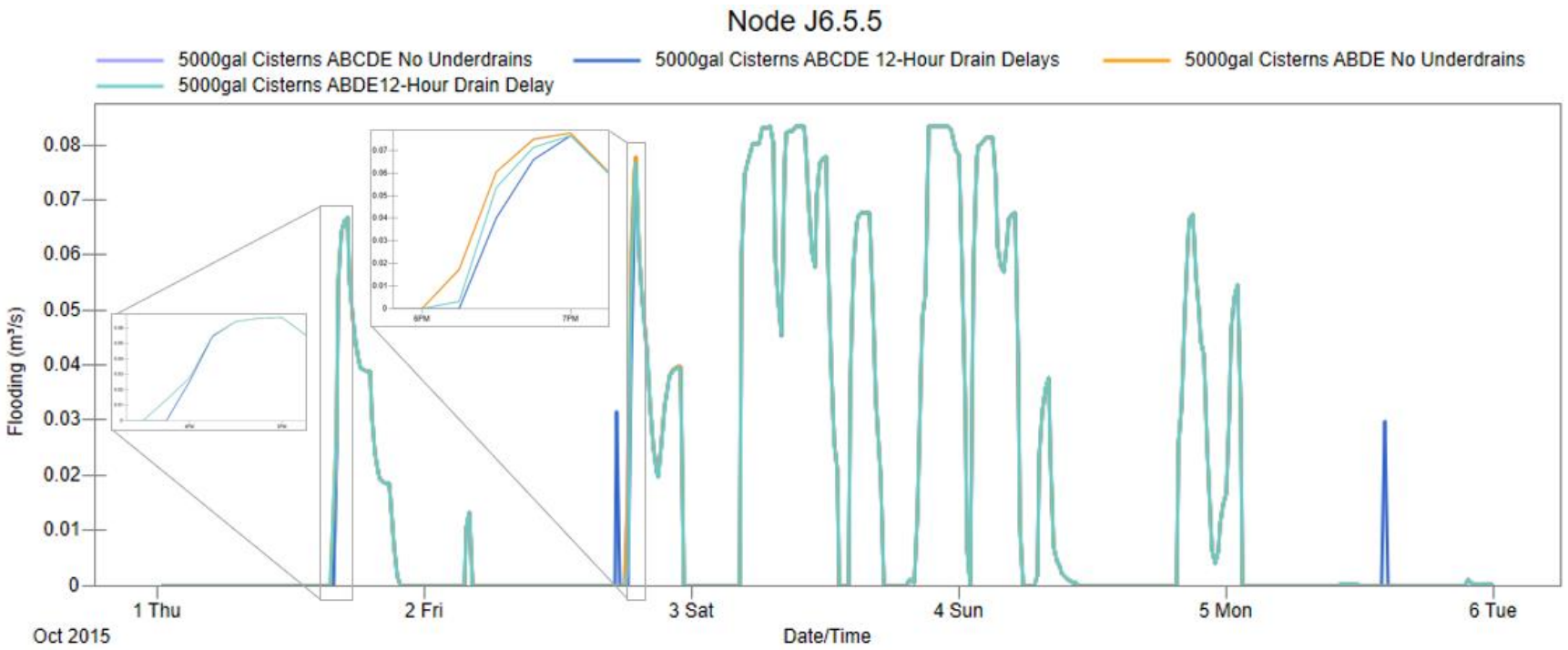

Figure D.13: Game 4 Junction 6.5.5 Flooding